











EXPERIMENTAL AND COMPUTATIONAL  
DETERMINATION OF GLOBAL RESONANCES  
IN SHIP STRUCTURES

by

MATTHEW EDWARD BARBER

B. S. Chemistry, University of New Mexico (1978)

Submitted to the Department of  
OCEAN ENGINEERING

In partial fulfillment of the requirements for the degrees of

NAVAL ENGINEER

and

MASTER OF SCIENCE IN MECHANICAL ENGINEERING

at the

MASSACHUSETTS INSTITUTE OF TECHNOLOGY

May 1991

© Matthew E. Barber

The author hereby grants to M.I.T. and to the U.S. Government permission to reproduce  
and to distribute copies of this thesis document in whole or in part.

---

A. Douglas Carmichael,  
Chairman Department Graduate Committee, Department of Ocean Engineering

10013  
B21714  
C.1

# EXPERIMENTAL AND COMPUTATIONAL DETERMINATION OF GLOBAL RESONANCES IN SHIP STRUCTURES

by

MATTHEW EDWARD BARBER

Submitted to the Department of Ocean Engineering  
on 10 May 1991 in partial fulfillment of the  
requirements of the degrees of Naval Engineer and  
Master of Science in Mechanical Engineering

## ABSTRACT

How machinery vibrations are transmitted through a foundation, into a hull and ultimately into the water is of great concern to ship designers. Global modes result from strong coupling between the vibration modes of a machine's foundation and the ship's hull, and can cause peaks in the radiated sound power spectrum. In simple structures the global modes can be identified and altered by making drive point mobility measurements and adding mass to the structure. Radiated sound power is altered because the added mass shifts the modal frequencies and modifies the coupling. In a more realistic structure with a higher impedance foundation there is more interaction with the hull and a greater density of modes making global mode identification harder, so additional methods are needed for identification. A finite element method is used to determine the vibration modes of a fluid loaded model foundation and hull. The forced response of the hull model is calculated and used in a boundary element method to predict the radiated sound power of the structure in water. The results are compared to experimental measurements from the actual model in a reverberant sound tank. Numerical methods are shown to be very useful in classifying the modes of a structure and predicting frequency shifts resulting in modal coupling to form global modes.

Thesis Supervisor: Richard H. Lyon

Title: Professor of Mechanical Engineering





## ACKNOWLEDGEMENTS

Thank you to Professor Richard Lyon for his interest in me and guidance throughout this research.

Thank you to Bolt Beranek and Newman Inc. especially Jeff Doughty for allowing me to use their acoustic facilities.

Thank you to Dr. David Goldsmith at DTRC Annapolis for taking interest in my project and allowing me access to the engineers and researchers at DTRC.

I owe my greatest thanks to my family; Matthew and Emma, who always brighten even my worst days, and mostly to my wife Bettye without whose support I could never have completed these three years at MIT or reached this point in my Naval career.



## Table of Contents

ABSTRACT .....	2
ACKNOWLEDGEMENTS .....	3
1 INTRODUCTION .....	8
1.1 Background .....	8
1.2 Research Goals .....	9
1.3 Thesis Organization and Content .....	11
2 THEORY .....	12
2.1 Modal Analysis .....	12
2.2 Radiated Power .....	20
2.3 Fluid Loading .....	23
2.4 Reverberant Sound Tank Acoustics .....	26
2.5 Global Mode Identification .....	30
2.6 Analytical Calculation .....	33
2.6.1 Radiation Efficiency .....	33
2.6.2 Average Modal Separation .....	37
2.7 Variable Listing .....	38
3 EXPERIMENTAL MODEL .....	43
3.1 Model Structure .....	43
3.2 Damping .....	45
3.3 Reverberant Water Tank .....	48
4 COMPUTATIONAL MODEL .....	52
4.1 Finite Element Program Description .....	52
4.2 Finite Element Model .....	52
4.2.1 Plate Element .....	53
4.2.2 Beam Element .....	54
4.2.3 Composite Model .....	55
4.2.4 Fluid Loading .....	56
4.3 Boundary Element Program Description .....	57
4.4 Boundary Element Model .....	58
5 COMPUTER ANALYSIS AND RESULTS .....	61
5.1 Computer Analysis .....	61
5.2 Results .....	70
5.3 Validation With Analytical Calculations .....	82
6 EXPERIMENTAL MEASUREMENTS AND RESULTS .....	84
6.1 Equipment Setup .....	84
6.2 Measurements .....	87
6.3 Drive Point Accelerance .....	88



6.4 Plate Acceleration .....	89
6.5 Waterborne Sound Pressure Level .....	90
6.6 Analysis .....	91
6.6.1 Experiment 1 .....	91
6.6.2 Experiment 2 .....	91
6.6.3 Experiment 3 .....	92
6.6.4 Experiment 4 .....	92
6.6.5 Experiment 5 .....	92
6.7 Validation of Results .....	93
7 CONCLUSIONS AND RECOMMENDATIONS .....	95
REFERENCES .....	98
APPENDIX A. DAMPING MEASUREMENTS .....	100
APPENDIX B. FINITE ELEMENT PROGRAM INPUT FILES .....	105
APPENDIX C. BOUNDARY ELEMENT PROGRAM INPUT FILE .....	123
APPENDIX D. FORTRAN PROGRAMS .....	134
APPENDIX E. MODAL FREQUENCY DATA .....	151
APPENDIX F. RADIATED POWER DATA .....	169





## Table of Figures

1. Model Isometric View .....	44
2. Hull and Foundation Model .....	45
3. Model Instrumentation for Damping Measurements .....	47
4. BBN Reverberant Sound Tank .....	49
5. Finite Element Model .....	53
6. Finite Finite Element and Boundary Element Plate Models .....	59
7. Foundation Model Mode Shapes with Clamped Ends .....	62
8. Foundation Model Mode Shapes With Simply Supported Ends .....	63
9. Foundation Mode at 490 Hz .....	65
10. Plate Mode at 468 Hz .....	66
11. Model Forcing Location .....	67
12. Radiated Power Spectrum for Foundation and Plate Model .....	68
13. Model With Weight Added to Foundation .....	70
14. Run # 1 Global Mode Pair .....	72
15. Run # 2 Global Mode Pair .....	73
16. Radiated Power Spectrum for Run # 0 and Run # 1 .....	75
17. Radiated Power Spectrum for Run # 0 and Run # 2 .....	76
18. Radiated Power Spectrum for Run # 0 and Run # 3 .....	77
19. Radiated Power Spectrum for Run # 0 and Run # 4 .....	78
20. Radiated Sound Power Spectrum for Run # 0 and Run # 5 .....	79
21. Location of Increased Sound Intensity in Run # 2 .....	81
22. Experimental Instrumentation Setup .....	84
23. Drive Point Accelerance for Experiments 1 - 5 .....	88
24. Plate Acceleration for Experiments 1 - 5 .....	89
25. SOund Pressure Level for Experiments 1 - 5 .....	90



## Table of Tables

1. Model Damping Loss Factors .....	48
2. Reverberant Sound Tank Data .....	50
3. Water Tank Reverberation Times .....	51
4. Element and Material Properties .....	55
5. Wave Number For Fluid Loaded and Free Plates .....	56
6. Modal Analysis Results .....	71
7. Hydrophone Placement in the Revererant Sound Tank .....	86



# 1 INTRODUCTION

## 1.1 Background

Machinery vibration on board ships is one of the main sources of sound transmitted into the water. Mechanical impact or rubbing in rotating or reciprocating machinery is transmitted via foundations to the hull and eventually into the water. This transmitted sound energy can be detected and the location and other characteristics of the ship compromised.

When designing new ships or alterations to existing ships the designer must be aware of possible sources of structural vibration, sound transmission paths and the possibility of increasing the radiated noise signature of the ship. For individual components care must be taken to eliminate or minimize possible sources of structural vibration, and for foundations the transmission of sound to the hull must be minimized. One method to minimize the transmission of sound between foundation and hull is through investigation of the vibration modes of the foundation and the hull.

By modal analysis the vibration of a foundation or the hull can be analyzed through its mode shapes and corresponding resonant frequencies. In the composite structure with the foundation attached to the hull three types of modes can be identified; a foundation mode, characterized by motion of the foundation with little hull motion, a hull mode, characterized by motion of the hull with little foundation motion, and a global mode, where there is motion of both the foundation and the hull.





Generation of volume velocity in the surrounding water by hull motion creates a sound source, therefore, hull and global modes would be expected to radiate sound into the water where foundation modes would not. Sound transmission from the foundation to the hull and into the water would be expected to be greatest in a global mode because both the foundation and the hull have a large response to excitation. If the designer could anticipate a global mode for a proposed foundation or identify one in an existing foundation he could make subtle alterations in the design to avoid it, or alter the existing foundation to eliminate it. This would allow the designer to reduce the radiated sound from the ship.

Previous research in [1], [2], and [3] has shown that global modes can be identified and altered in simple structures such as a beam attached to a plate. Correlation was shown between the existence of a global mode pair and a peak in the radiated sound pressure spectrum in water. However, when a higher impedance structure was attached to a plate to better model a real foundation hull interaction global mode identification became more difficult and required modal analysis by means of a finite element method to help in identifying global modes.

## **1.2 Research Goals**

The purpose of this research is to further examine the identification of global modes in a waterborne foundation and hull model. By using computer methods to



model, predict, and estimate the radiated power of the global modes of a foundation and hull a ship design can be modified before production to try and eliminate global modes and hence reduce the radiated sound signature of the ship.

A modal analysis of a foundation and hull model will be done using a finite element method. An added mass approximation is used to account for the fluid loading of the water on the hull. The mode shapes and resonant frequencies will be used to aid in the identification of global modes, and to predict the frequency response of the hull. From the model's forced response at specified frequencies the model velocity amplitude and phase will be determined. A boundary element program will then be used to predict the radiated sound power spectrum using the plate velocity as the input boundary condition.

A global mode occurs when two of the resonant modes of the individual structures are close in frequency, and should be seen as two closely spaced resonant frequencies for the composite structure. To form a global mode in the computer model a foundation mode will be selected from an analysis of the model mode shapes, then a mass added to the foundation to lower its frequency. The mode should couple with a lower frequency mode and form a global mode pair and a subsequent increase in the calculated radiated sound power at the frequency of the global mode should be seen.

The predicted sound power from the foundation and hull model will be compared to experimental data taken from the real model in a reverberant sound tank. Drive point acceleration measurements taken from the model should help identify the



resonant frequencies of global modes and the radiated sound pressure measurements taken should correlate with the appearance and disappearance of peaks in the radiated sound power spectrum as the global modes are altered.

### **1.3 Thesis Organization and Content**

The motivation and goals described above form the basis for this research. Chapter 2 describes the theory used to perform the analysis and calculations. The experimental model used in this research is described in Chapter 3, and the computer models are described in Chapter 4. The computer analysis and results are discussed in Chapter 5, and the experimental setup and measurements are discussed in Chapter 6. Chapter 7 summarizes the results of the analyses and states the conclusions and recommendations for future work. There are several Appendices included that contain graphical data displays of damping measurements, examples of finite element program input files, examples of boundary element input files, computer programs that were generated, a listing of the resonant frequencies of the various models, and the Radiated Power output data from the boundary element program.





## 2 THEORY

The identification of vibrational modes in a structure requires a knowledge of modal analysis, which involves solving the equations of motion for the eigenvalues and eigenvectors. For simple systems this can be done analytically, but in general it requires approximating the structure with discrete elements and solving the problem numerically. Subsequently, the calculation of the forced response and radiated sound power from a structure involves discretization and numerical solution. The results of these calculations can be used in a systematic way to classify the modes of a structure into foundation, plate, or global modes to help identify and alter the radiated sound.

### 2.1 Modal Analysis

Standard terminology used in this chapter:

- $\{ \}$  Denotes a vector
- $[ ]$  Denotes a matrix
- $\ddot{x}$  Denotes the second derivative with respect to time.

In modal analysis the forced response of each of the vibrational modes of the structure is calculated and added together to give the structure's response. In continuous structures however there are an infinite number of modes and resonant frequencies, so approximations are made to achieve a solution. One method used is to



discretize the structure into smaller elements and do the modal analysis and forced response by computational methods. The finite element method does this by dividing the structure into many smaller connected elements whose masses and physical properties are used to approximate a complex continuous structure. The problem becomes that of solving  $n$  equations in  $n$  unknowns, where  $n$  is the number of degrees of freedom or the number of discrete points in the structure times the number of displacements or rotations that the points are free to move in. Because  $n$  can become large using computers makes the solution manageable. The following paragraphs outline the general methods used to evaluate structures using modal analysis.

The equations of motion for the free vibration of a discretized undamped elastic structure can be written in matrix notation as:

$$[M]\{\ddot{u}\} + [K]\{u\} = \{0\} \quad (2.1)$$

where,  $[M]$  is the mass matrix,  $[K]$  is the stiffness matrix, and  $\{u\}$  is the displacement vector. The eigenvalue problem can be solved by assuming a solution of the form:

$$u_i(t) = X_i T(t), \quad i=1,2,\dots,n \quad (2.2)$$

where,  $u_i$  is the  $i^{\text{th}}$  component of the displacement vector,  $X_i$  is a constant, and  $T$  is a function of time. By substituting equation (2.2) into the equation of motion the following two equations result:



$$\ddot{T}(t) + \omega^2 T(t) = 0 \quad (2.3)$$

$$[[K] - \omega^2 [M]] \{X\} = \{0\} \quad (2.4)$$

The solution to equation (2.3) can be expressed as

$$T(t) = A e^{i(\omega t + \phi)} \quad (2.5)$$

where the constants  $A$  and  $\phi$  are the amplitude and phase and  $\omega$  is a characteristic frequency. The characteristic frequencies of the system  $\omega$  can only take on values determined by the eigenvalues of equation (2.4). For a nontrivial solution the determinant of the coefficient matrix  $[[K] - \omega^2 [M]]$  must be zero. When the determinant is evaluated an  $n^{\text{th}}$  order polynomial results with roots  $\omega_1^2, \omega_2^2, \dots, \omega_n^2$ , the eigenvalues or natural frequencies of the system. Substituting back into equation (2.4) gives the characteristic eigenvectors or mode shapes  $\{X^{(i)}\}$ .

When determining the response of the structure to a prescribed force,  $\{F(t)\}$ , the equation of motion becomes:

$$[M] \{\ddot{u}\} + [K] \{u\} = \{F(t)\} \quad (2.6)$$

which is a set of  $n$  coupled second order ordinary differential equations. The equations can be uncoupled if generalized coordinates are used.





To solve for the forced response the mode shapes and natural frequencies are found from the unforced case, then the expansion theorem described in [4] is used to find the solution as a linear combination of the normal modes.

$$\{u(t)\} = q_1(t)\{X^{(1)}\} + q_2(t)\{X^{(2)}\} + \dots + q_n(t)\{X^{(n)}\} \quad (2.7)$$

where,  $\{X^{(i)}\}$  is the eigenvector or mode shape of the  $i^{\text{th}}$  mode, and each  $q_{(i)}(t)$  is a time dependent generalized coordinate known as a modal participation coefficient. A modal matrix,  $[X]$ , can be formed from the mode shapes where the  $i^{\text{th}}$  column is the vector  $\{X^{(i)}\}$ , then if the mode shapes are normalized with respect to the mass matrix the following equations are true,

$$\{X^{(i)T}\}[M]\{X^{(i)}\} = 1 \quad (2.8)$$

$$[X]^T[M][X] = [I] \quad (2.9)$$

$$[X]^T[K][X] = [\omega^2]. \quad (2.10)$$

Where  $[\omega^2]$  is the diagonal matrix of eigenvalues. The applied forces,  $\{F(t)\}$ , can be expressed as generalized forces  $\{Q(t)\}$  by:



$$\{Q(t)\}=[X]^T\{F(t)\} \quad (2.11)$$

and the equations of motion written in a generalized matrix form are:

$$\{\ddot{q}(t)+[\omega^2]\{q(t)\}=\{Q(t)\}. \quad (2.12)$$

This denotes a set of  $n$  uncoupled second order ordinary differential equations, which can be solved for  $\{q(t)\}$  and the displacements  $\{u(t)\}$  found from:

$$\{u(t)\}=[X]\{q(t)\}. \quad (2.13)$$

The response for a structure with damping can be calculated in a similar manner if the modal damping ratios are known for the structure. The generalized equations of motion become:

$$\{\ddot{q}_i(t)\}+2\xi_i\omega_i\{\dot{q}_i(t)\}+\omega_i^2\{q_i(t)\}=\{Q_i(t)\}, \quad i=1,2,\dots,n \quad (2.14)$$

where,  $\xi_i$  is the modal damping ratio of the  $i^{\text{th}}$  mode.

In finite element analysis the mode shapes and resonant frequencies are found by solving these equations numerically. The mass matrix comes from the discretized element masses and the stiffness matrix depends on the type of elements used eg. beam or plate/shell, the geometry of the structure, and an assumed displacement function within the elements.



Each element is defined by points or nodes in the structure. The nodal displacements in three orthogonal directions  $u$ ,  $v$ , and  $w$  are expressed as a function of the  $x$ ,  $y$ , and  $z$  coordinates of the nodes:

$$\begin{aligned} u(x, y, z) &= \alpha_1 + \alpha_2 x + \alpha_3 y + \alpha_4 z + \alpha_5 xy + \dots \\ v(x, y, z) &= \beta_1 + \beta_2 x + \beta_3 y + \beta_4 z + \beta_5 xy + \dots \\ w(x, y, z) &= \gamma_1 + \gamma_2 x + \gamma_3 y + \gamma_4 z + \gamma_5 xy + \dots \end{aligned} \quad (2.15)$$

The coefficients are the generalized coordinates. Written in matrix form:

$$\{u\} = [\Phi] \{\alpha\} \quad (2.16)$$

where,  $[\Phi]$  is the matrix of polynomial terms in  $x$ ,  $y$ , and  $z$  and  $\{\alpha\}$  is the vector of generalized coordinates.

The strain can be expressed as:

$$\{\varepsilon\} = [E] \{\alpha\} \quad (2.17)$$

where,  $\{\varepsilon\}$  is the generalized strain vector and  $[E]$  is the matrix of polynomial elements taken from  $[\Phi]$  and the strain displacement relationship. The generalized strain vector depends on the type of element used. For example for a plane strain element:



$$\{\epsilon\}^T = \{\epsilon_{xx}, \epsilon_{yy}, \gamma_{xy}\} \quad (2.18)$$

and plate bending:

$$\{\epsilon\}^T = \{\kappa_{xx}, \kappa_{yy}, \kappa_{xy}\} \quad (2.19)$$

$$\text{where, } \epsilon_{xx} = \frac{\partial u}{\partial x}, \quad \epsilon_{yy} = \frac{\partial v}{\partial y}, \quad \gamma_{xy} = \frac{\partial u}{\partial y} + \frac{\partial v}{\partial x}, \quad \kappa_{xx} = -\frac{\partial^2 w}{\partial x^2}, \quad \kappa_{yy} = -\frac{\partial^2 w}{\partial y^2}, \quad \kappa_{xy} = 2\frac{\partial^2 w}{\partial x \partial y}.$$

[E] is derived from the specific strain displacement operation performed on the polynomial terms in  $[\Phi]$  as defined in the respective strain vector.

The generalized stress vector,  $\{\tau\}$ , can then be obtained by:

$$\{\tau\} = [C]\{\epsilon\} \quad (2.20)$$

where, [C] is the generalized elasticity matrix for the specific element type. The elasticity matrix for a plane strain element is:

$$[C] = \begin{bmatrix} \frac{E}{(1-\nu^2)} & \frac{\nu E}{(1-\nu^2)} & 0 \\ \frac{\nu E}{(1-\nu^2)} & \frac{E}{(1-\nu^2)} & 0 \\ 0 & 0 & \frac{E}{2(1+\nu)} \end{bmatrix} \quad (2.21)$$





and the elasticity matrix for plate bending is:

$$[C] = \begin{bmatrix} \frac{Eh^3}{12(1-\nu^2)} & \frac{\nu Eh^3}{12(1-\nu^2)} & 0 \\ \frac{\nu Eh^3}{12(1-\nu^2)} & \frac{Eh^3}{12(1-\nu^2)} & 0 \\ 0 & 0 & \frac{Eh^3}{24(1+\nu)} \end{bmatrix} \quad (2.22)$$

The stiffness matrix is obtained from the summation over all of the elements of these combined matrix operations to convert displacement to stress.

The type of elements used to evaluate the model for this research is a four node plate/shell element with five degrees of freedom at each node, three translational degrees and two rotational (the rotation normal to the plane of the element is fixed). The assumed functional relationship between the displacement at the nodes is given by the constant linear stress triangle and the Hsieh, Clough, and Tocher methods described in [5]. The stress, strain, displacement and elasticity for this type of element is obtained by superimposing the respective matrices and vectors for the plane strain and plate bending elements described above. The strain vector is:

$$\{\epsilon\}^T = \{\epsilon_{xx}, \epsilon_{yy}, \gamma_{xy}, \kappa_{xx}, \kappa_{yy}, \kappa_{xy}\}, \text{ and the stress vector is:}$$

$$\{\tau\}^T = \{\tau_{xx}, \tau_{yy}, \tau_{xy}, M_{xx}, M_{yy}, M_{xy}\}.$$

Combining the nodal displacement vector with the generalized coordinates, the nodal locations, the mass matrix and the stiffness matrix as described above results in



an eigenvalue and forced response problem that is solved numerically. The output is the displacement amplitude and phase of each node in the structure as it responds to the applied force.

## 2.2 Radiated Power

The motion of the boundary to an acoustic medium can be used to calculate the radiated power into the medium by solving the acoustic wave equation. This solution can be done analytically for only the simplest geometries and in general approximate methods must be used.

The boundary element method (BEM) is a computational method of solving the acoustic wave equation. In the BEM the boundary of the acoustic domain is modeled with a discrete two dimensional lattice of nodes. The boundary velocity ( $v$ ) or pressure ( $p$ ) is specified at each node, then for each point on the boundary the Helmholtz integral equation is solved numerically to form a system of algebraic equations in the unspecified variable ( $p$  or  $v$ ). The algebraic system is solved for the unknown and then the value of  $p$  or  $v$  can be found anywhere in the acoustic medium.

The usefulness of the BEM is that it relies on only the geometry and the boundary conditions of the problem. Analytical results are available for simple shapes such as spheres, but introducing even slight deviations to the shape will severely complicate the results. In the BEM an arbitrary bounding surface is



modelled two dimensionally with a series of points. The velocity or pressure at the surface points can be found by other methods such as a finite element analysis of the structure.

The BEM formulation for the sound radiation from a surface S into an infinite acoustic medium is shown below (from [7] and [8]).

The three dimensional Helmholtz integral equation can be expressed as:

$$C(P)p(P) = \int_S \{p(Q)G'(P, Q) + iz_0kv(Q)G(P, Q)\}dS(Q) \quad (2.23)$$

where, Q is any point on S

P is any point

$p(P)$  is the acoustic pressure at P satisfying  $\nabla^2 p + k^2 p = 0$

$v(Q)$  is the velocity amplitude at Q on S

G is the free surface Green's function  $G(P, Q) = \frac{e^{-ikR(P, Q)}}{R(P, Q)}$

$R = |P-Q|$

k is the wave number,  $\left(\frac{\omega}{c}\right)$

$G'(P, Q)$  is the normal gradient of the Green's function at Q

$z_0$  is the characteristic impedance of the medium

$C(P) = 0$ , for P in the body

$= 4\pi$ , for P in the medium



$$= 2\pi, \text{ for } P \text{ on } S$$

(For  $P$  at an edge or corner of  $S$ ,  $C(P)$  has a different value which is a function of the local geometry.

$$C(P) = 4\pi + \int_S \frac{\partial}{\partial \eta} \left\{ \frac{1}{R(P, Q)} \right\} dS(Q) \quad (2.24)$$

$\eta$  is the unit normal on  $S$  out of the body.

The solution strategy is to specify either  $p$  or  $v$  on  $S$ , then perform the integration to form a set of algebraic equations in the unknown variable. Solve the system of equations numerically to obtain the unknown  $p$  or  $v$ . When  $p$  and  $v$  are known on the bounding surface they can be found in the acoustic medium by numerical quadrature. Then the radiated power can be found from:

$$W = \frac{1}{2} \int_S \text{Re} \{ p^*(Q) v(Q) \} dS(Q) \quad (2.25)$$

where, the  $*$  is the complex conjugate. This integration can be done numerically.

A shortcoming of the BEM has been in the boundary integral equation formulation for the exterior problem where sound is radiated from a body into an infinite or semi-infinite medium. There is a nonuniqueness of solution at certain characteristic frequencies, "fictitious eigenfrequencies" with no physical significance. Schenk, [7], solved the nonuniqueness problem in his combined Helmholtz integral





equation formulation or CHIEF method. This method places additional points inside the body to overdetermine the solution at the surface. The boundary element program uses the CHIEF method.

## 2.3 Fluid Loading

A body radiating into an acoustic medium will experience a loading on its surface due to the radiation resistance of the fluid and the added mass of the fluid that must be moved by the body. At very low frequencies it is known, [9] and [10], that the fluid appears to the structure like an added mass. In spherical shell structures it is found, [11], that the added mass approximation is adequate for  $ka < 1$ , where  $ka$  is the ratio of the circumference of the spherical shell to the acoustic wavelength. At higher frequencies the fluid impedance (ratio of pressure and velocity) involves both mass-like and damping-like effects, and at very high frequencies,  $ka > 5$ , the radiation resistance effect dominates. If the circumference of the spherical shell ( $a$ ) is replaced by a characteristic length of the structure then for  $ka < 1$  the added mass approximation to the fluid loading should be adequate. For example, if  $a = 4$  feet, in the frequency range 400 to 600 Hz,  $ka$  varies from .52 to .78 so the added mass effect will dominate.

There are many examples in the literature of using numerical methods to approximate the fluid structure interaction, [8], [9], [10], [11], [12], and [13]. However, at the low frequencies examined in this research an added mass approximation will be adequate.



In [6] the fluid loading at low frequencies is predicted by the added mass of a layer of fluid  $\lambda_b/2\pi$  thick, where  $\lambda_b$  is the wave length of the flexural waves in the plate. These waves cause the most motion at the surface of the plate so are responsible for most of the radiated sound.

The wave number of flexural waves in a plate ( $k_b$ ) is calculated from:

$$k_b^2 = \frac{\omega}{\kappa C_l} \quad (2.26)$$

However, the wave number of the plate will be modified by the fluid loading. In [14], this effect is determined by solving the equations governing the flexural motions in the plate with the fluid loading.

$$D \nabla^4 \omega + \rho_s \frac{\partial^2 \omega}{\partial t^2} = -p \big|_{z=0} \quad (2.27)$$

where,  $\rho_s$  is the area density of the plate,  $p|_{z=0}$  is the pressure due to the fluid loading, and  $p$  must be a solution to the wave equation:  $\nabla^2 p - (c^2) \frac{\partial^2 p}{\partial t^2} = 0$ . The boundary condition between the fluid and the plate that must be satisfied is:

$$\frac{\partial p}{\partial z} \bigg|_{z=0} = -\rho_f \frac{\partial^2 \omega}{\partial t^2} \quad (2.28)$$



where,  $\rho_f$  is the fluid density. By requiring a solution to equations (2.27) and (2.28) of the form:

$$\omega = W e^{i(k_b x - \omega t)} \quad (2.29)$$

the system can be solved if the following dispersion relation is satisfied:

$$\frac{\rho_f \omega}{\sqrt{k_b^2 - k^2}} + \omega \rho_s \left( 1 - \frac{D k_b^4}{\rho_s \omega^2} \right) = 0 \quad (2.30)$$

where,  $k$  is the acoustic wave number and  $D$  is the flexural rigidity of the plate,  $D = Eh^3/12(1-\nu^2)$ .

This equation has 5 roots for  $k_b$ , one pure real root (subsonic wave) and two complex conjugates (super sonic waves). At the frequencies of interest (400 Hz - 600 Hz) the radiation loading of the plate is insignificant and the added mass of the fluid is the dominant factor in the fluid loading of the plate. The pure real root will give the fluid loaded wave number of the plate.

Rewriting the dispersion relation gives:

$$k_b^4 = \frac{\rho_s \omega^2}{D} + \frac{\rho_f \omega^2}{D \sqrt{k_b^2 - k^2}} \quad (2.31)$$

which can be solved at a given frequency for the one real root by iteration.



## 2.4 Reverberant Sound Tank Acoustics

For an enclosed volume the geometry of the enclosed space defines an infinite set of mode shapes that sound waves can exist in. In [15] the modal analysis of a room is discussed and equations for the modal density, modal energy, and power of a room presented. These equations are used to determine the acoustic limits for use of a reverberant tank and to calculate the radiated sound power of a sound source from the measured sound pressure.

For a rectangular enclosure the number of modes at a given frequency can be approximated by the following equation:

$$N(\omega) \approx \frac{\omega^3 V}{6\pi^2 c^3} \quad (2.32)$$

where  $V$  is the volume of the enclosure and  $c$  is the speed of sound in the acoustic medium. Then the modal density is:

$$n(\omega) = \frac{dN(\omega)}{d\omega} \approx \frac{\omega^2 V}{2\pi^2 c^3} \quad (2.33)$$

and the modal separation:





$$\delta\bar{f} = \frac{1}{n(\omega)}. \quad (2.34)$$

The frequency of the  $M^{\text{th}}$  mode of the enclosure,  $f_M$ , is calculated from:

$$f_M^2 = \frac{c^2}{4} \sum_{j=1}^3 \frac{m_j^2}{L_j} \quad (2.35)$$

where,  $j$  represents the coordinate axes,  $m_j$  is the mode number, and  $L_j$  is the length of the enclosure in the  $j^{\text{th}}$  direction. From the mode density, modal separation and the lowest frequency mode an estimate of the frequency response of the enclosure can be made for acoustic measurements.

When sound power is radiated into an enclosure each of the modes of the enclosure will contain a portion of the total energy. An estimate of the sound power in a specific frequency band can be made if the sound pressure in that band is measured. The following equations show how the sound power can be calculated.

The average of the energy in a particular mode  $M$  is given by:

$$\langle E_M \rangle = \frac{\langle p_M^2 \rangle_{r,t}}{\rho_f c^2} \quad (2.36)$$



where the modal pressure is averaged over space and time. Since the natural modes of the enclosure are spatially orthogonal the average squared pressure is the sum of the modal contributions, and the total average energy is the sum of the average modal energies. The total energy in a frequency band  $\Delta\omega$  is:

$$\langle E \rangle_t = \sum_M \langle E_M \rangle_t = n(\omega)\Delta\omega \langle E_M \rangle_{t,M} \quad (2.37)$$

If the average pressure is measured in a frequency band then the average energy in that band can be calculated.

The total sound energy in an enclosure can be thought of as the sum of the contributions from the direct field of the sound source and the reverberant field. The remainder of the power is dissipated at the enclosure walls. The fraction of incident power that is absorbed by the walls is given by the absorption coefficient,  $\alpha$ . The absorption coefficient is calculated from the reverberation time ( $T_R$ ) of the enclosure, which is the time it takes the sound energy in the enclosure to decay by 60 decibels (dB). From [6],  $\alpha$  in terms of  $T_R$  and collision rate ( $\nu$ ) is:

$$\alpha = \frac{13.8}{T_R \nu} \quad (2.38)$$

$$\nu = \frac{cS}{4V} \quad (2.39)$$



If the radiated sound power of the source is  $\Pi_s$ , then the power absorbed at the walls from the direct field is  $\alpha\Pi_s$  and the power injected into the reverberant field is  $(1-\alpha)\Pi_s$ . The total energy in the room in the reverberant field is  $VE_R$  where  $E_R$  is the energy in the reverberant field. The power dissipated in the walls from the reverberant field is  $\alpha v(VE_R)$ . To get the energy in the reverberant field an energy balance is done:

$$\frac{d}{dt}(VE_R) = (1 - \alpha)\Pi_s - \alpha v(VE_R). \quad (2.40)$$

For steady state  $VE_R$  is constant so,

$$E_R = \frac{\Pi_s}{vV} \frac{1 - \alpha}{\alpha} \quad (2.41)$$

and power radiated from the source is:

$$\Pi_s = \frac{\alpha v V E_R}{1 - \alpha}. \quad (2.42)$$



By measuring the acoustic sound pressure in the enclosure at least one acoustic wavelength away from the source and averaging it in space and time, the average energy in the reverberant field can be calculated from equation (2.38). Then, knowing  $T_R$ ,  $\Pi_s$  can be calculated from equations (2.39), (2.40), and (2.43).

## 2.5 Global Mode Identification

In a structure consisting of a foundation and plate vibration modes can be identified as foundation, plate, or global. A foundation mode involves predominantly foundation motion and little plate motion, and a plate mode involves predominantly plate motion and not foundation motion. A global mode is the result of coupling between a mode of the foundation and a mode of the plate and involves significant motion of both the foundation and plate. These modes can be identified using a systematic method of modifying the foundation and foundation hull junction with masses and observing how resonant peaks from modal analysis of drive point mobility measurements shift in frequency.

In [1] it was shown that global modes could be identified in a simple structure consisting of a beam and plate by making drive point mobility measurements. Small masses were added to the beam or beam/plate junction and vibration modes were identified as beam, plate or global by observing how peaks in the drive point mobility shifted as the weights were added. The frequency of a beam mode lowers when mass is added to the beam and doesn't shift when mass is added to the junction, because





this mode involves beam motion and not plate motion. The frequency of a plate mode lowers when mass is added to the junction and doesn't shift when mass is added to the beam, because this mode involves plate motion and not beam motion. Global modes may couple or uncouple when a mass is added to either the beam or the plate because the frequencies of the mode pair shift apart or closer together. By systematically adding weights to the foundation and foundation and hull junction global modes can be identified.

The method for identifying global modes was confirmed in [2], and it was shown that there was some correlation between the presence of a global mode and a peak in the radiated sound pressure in water for a simple plate and beam structure. Because a global mode is characterized by the coupling of two modes and involves motion of both the plate and the foundation it is expected that the transmission of sound energy from the foundation to the hull and into the water will be greatest at the frequency of the global mode pair. Therefore, at this frequency there should be a peak in the radiated sound pressure. It is then possible to confirm the presence or absence of a global mode by a relative increase or decrease the radiated sound power as the global mode pair separation is shifted. This coupling or uncoupling of a global mode pair is accomplished by adding a mass to the foundation or the foundation and hull junction.

In a simple beam and plate structure the modal density of the beam is low. In a more complex foundation structure the modal density is higher and if the junction impedance is increased there is greater interaction between the hull and the foundation. This is a more realistic model of an actual foundation and hull junction.



In [3] it was found that this made the identification of global modes more difficult, so to aid in the identification of global modes a modal analysis of the structure is needed. For this purpose a finite element method can be used.

To help identify global modes in the composite structure, the foundation can be modeled by itself to determine the mode shapes and the resonant frequencies. Fixed and simply supported boundary conditions need to be applied at the junction point of the foundation to fully understand what the mode shapes and frequencies will be. These conditions are extremes of the actual condition at the junction and should bracket the actual frequency at which a foundation mode would occur.

The composite structure is modeled and the mode shapes and resonant frequencies determined. If a mode shape can be found that has little plate motion and significant foundation motion similar to a previously determined foundation mode then it is classified a foundation mode. If the mode below it in frequency is approximately  $180^\circ$  out of phase, then this mode pair may be a good candidate to form a global mode pair. To shift the foundation mode down in frequency a mass is added to a node on the foundation. The modal analysis is repeated with this alteration to the foundation.

Since global modes should signify where peaks in the radiated sound power should occur the computer analysis is used to calculate a radiated sound power spectrum in a frequency band around the foundation mode for both the modified and unmodified models. A coupling of the selected modes will be indicated by an increase in the radiated sound power at the frequency of the mode pair.



## 2.6 Analytical Calculation

For evaluation of computer or experimental results it is useful to compare them to analytical calculations that give exact results or estimates of calculated or measured values. The following discussion will give analytical estimates of modal density and radiation efficiency of a flat plate.

### 2.6.1 Radiation Efficiency

For a free plate vibrating in a fluid at frequencies below the critical frequency ( $f_c$ ) theoretically the plate does not radiate sound. Below  $f_c$  the bending waves in the plate are subsonic, the pressure and particle velocity at the plate surface are  $90^\circ$  out of phase and the fluid simply presents a mass reactance to the vibration. An equation for the calculation of  $f_c$  is given in [6]:

$$f_c = \frac{c^2}{2\pi\kappa c_l} \quad (2.43)$$

where,  $c$  is the speed of sound in the acoustic medium,  $\kappa$  is the radius of gyration of the plate, and  $c_l$  is the speed of longitudinal waves in the plate. For a .25 inch steel plate in water  $f_c = 3837$  Hz.



A bending wave in a plate below  $f_c$  can radiate sound if there is a constraint placed on the plate that inhibits its free vibration. When a bending wave meets an attachment or foundation on the plate there is a reaction force from the mass resisting the wave motion. The plate will radiate sound because the reaction force acts like a force on the plate. From [6] the radiated pressure ( $p_{rad}$ ) from a point force ( $l_s$ ) on a plate is:

$$p_{rad} = \frac{l_s \rho_f}{2\pi \rho_s r} \quad (2.44)$$

where,  $\rho_f$  is the density of the acoustic medium,  $\rho_s$  is the area density of the plate, and  $r$  is the distance from the plate. Then from the intensity ( $I$ ):

$$I = \frac{\langle p_{rad}^2 \rangle}{\rho_f c} \quad (2.45)$$

and the plate radiating into half space, the radiated power ( $\Pi_{rad}$ ) can be calculated:

$$\Pi_{rad} = \frac{\rho_f \langle l_s^2 \rangle}{2\pi \rho_s^2 c}. \quad (2.46)$$

The relationship between the point force on a plate and plate velocity ( $v_p$ ) is given by:





$$l_s = \frac{v_p}{G_p} \left( \frac{1}{1 + \frac{Y_m}{G_p}} \right) \quad (2.47)$$

where,  $Y_m$  is the mobility of the foundation and  $G_p$  is the drive point conductance of the plate given by  $G_p = 1/8\rho_s\kappa c_l$ .

If the simplest case is assumed where the foundation holds the plate fixed the foundation mobility is equal to the drive point conductance. Then the average mean squared point force ( $\langle l_s^2 \rangle$ ) as a function of the average mean squared plate velocity ( $\langle v_p^2 \rangle$ ) is:

$$\langle l_s^2 \rangle = 64\rho_s^2\kappa^2c_l^2 \langle v_p^2 \rangle \quad (2.48)$$

and the radiated power becomes:

$$\Pi_{rad} = \frac{32}{\pi c} \rho_f \kappa^2 c_l^2 \langle v_p^2 \rangle \quad (2.49)$$

A common way to express radiated power is by comparing it to the sound radiated by a piston in a tube:  $\Pi_{rad} = A_p \rho c \langle v^2 \rangle_{x,t}$ . The radiated power from an arbitrary vibrating structure can then be equated to this power by the radiation efficiency ( $\sigma_{rad}$ ). From [6]:

$$\Pi_{rad} = A_p \rho c \langle v^2 \rangle_{x,t} \sigma_{rad} \quad (2.50)$$



Then  $\sigma_{rad}$  can be calculated by:

$$\sigma_{rad} = \frac{32\kappa^2 c_l^2}{\pi A_p c^2} \quad (2.51)$$

For a .25 inch steel plate with an area of 1.43 m<sup>2</sup>,  $\sigma_{rad} = 0.0275$ . If the mobility of the foundation on the plate is assumed to be a 2 Kg mass at 475 Hz then the magnitude of the mobility, given by  $1/M\omega$ , is  $1.7 \times 10^{-4}$  (MKS). Recalculating the radiation efficiency gives  $\sigma_{rad} \approx 3 \times 10^{-6}$ . These values can be used to check the results of the boundary element model of the plate.

Another check on the model can be made from comparing the radiation efficiency calculated by the boundary element program to that measured in the experiment. By measuring  $\Pi_{rad}$  and  $\langle v_p^2 \rangle$ ,  $\sigma_{rad}$  can be calculated by:

$$\sigma_{rad} = \frac{\Pi_{rad}}{A_p \rho_f c \langle v_p^2 \rangle} \quad (2.52)$$



## 2.6.2 Average Modal Separation

A check on the modal analysis of the plate by the finite element program can be done by doing simple calculations of the expected average modal density and average modal separation of the plate. In [6] the average modal density of a plate as a function of frequency ( $n(f)$ ) is:

$$n(f) = \frac{A_p}{2\kappa c_l} \quad (2.53)$$

and the average modal separation ( $\delta\bar{f}$ ) is:

$$\delta\bar{f} = \frac{2\kappa c_l}{A_p} \quad (2.54)$$

For a .25 inch thick steel plate with  $A_p = 1.43 \text{ m}^2$ ,  $n(f) = 0.0765 \text{ modes/Hz}$  and  $\delta\bar{f} =$

13.1 Hz/mode.



## 2.7 Variable Listing

### Section 2.1

$[M]$	Mass matrix
$[K]$	Stiffness matrix
$\{u\}$	Displacement vector
$\{\ddot{u}\}$	Acceleration vector
$\{0\}$	Zero vector
$\omega$	Radian frequency (radians/second)
$\{X^{(i)}\}$	Mode shape for the $i^{\text{th}}$ mode
$\{F(t)\}$	Force vector
$q_i(t)$	Modal participation coefficient for the $i^{\text{th}}$ mode
$[I]$	Identity matrix
$[\omega^2]$	Diagonal matrix of eigenvalues
$\{Q(t)\}$	Generalized force vector
$\xi_i$	Damping ratio for the $i^{\text{th}}$ mode
$u$	Displacement in the x direction
$v$	Displacement in the y direction
$w$	Displacement in the z direction
$\{\alpha\}$	Vector of generalized coordinates
$[\Phi]$	Matrix of polynomial terms in x, y, and z
$\{\epsilon\}$	Strain vector





[E]	Strain-Displacement relationship matrix
{ $\tau$ }	Stress vector
$\epsilon_{xx}$	$= \frac{\partial u}{\partial x}$
$\epsilon_{yy}$	$= \frac{\partial v}{\partial y}$
$\gamma_{xy}$	$= \frac{\partial u}{\partial y} + \frac{\partial v}{\partial x}$
$\kappa_{xx}$	$= -\frac{\partial^2 w}{\partial x^2}$
$\kappa_{yy}$	$= -\frac{\partial^2 w}{\partial y^2}$
$\kappa_{xy}$	$= 2\frac{\partial^2 w}{\partial x \partial y}$
[C]	Elasticity matrix
E	Young's modulus
$\nu$	Poisson's ratio
$h$	Plate thickness

## Section 2.2

S	Arbitrary surface in an acoustic medium
Q	Arbitrary point on the surface S
P	Arbitrary point
$p$	Acoustic pressure
$v$	Velocity
$\nabla^2$	Laplacian operator $= \frac{\partial^2}{\partial x^2} + \frac{\partial^2}{\partial y^2} + \frac{\partial^2}{\partial z^2}$
$G(P,Q)$	Free surface Green's function $G(P,Q) = \frac{e^{-ikR(P,Q)}}{R(P,Q)}$
$G'(P,Q)$	Normal gradient of the Green's function at Q



R	$ P-Q $
k	Wave number ( $\frac{\omega}{c}$ )
c	Speed of sound
$z_0$	Characteristic impedance of the medium
C(P)	$= 0$ , for P in the body $= 4\pi$ , for P in the medium $= 2\pi$ , for P on S
	For P at an edge or corner of S, C(P) has a different value which is a function of the local geometry.
	$C(P) = 4\pi + \int_S \frac{\partial}{\partial \eta} \left\{ \frac{1}{R(P,Q)} \right\} dS(Q)$
$\eta$	Unit normal on S out of the body
W	Power

### Section 2.3

$k_b$	Wave number of plate flexural waves
$\lambda_b$	Wave length of plate flexural waves
$\kappa$	Radius of gyration of a plate $\frac{h}{2\sqrt{3}}$
$h$	Plate thickness
D	Flexural rigidity $Eh^3/12(1-\nu^2)$
E	Young's modulus
$\nu$	Poisson's ratio



$\rho_s$	Area density of a plate
$\rho_f$	Density of the acoustic medium
$k$	acoustic wave number

## Section 2.4

$N(\omega)$	Number of acoustic modes in an enclosure at $\omega$
$V$	Volume of the enclosure
$n(\omega)$	Modal density of the enclosure at $\omega$
$\delta\bar{f}$	Modal separation in the enclosure at $\omega$
$f$	Cyclic frequency (cycles/second)
$\langle E_M \rangle$	Average energy of the $M^{\text{th}}$ mode
$\langle p_M^2 \rangle_{r,t}$	Spatial and time average pressure squared of the $M^{\text{th}}$ mode
$\rho_f$	Density of the acoustic medium
$\alpha$	absorption coefficient
$T_R$	Reverberation time
$v$	collision rate
$S$	Total surface area of all walls in an enclosure
$\Pi_s$	Radiated sound power from a source
$E_R$	Energy in the reverberant field



## Section 2.6

$f_c$	Critical frequency
$c$	Speed of sound in the acoustic medium
$\kappa$	Radius of gyration of a plate $= \frac{h}{2\sqrt{3}}$
$c_l$	Speed of longitudinal wave (5100 m/sec)
$p_{rad}$	Radiated pressure
$l_s$	Point force
$\rho_f$	Density of the acoustic medium
$\rho_s$	Area density of plate
$r$	Distance from the plate in the acoustic medium
$Y_m$	Mobility of obstruction on plate
$G_p$	Drive point conductance of plate $= 1/8\rho_s\kappa c_l$
$\Pi_{rad}$	Radiated power
$\sigma_{rad}$	Radiation efficiency
$A_p$	Area of plate
$n(f)$	Average modal density of a plate
$h$	Plate Thickness
$\delta\bar{f}$	Average modal separation of a plate





### 3 EXPERIMENTAL MODEL

#### 3.1 Model Structure

The model was constructed to closely model a section of a ships hull with an attached foundation. This model was used previously in [3]. In [2], foundations of various impedance levels were modeled using a series of pipes from .313" OD x .25" ID to 1.0" OD x .75" ID. The smaller pipes modeled foundations of small pumps and auxiliary equipment and the larger pipes modeled larger ship board equipment such as main propulsion elements and turbine generators. The model used in this research is more representative of actual machine foundations with higher modal density and attachment to the hull at more than one point.

The foundation model consists of a four legged pipe frame with each leg joined by a cross member to form a box like structure. Each of the sides is varied in length to avoid symmetrical resonant frequencies. The pipe is 1/2 inch schedule 80 steel pipe welded at the joints with each leg tapped to allow for bolting to the steel plate. The hull is modelled with a 48" x 48", .25" thick steel plate. The corners of the plate are cut at odd angles to reduce symmetry to more closely model an actual hull.

To allow the model to float on water the model was given wooden sides. Four 1 X 6 inch boards were cut to length and fastened to the model edges with wood screws and glue. The joints were treated with water proof caulking to provide additional watertight integrity. This arrangement proved to be satisfactory with the model



floating in water with three inches of freeboard.

The complete model weighs about 300 pounds, so four lifting lugs were added for hoisting the model.

Drawings of the model are shown in Figures [1] and [2].

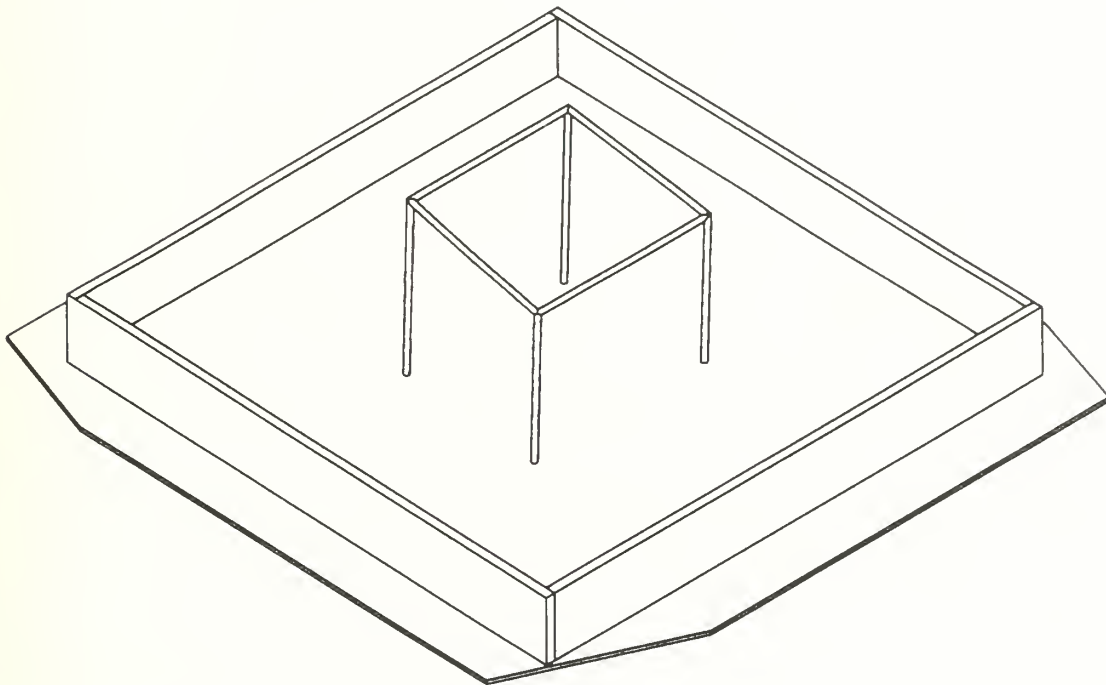


Figure 1. Model Isometric View



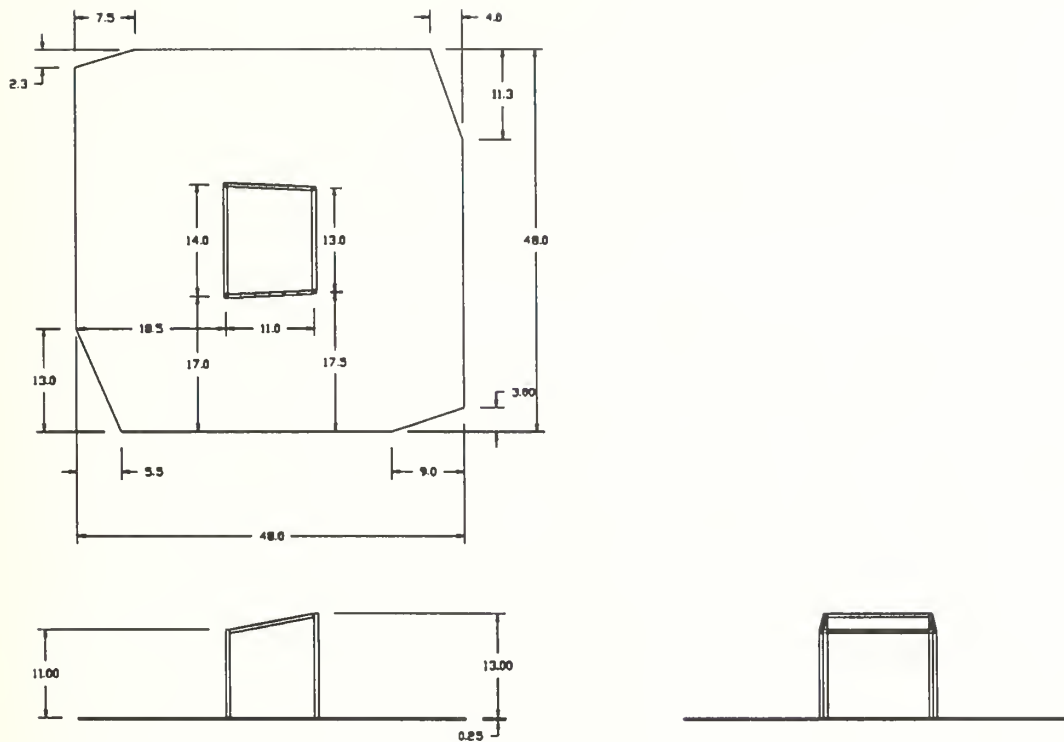


Figure 2. Hull and Foundation Model (Dimensions in Inches)

### 3.2 Damping

The model structure has a natural damping loss factor of only about .2% in the frequency range 0 - 2500 Hz, whereas actual ship structures would be expected to have damping loss factors of the order of 2%. To increase the damping of the structure damping material was added in [3]. This treatment consisted of .070 inch thick viscoelastic damping material (TEC Damping Sheet by Eckel Industries Inc.)



glued to the surface of the plate. Epoxied to the viscoelastic material was 1/32 inch thick stainless steel sheet to allow for shear loading. A portion of the damping material had been removed from the model and was reapplied. After modification the damping consisted of a 10 inch thick band around the perimeter of the plate between the wooden sides and the foundation mounting holes.

To confirm the value of the damping loss factor the damping of the waterborne model was measured in 1/3 octave bands from 200 Hz to 1000 Hz. The integrated impact method for determining damping loss factor of [16] was used. The vibration amplitude decay with time was measured and the decay rate (DR) determined. Measuring DR on a plot of Amplitude versus Time is difficult and may lead to erroneous results. In [16] it is shown that the area under the amplitude squared curve decays at the same rate as the amplitude, so the area under the amplitude squared curve is plotted versus time and the slope of this curve is the decay rate. Decay rate from this method is less prone to errors and is easy to produce. In [2] a computer program was written using the TSL2 language of the General Radio 2515 multichannel analyzer to compute and plot this curve. Using this analyzer and computer program the damping loss factor of the structure in water was measured.

Figure [3] shows the experimental setup used for the damping measurements. With the GenRad 2515 multichannel analyzer a Wilcoxon Research model 408M accelerometer was used with an ENDEVCO 2721B charge amplifier. With the model floating in the water it was impacted with a hammer and the decay of the vibrations





recorded on the analyzer. The record was input into the computer program and the amplitude decay and amplitude squared integration displayed and plotted. The plots obtained are included in Appendix [A].

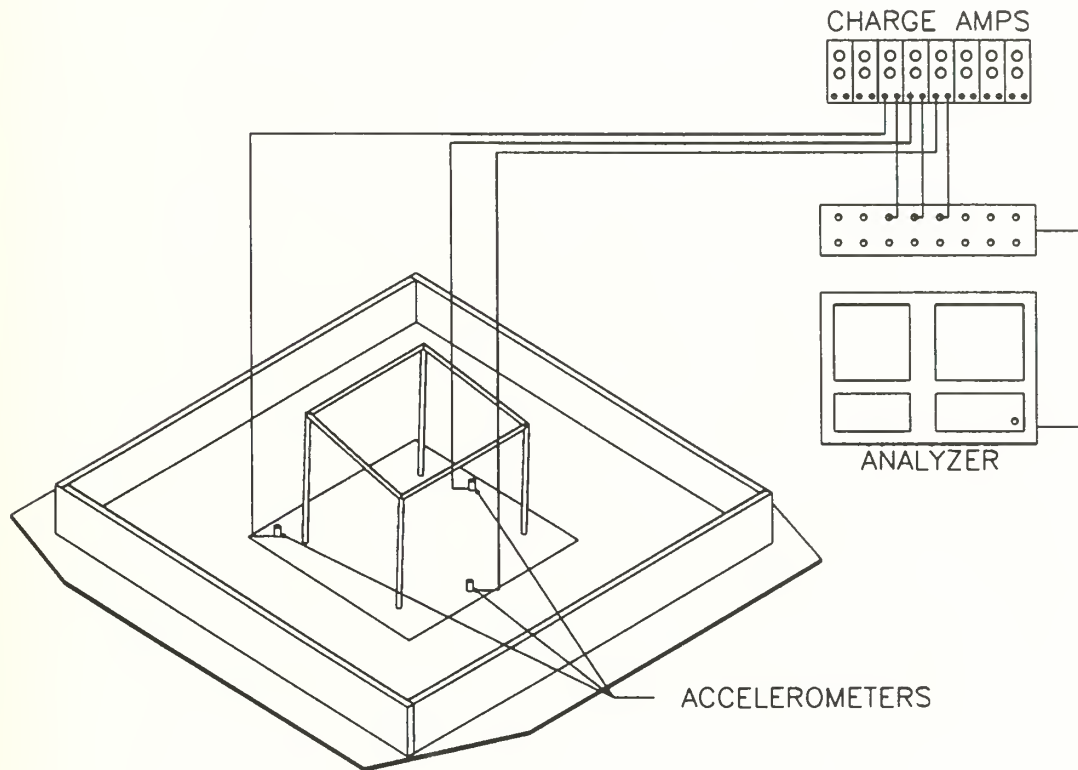


Figure 3. Model Instrumentation for Damping Measurements



From [6] the decay rate ( $DR$ ) in terms of loss factor ( $\eta$ ) and frequency ( $f$ ) is:

$$\eta = \frac{DR}{27.3f} \quad (3.1)$$

Table [1] summarizes the damping loss factors measured for the model in water.

1/3 Octave Band (Hz)	$DR$ (dB/sec)	$T_R$ (sec)	$\eta$
200	140	0.43	0.026
250	190	0.32	0.028
315	200	0.30	0.023
400	240	0.25	0.022
500	330	0.18	0.024
630	330	0.18	0.019
800	350	0.17	0.016
1000	330	0.18	0.012

Table 1. Model Damping Loss Factors

### 3.3 Reverberant Water Tank

To make vibration and sound pressure level measurements the reverberant water tank at Bolt, Beranek and Newman INC. was used. The construction of the tank is



such that no two walls are parallel, the modal density of the tank is increased, and hence the tank supports resonant modes with close spacing in frequency. The tank walls have a radiation absorption coefficient of .05.

The dimensions of the tank are shown in Figure [4]. At a given frequency the number of modes in the tank, the modal density, and the modal separation can be approximated by equations (2.32), (2.33), and (2.34). These are listed in Table [2] for 400 and 600 Hz.

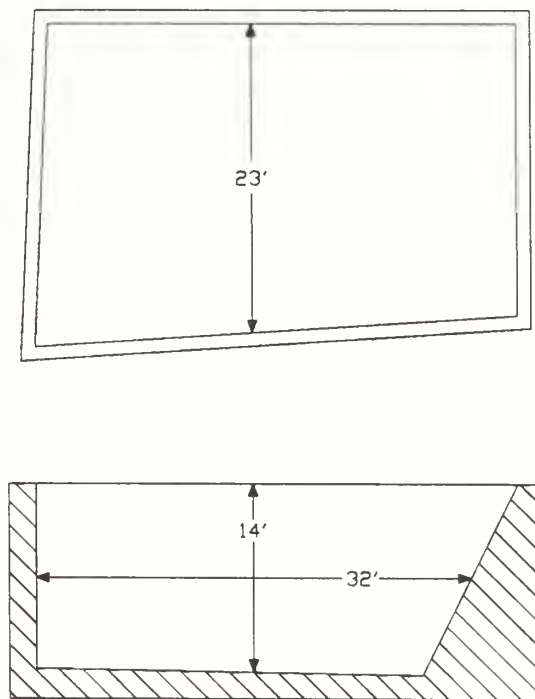


Figure 4. BBN Reverberant Sound Tank



Frequency (Hz)	$N(\omega)$	$n(\omega)$	$\delta\bar{f}$
400	24	0.029	34
600	81	0.065	16

Table [2] Reverberant Sound Tank Data

The frequency of the  $M^{\text{th}}$  mode of the tank is calculated from equation (2.35). Using the average dimensions in each direction for the tank, 32 feet long 23 feet wide and 14 feet deep, and a mode number of 1 the lowest mode supported in the tank can be estimated. Using these numbers  $f_1=217$  Hz and the useful range of the tank as a reverberant tank has a lower limit set by BBN at the 1/3 octave band centered at 315 Hz.

The reverberation time for the tank was obtained from BBN, and 1/3 octave bands of interest are listed in Table [3]. The measurements were obtained for the tank without the model, but because the model dimensions are small compared to the tank the error in the reverberation time is slight.





1/3 Octave Band (Hz)	$T_R$ (sec)
315	0.192
400	0.199
500	0.202
630	0.270
800	0.268
1000	0.383

Table 3. Water Tank Reverberation Times



## 4 COMPUTATIONAL MODEL

### 4.1 Finite Element Program Description

The finite element program used for this research is ALGOR, from ALGOR Interactive Systems INC. of Pittsburgh, Pennsylvania. The program is a general purpose finite element program that can be run on a personal computer with a 80386 microprocessor and a math coprocessor with at least 20 megabytes of memory. This research required the use of the modal analysis program, SSAP1H, and frequency response program, SSAP5H. The program also has a model generation CAD program that was used to construct the model, and a post processing viewing program to observe the displaced shape of the structure at each modal frequency. A complete description of the ALGOR programs can be found in [5].

### 4.2 Finite Element Model

The finite element model was constructed of 228 two dimensional shell/plate elements that modeled the 1/4 inch steel plate and 80 beam elements that modeled the 1/2 inch diameter schedule 80 steel pipe foundation. To give accurate results the model was made of enough elements so that there are at least six plate elements per wavelength in any linear direction along the plate or beams. The model will accurately model up to three flexural wave lengths in any direction. The model is



shown in Figure [5].

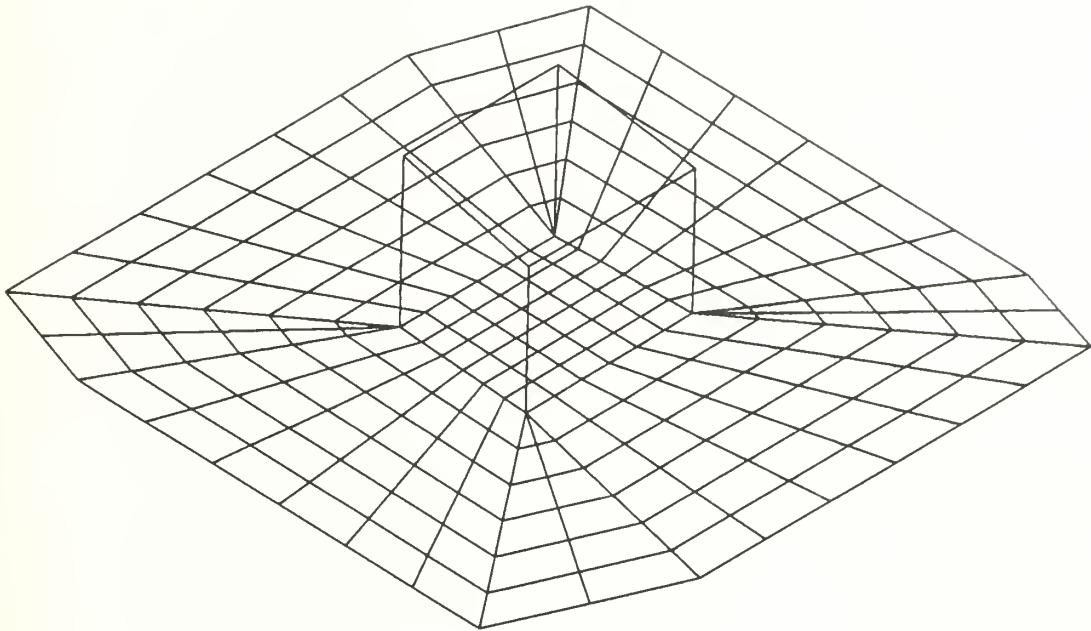


Figure 5. Finite Element Model

#### 4.2.1 Plate Element

A plate element consists of four nodes with 5 degrees of freedom at each node (three translational degrees and two rotational degrees, the rotation in the plane of the element is fixed). The location of each node is specified by its three global coordinates relative to a global frame of reference. Each four nodes that



make up an element are specified by a connectivity table. The table contains one entry for each element, the nodes that make it up and the plate thickness. From the nodal locations and connectivity table the geometry of the model is determined. The material properties of the plate specified are the modulus of elasticity ( $E$ ), Poisson's ratio ( $\nu$ ) and density ( $\rho$ ). From these values a mass matrix and a stiffness matrix are formed.

#### 4.2.2 Beam Element

A beam element consists of three nodes, two nodes define the ends of the beam and a third node is needed to define the orientation so the cross sectional areas and moments of inertia are interpreted correctly. The location of each node is specified by its global coordinates in a global frame of reference. To define the stiffness matrix of the beam elements the following properties are needed: the cross sectional area ( $A$ ), the shear area with respect to the local vertical and horizontal axes ( $S_2$  and  $S_3$ ), the moments of inertia about the local vertical and horizontal axes ( $I_2$  and  $I_3$ ), and the polar moment of inertia about an axis perpendicular to the plane of the cross sectional area through the centroid ( $J_1$ ). The material properties specified are  $E$ ,  $\nu$ , and  $\rho$ . With this data mass and stiffness matrices can be formed.





### 4.2.3 Composite Model

The dimensions of the model are those of the actual plate and pipe frame foundation used in the experimental model. The physical parameters used are listed in Table [4], and the model dimensions are shown in Figure [2].

Beam	
A	0.32 in <sup>2</sup>
S <sub>1</sub>	0.048 in <sup>2</sup>
S <sub>2</sub>	0.048 in <sup>2</sup>
I <sub>1</sub>	0.02015 in <sup>4</sup>
I <sub>2</sub>	0.0215 in <sup>4</sup>
J <sub>1</sub>	0.04015 in <sup>4</sup>

Plate	
t	0.25 in

Material	
E	30,000,000 psi
v	.3
ρ	.283 lb/in <sup>3</sup>

Table 4. Element and Material Properties

Because the computational model will be compared to the experimental results a .5 lb mass load was added at the foundation corner node 303 to account for the supported weight of the shaker used in the experimental measurements.



#### 4.2.4 Fluid Loading

The model hull and foundation float on the surface of the reverberant sound tank for taking measurements. The added mass effect of the fluid will effect the wave number of the elastic waves in the plate. The wave number of the plate modified by the fluid loading is calculated by iterating equation (2.31). The loaded plate wave numbers for selected frequencies are shown in Table [5].

Frequency (Hz)	Free Plate Wave Number (in <sup>-1</sup> )	Loaded Plate Wave Number (in <sup>-1</sup> )
400	1.76	1.91
425	1.81	1.96
450	1.86	2.02
475	1.91	2.07
500	1.95	2.12
525	2.00	2.17
550	2.04	2.22
575	2.09	2.27
600	2.13	2.31

Table 5. Wave Number For Fluid Loaded and Free Plates

For the finite element analysis this approximate approach was used to account for the fluid loading of the plate. To each plate node a mass load was



added. The amount of mass added was determined by averaging the area of the plate elements surrounding the node and multiplying by the thickness of the fluid layer,  $\lambda_v/2\pi$ , and  $\rho_f$ .

The added mass varies with the frequency so a mean frequency in the frequency band of interest was chosen as an approximation. The mass loading used in the finite element model was for 475 Hz giving a loaded plate wave number of  $2.07 \text{ in}^{-1}$  and a fluid layer .48 inches thick. The added mass values for the plate nodes can be seen in the finite element program input file included in Appendix [B].

### 4.3 Boundary Element Program Description

The boundary element program used is BEMAP version 2.43, [17], developed for prediction of acoustic fields by Spectronics INC. of Lexington, Kentucky. The program is a general purpose boundary element program and can be used to solve both interior and exterior radiation problems. The acoustic space can be defined as infinite or semi-infinite with a plane boundary described as pressure release or perfectly reflective. Also, the radiating body can be located anywhere with respect to a semi-infinite plane including being part of the plane, where the plane is considered a baffle. The program can be run on a personal computer with a 80386 microprocessor and a 80387 math coprocessor. It has no interactive interface like the finite element



program so the model is defined by inputting the node locations and connectivity. The boundary element model was constructed using the finite element model nodal coordinates so they would be compatible.

#### 4.4 Boundary Element Model

The boundary element model is constructed of curvilinear quadrilateral and/or triangular elements. Quadratic elements are constructed of three nodes per side for a total of eight nodes in each element. The triangle element also has eight nodes but one of the sides is collapsed to a point so that one point has three local node numbers associated with it. Each quadrilateral is mapped onto a square and each triangular element is mapped to an equilateral triangle. The mapping approximates the cartesian coordinates of the elements in terms of quadratic or linear shape functions that are intrinsic to the boundary element program. The specified variables on the boundary are also approximated in terms of these shape functions.

Each node is located with three orthogonal coordinates in an arbitrarily established global coordinate system. To establish the geometry of the elements a connectivity table is used where each element is given a number and local node numbers are correlated to the global node numbers. The node and element numbering is shown in the BEM input file included as Appendix [C].

The node and element numbering are different between the finite element program and the boundary element program. To facilitate the ease of file transfer a





fortran program was written to convert the finite element frequency response output to the boundary element program input file. This program is included and made available for the use of others in Appendix [D]. The finite element node numbering is converted to the boundary element numbering. To do this some nodes in the finite element model are not used so the finite element model plate has 241 nodes and 228 elements and the boundary element model has 184 nodes and 57 elements. This is illustrated in Figure [6].

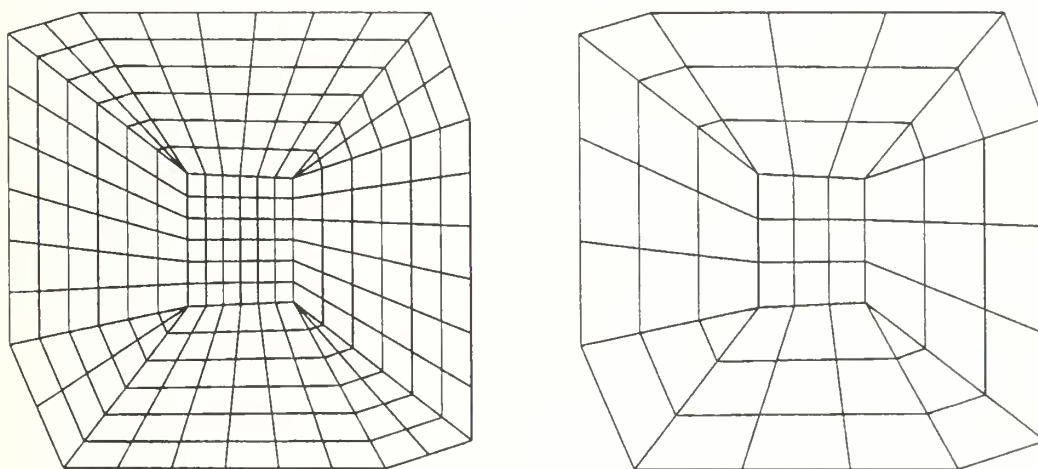


Figure 6. Finite Element Plate Model (Left), Boundary Element Plate Model (Right).

The finite element frequency response program output is displacement amplitude and phase at each node. This is converted to velocity amplitude and phase at the boundary element model nodes for input as the boundary conditions using equations (4.1) and (4.2).



$$u = D e^{i\omega x + \phi} \quad (4.1)$$

$$v = \frac{\partial u}{\partial t} = i\omega D e^{i\omega x + \phi} \quad (4.2)$$

The boundary element program treats the steel plate as a vibrating surface in an infinite baffle. The plane of the water surface is specified as the baffle with the steel plate set into it. A pressure release boundary condition is specified for the baffle. The other constants of the problem specified in the boundary element program are: Speed of sound = 58320 inches/second and density of the acoustic medium = .0361 lb/in<sup>3</sup>. To be consistent with the finite element program the units remain in inches, pounds, and seconds and the results are converted to watts.



## 5 COMPUTER ANALYSIS AND RESULTS

### 5.1 Computer Analysis

The computer analysis was run on an IBM P/S2 model 70, which has a 80386 microprocessor, 80387 math coprocessor, 4 Megabytes of RAM, and a 80 Megabyte hard drive. On the average the modal analysis up to 600 Hz took 13 hours computer time, the frequency response analysis for 50 frequencies took 4 hours computer time, and the boundary element program took 18 hours for 50 frequencies.

The finite element program was used to predict the mode shapes and resonance frequencies of the foundation alone. Both clamped and simply supported boundary conditions were evaluated to attempt to bracket the actual boundary condition of the foundation mounting onto the plate. The results are displayed in Figures [7] and [8].



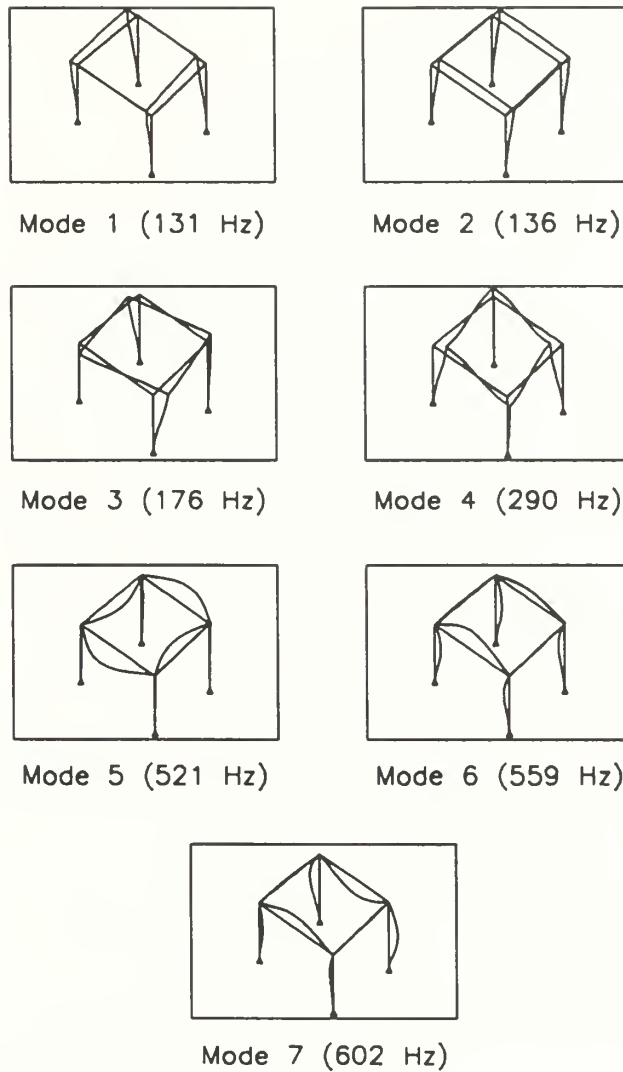


Figure 7. Foundation Model Mode Shapes With Clamped Ends

Once the foundation mode shapes were established the composite model with the foundation attached to the plate was analyzed. The general steps followed in the course of the computer analysis are outlined in the following list.





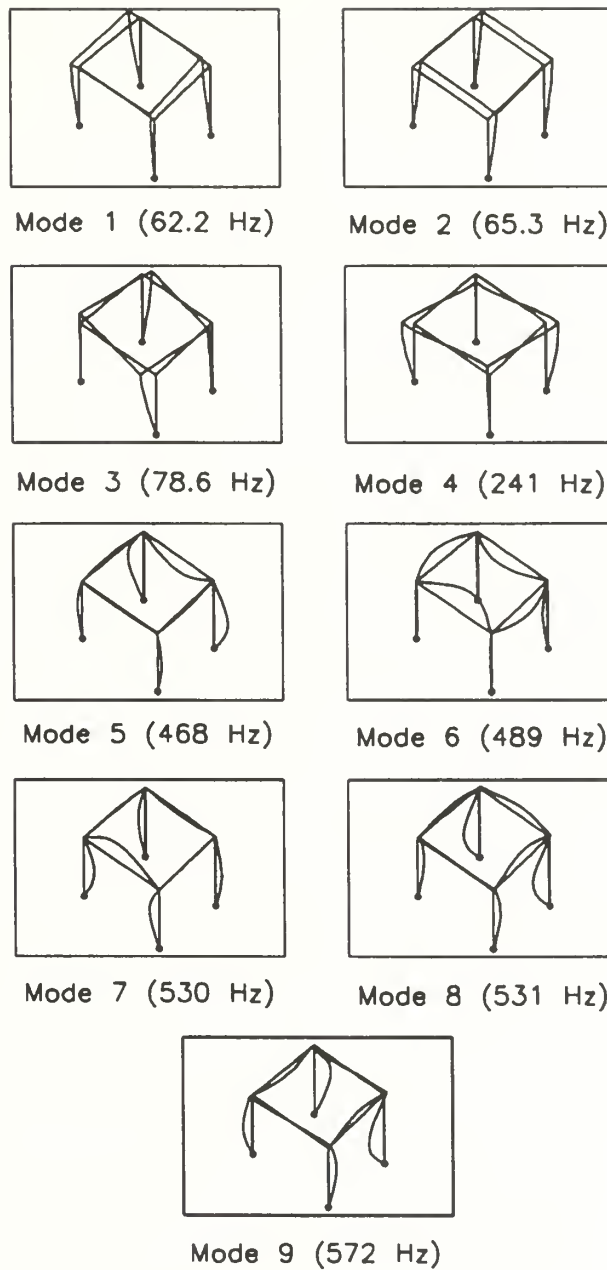


Figure 8. Foundation Model Mode Shapes with Simply Supported Ends



1. Construct finite element model as described in section 4.2.
2. Add discrete mass to each node to model fluid loading as calculated in section 4.2.4.
3. Add discrete mass to foundation to model shaker mounting.
4. Solve for mode shapes and resonant frequencies up to 600 Hz.
5. Solve for the nodal displacement and phase for the plate nodes for the structure subject to sinusoidal forcing at a series of selected frequencies using the frequency response program.
6. Convert the finite element program geometry and frequency response program output into the boundary element program input file.
7. Solve for the radiated power at each frequency in the series using the boundary element program.

An example finite element modal analysis program input file for the plate and foundation model as constructed in the previous section is included as Appendix [B].

The modal analysis resulted in 79 modes from 0 - 600 Hz including 6 rigid body modes. The resonant frequencies are listed in Appendix [E]. A foundation mode of the model was identified by examining the mode shapes in the frequency band from 400 to 600 Hz. A foundation mode is characterized by mostly foundation motion and little plate motion. Figure [9] displays the 66<sup>th</sup> mode shape at a resonant frequency of 490 Hz. This figure displays the mode shape superimposed on the undisturbed model, note that the plate shows almost no motion while the foundation has large



displacements (the displacements calculated in the finite element model are scaled up significantly to show the relative displacement). This mode shape is similar to mode # 5 (521 Hz) in the foundation model with clamped ends and mode # 6 (489 Hz) in the foundation model with simply supported ends.

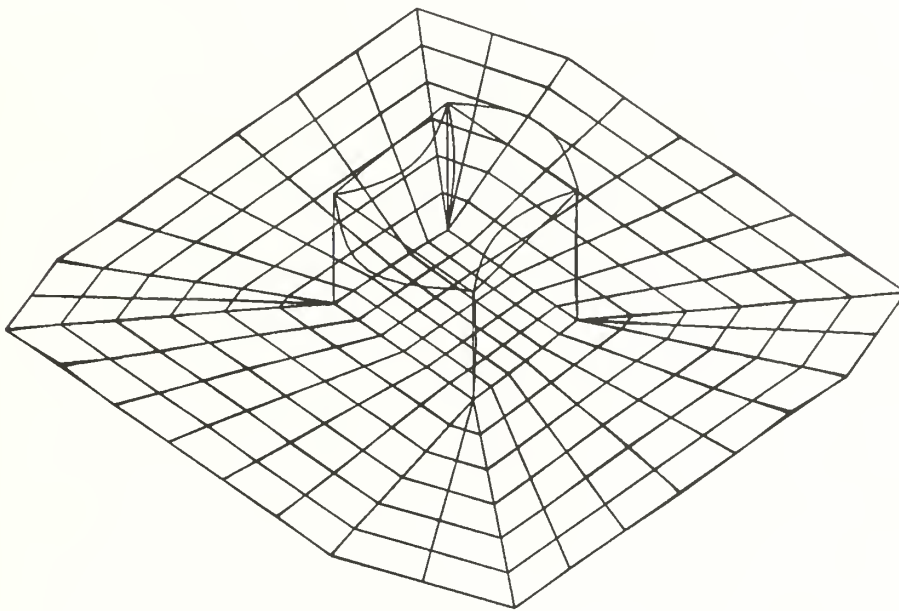


Figure 9. Foundation Mode at 490 Hz

A plate mode was also identified by examining the mode shapes. Figure [10] displays the 63<sup>rd</sup> mode at a resonant frequency of 468 Hz, note the large plate motion compared to relatively little foundation motion.



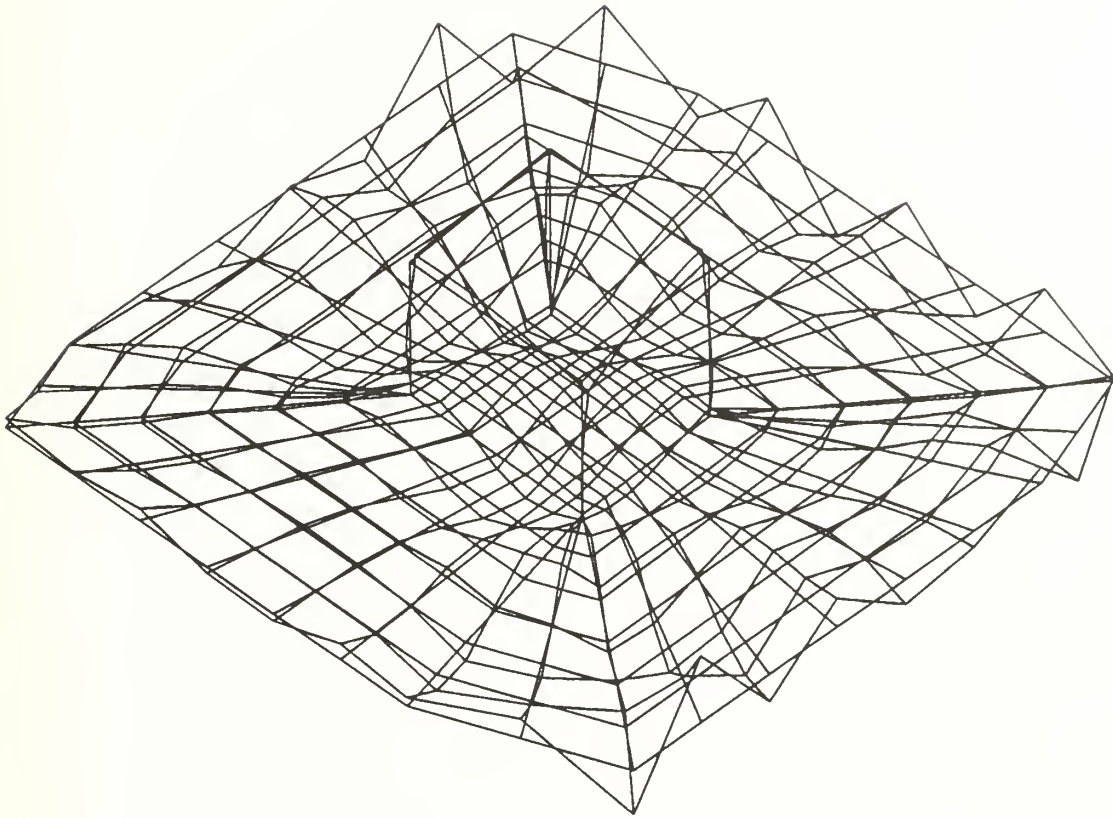


Figure 10. Plate Mode at 468 Hz

The frequency response program from the ALGOR finite element program was run with a force applied to the structure at node number 303 as indicated in Figure [11].





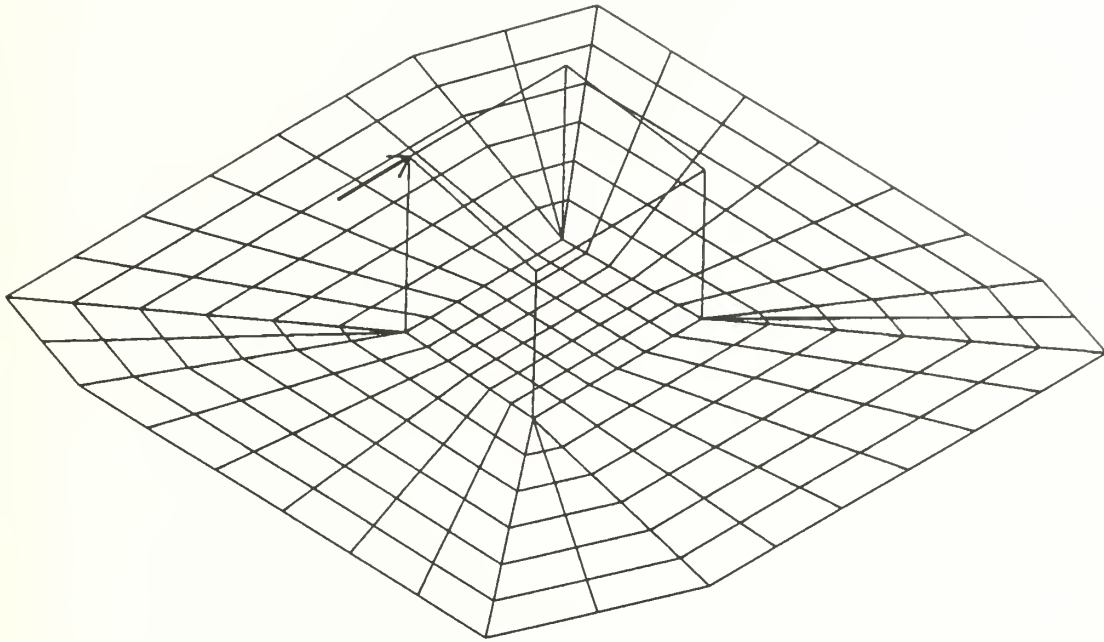


Figure 11. Model Forcing Location

The force amplitude was 1.225 lbs (corresponding to .75 lbs rms force, the rms force from the shaker to be used in the experimental measurements), the damping loss factors measured in chapter 3.2 were input to the program as the modal damping loss factors, and the frequency was stepped in 1 Hz increments from 450Hz to 500 Hz to calculate the response in a 50 Hz band. This band was chosen because the frequency of the foundation mode was 490 Hz and the plate mode 468 Hz. A limit of 50 Hz was selected because of the computation time involved. The frequency response program calculates the displacement amplitude and phase for each node on the plate. This was



edited using the fortran programs in Appendix [D] to form the input file for the boundary element program. The boundary element program calculates pressure, velocity, and intensity at each node on the plate and power radiated by each element. The power is integrated over the plate to give the total radiated power of the plate. The calculated radiated power spectrum for the plate model floating on a semi-infinite water surface is shown in Figure [12].

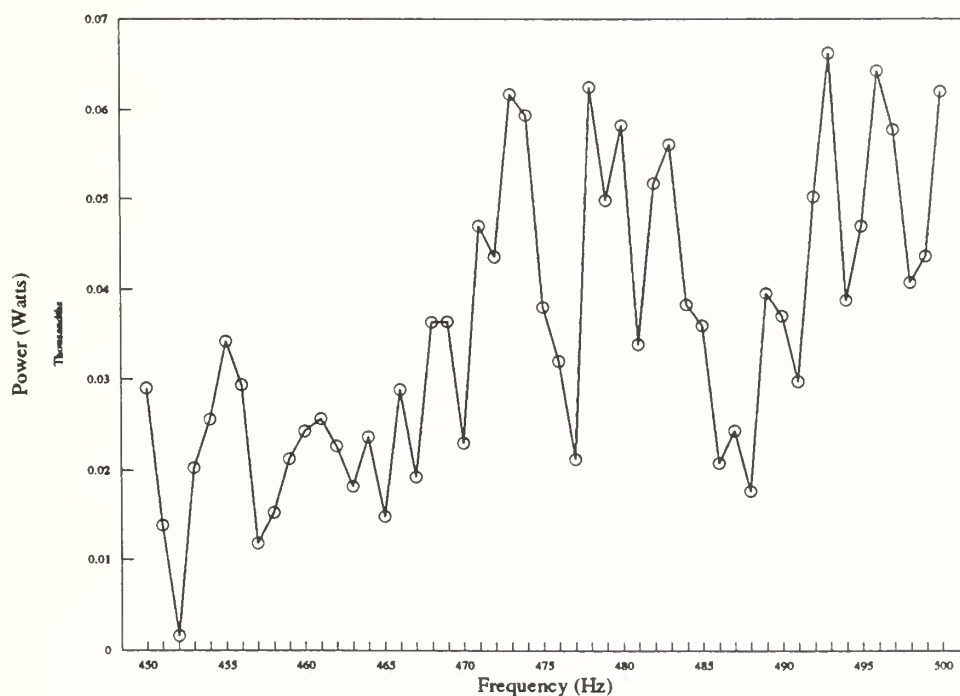


Figure 12 Radiated Power Spectrum for Foundation and Plate Model



Note that there is a significant dip in the radiated power spectrum in the vicinity of the foundation mode frequency probably due to the lack of plate motion in this mode.

To attempt to form a global mode pair by shifting the foundation mode down in frequency mass is added to the foundation. Several different variations were analyzed designated Runs 1 through 5.

- 1 - 0.375 lb weight added to node # 285
- 2 - 0.750 lb weight added to node # 285
- 3 - 1.500 lb weight added to node # 285
- 4 - 0.750 lb weight added to node # 277
- 5 - 2, 0.750 lb weights added to opposite cross  
beams

A depiction of a weight added to node number 285 (the middle of the cross beam) is shown in Figure [13]. Node number 277 is approximately at the 1/4 point on the same cross beam, and in run 5 an additional weight was added to the opposite beam to that shown in the figure. The procedural steps 4 through 7 were repeated with the modified models.



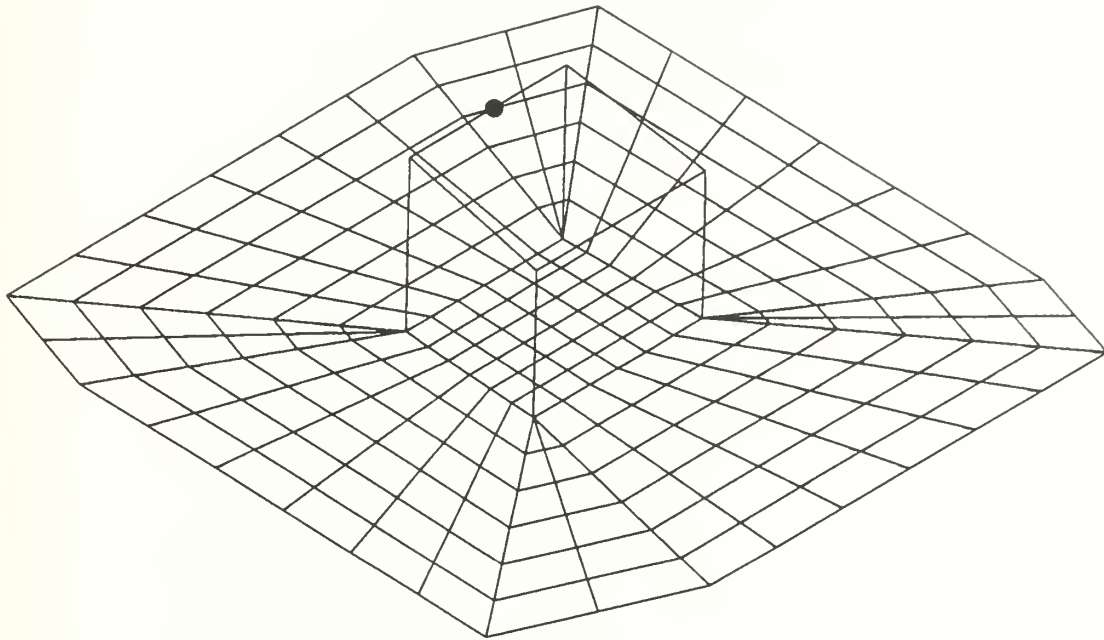


Figure 13. Model With Weight Added to Foundation.

## 5.2 Results

All of the modal frequencies resulting from the modal analyses are listed in Appendix [E]. The frequencies between 450 Hz and 500 Hz are tabulated in Table [6] with a brief description of their mode shape. (A mode shape designated "foundation"





has foundation motion with insignificant plate motion, a mode shape designated "plate" has plate motion with insignificant foundation motion , and a mode shape designated "both" has significant motion in both the foundation and plate.)

Run	Freq. (Hz)	Shape	Run	Freq. (Hz)	Shape
0	452	Both	3	452	Both
	459	Both		458	Both
	468	-Plate-		468	-Plate-
	477	Both		471	Foundation
	485	Both		477	Both
	490	Foundation		485	Both
	497	Both		497	Both
1	451	Both	4	452	Both
	460	Both		459	Both
	468	-Plate-		468	-Plate-
	477	Both		477	Both
	484	Both		485	Both
	486	Both		489	Foundation
	497	Both		497	Both
2	455	Both	5	451	Both
	467	Both		459	Both
	468	Both		467	Both
	479	Foundation		468	Foundation
	485	Both		477	Both
	490	Both		485	Both
	498	Both		497	Both

Table 6. Modal Analysis Results

In Run # 1 the foundation mode apparently coupled to form what may be a global mode pair at 484 Hz and 486 Hz. Each mode shows both plate and foundation



motion, and the foundation mode seen previously in Run # 0 is no longer evident. The foundation motion in the pair is of the same shape as the Run # 0 foundation mode. Figure [14] shows the apparent global mode pair.

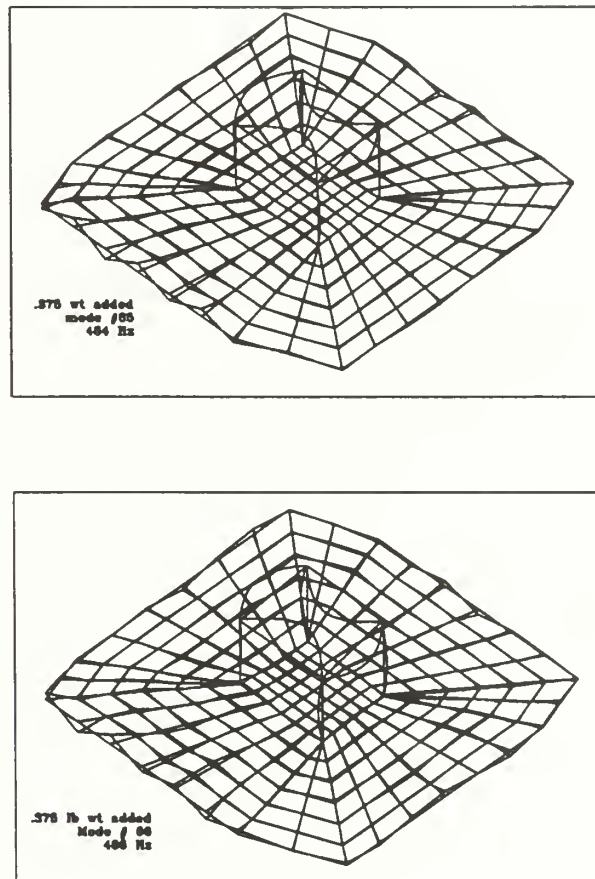


Figure 14. Run # 1 Global Mode Pair

In Run # 2 the foundation mode shifted down in frequency by 11 Hz to 479 Hz. The plate mode seen in Run # 0 at 468 Hz is no longer evident, but there is a mode



pair at 467 Hz and 468 Hz that shows both foundation and plate motion. The foundation motion has a shape similar to the foundation mode from Run # 0. Apparently the frequency of the foundation mode in Run #0 shifted down enough to coupled with the plate mode to form an apparent global mode pair. These mode shapes are shown in Figure [15].

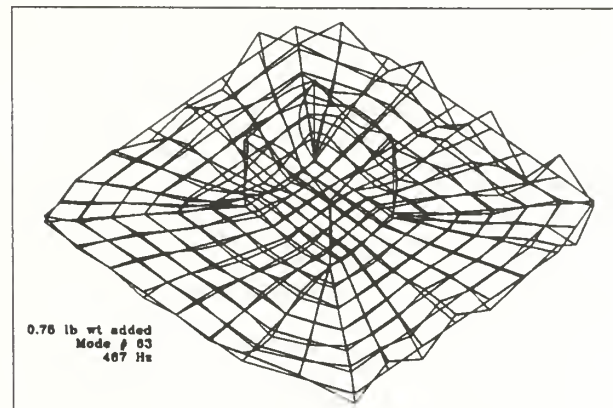
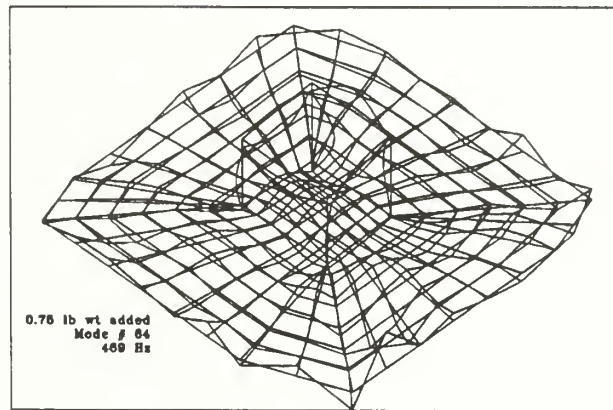


Figure 15. Run # 2 Global Mode Pair



In Run # 3 where the most weight was added to node # 285 the foundation mode shifted by 19 Hz to 471 Hz and the plate mode did not shift remaining at 468 Hz. There seems to be no coupling of these modes as the foundation and plate mode shapes remained as in Run # 0.

In Run # 4 there was little shift in frequency of the foundation mode (1 Hz to 489 Hz) and no other obvious changes to the mode shapes.

In Run # 5 the foundation mode shifted 22 Hz down to 468 Hz, and the plate mode is no longer evident. The mode at 467 Hz apparently is the result of slight coupling between the plate and foundation mode, because the shape of the foundation motion in this mode is the same as the Run # 0 foundation mode. This mode pair appears to be due to weak coupling of the Run # 0 plate and foundation modes, although the foundation mode now at 468 Hz does not show significant plate motion.

The following 5 figures shown the results of the boundary element program radiated power calculations for each of the Runs. The baseline calculated power spectrum of the model without weight added is shown with each spectrum.





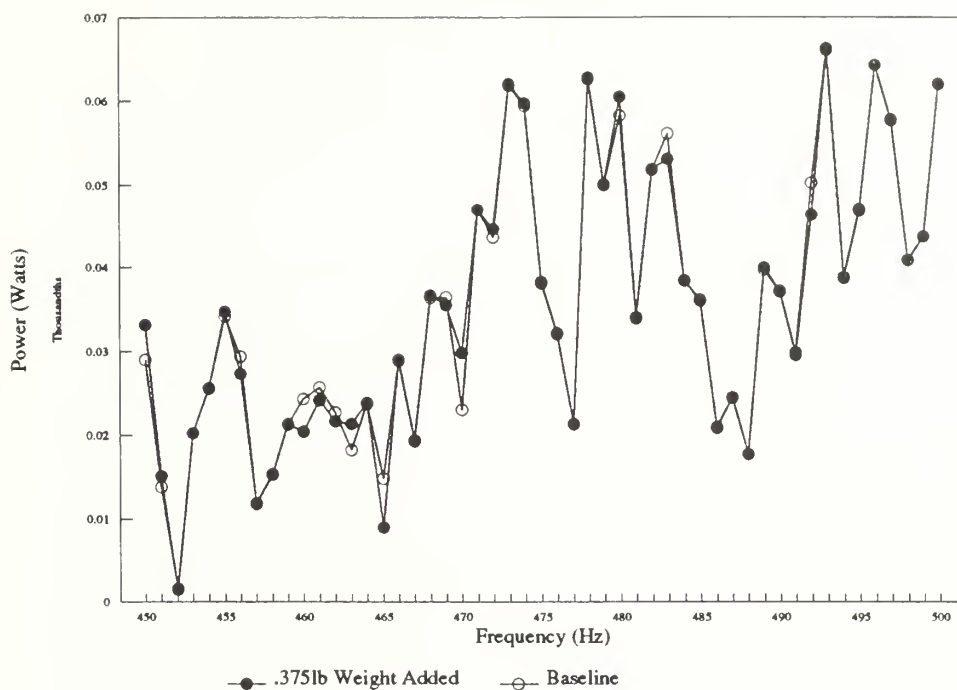


Figure 16. Radiated Power Spectrum for Run # 0 and Run # 1

In Run # 1 the peaks in the calculated power spectrum at 480 Hz and 483 Hz slightly raised and lowered respectively. This change may be due to the coupling of the foundation mode. The mode shapes at 484 Hz and 486 Hz indicate a global mode pair which should result in increased radiated power, but none is evident. Close analysis of the mode shapes shows that plate deflections are small compared to other modes which may account for the lack of radiated power increase. There is also some change in the peaks from 460 Hz to 465 Hz. This is probably due to nonresonant effects since the closest resonant modes are at 458 Hz and 468 Hz.



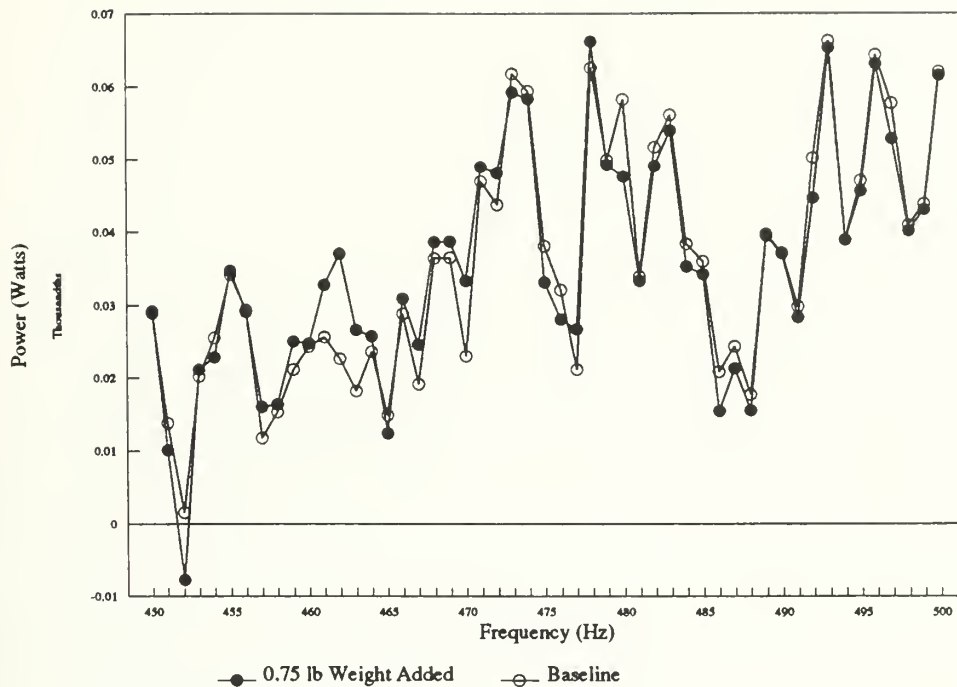


Figure 17. Radiated Power Spectrum for Run # 0 and Run # 2

In Run # 2 the calculated power from 466 Hz to 471 Hz is higher than the calculated power for the unmodified model and at frequencies above 475 Hz the power is generally lower. Run # 2 shows a strong single peak at 462 Hz where Run # 0 had a lower power double peak. The mode shapes indicate a global mode pair at 467 Hz and 468 Hz which correlates to the increase in calculated power. The lower power at frequencies greater than 475 Hz may be due to the uncoupling of the global modes as the foundation mode is shifted down in frequency. The peak at 462 Hz is due to nonresonant effects since the closest resonant frequencies are at 455 Hz and 468 Hz.



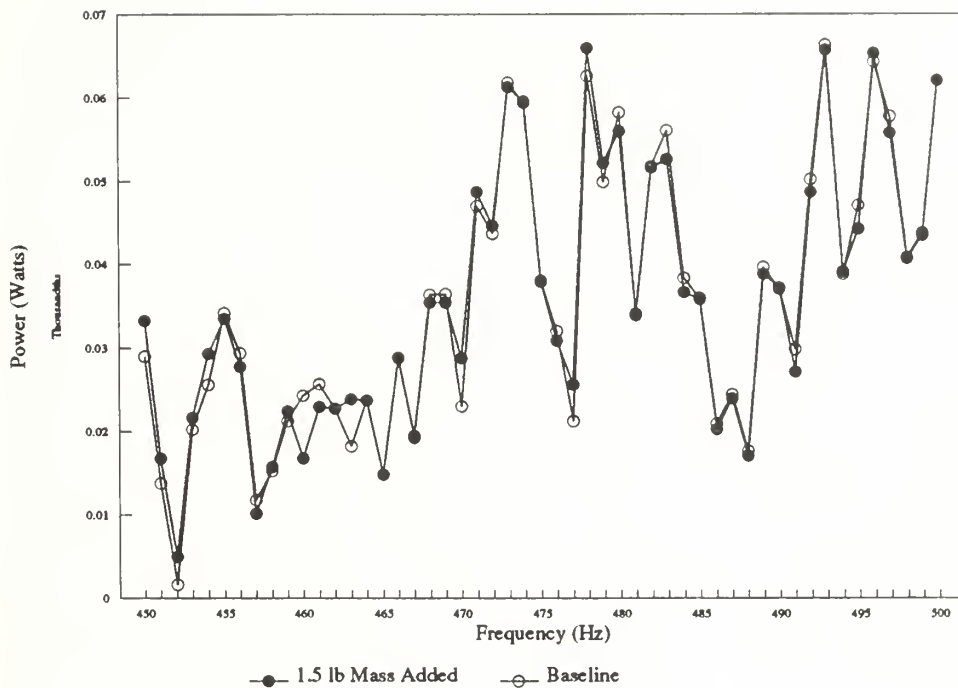


Figure 18. Radiated Power Spectrum for Run # 0 and Run # 3

In Run # 3 the peak at 463 Hz has decreased. The analysis of the mode shapes showed no coupling of the foundation and plate modes, so the extra weight (1.5 lbs) apparently caused the uncoupling of the global mode pair at 467 Hz and 468 Hz that was seen in Run # 2. However, there is still some shifting of the peaks from 460 Hz to 465 Hz due to nonresonant effects. The calculated power spectrum above 485 Hz appears unchanged from the baseline, but the slight change in the peaks from 470 Hz to 485 Hz may be because of the shifting of the foundation mode to 471 Hz.



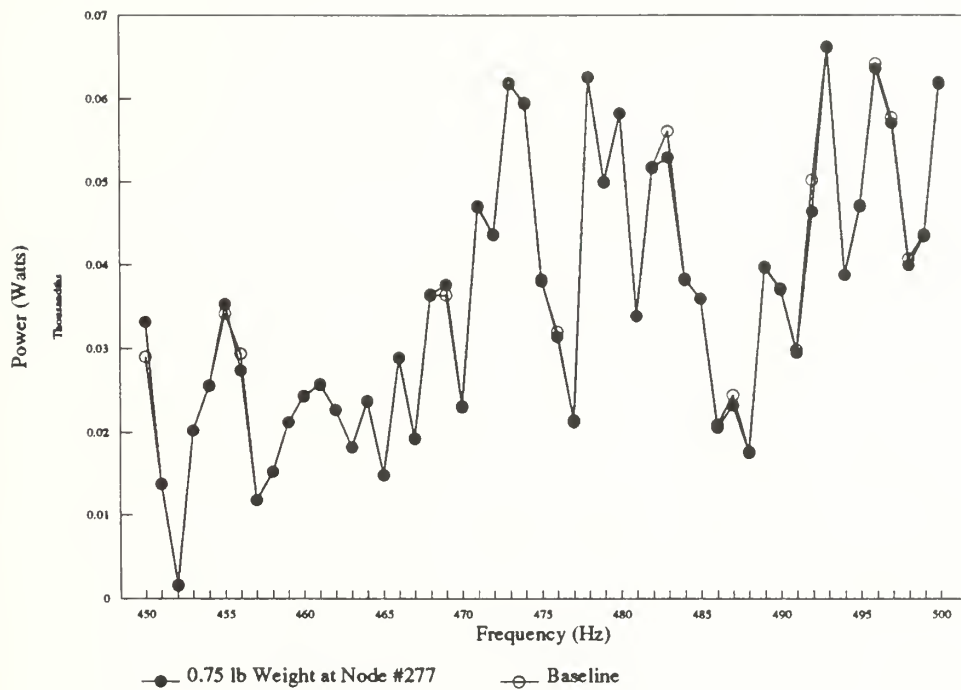


Figure 19. Radiated Power Spectrum for Run # 0 and Run # 4

As expected from the relatively slight frequency shifts from the modal analysis, there is almost no change in the calculated power spectrum for Run # 4. There is only evidence of slight power changes.





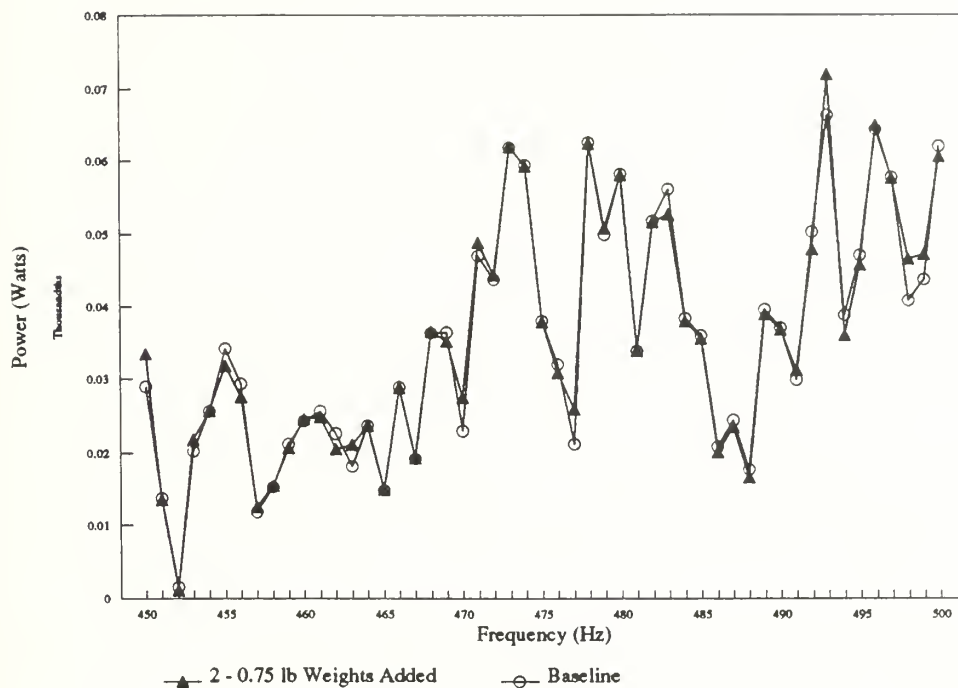


Figure 20. Radiated Power Spectrum for Run # 0 and Run # 5

In Run # 5 the foundation mode is shifted closer to the plate mode than in any other run. The shape of the mode at 467 Hz indicates some coupling with the foundation mode because the displaced shape of the foundation is the same, the calculated power spectrum shows changes in the peaks from 460 Hz to 465 Hz as was seen before when the plate mode from Run # 0 coupled.

In the series of computer calculations the mode shapes generated indicate the possibility of 2 global mode pairs being formed. One from Run # 1 (.375 lb weight added) where the foundation mode of Run # 0 shifted and a global mode pair appears



at 484 Hz and 486 Hz. However, the calculated radiated power does not show an increase in radiated power at the frequency of the pair. The other possible global mode pair occurs in Run # 2 at 467 Hz and 468 Hz. There is an increase in the calculated power from 466 Hz to 471 Hz and a peak in the calculated power at 462 Hz. The 462 Hz peak is due to nonresonant effects possibly involving interaction between the plate and the fluid, diffraction effects, or modal overlap on the plate. In addition to this nonresonant power peak the calculated radiated power spectrum in general shows 14 - 15 peaks in the 450 Hz to 500 Hz band, which is almost double the structural modes in this band. There are nonresonant effects contributing to the calculated radiated sound power which could be masking the expected peaks due to global mode formation.

Diffraction occurs when the sound radiated from a surface has an acoustic wavelength short enough so reflected sound interferes with the radiated sound at some angle from the surface. This results in small side lobes in the radiated sound. Although the intensity of these diffraction lobes is generally only 2% of the main lobes there are pressure variations that occur across the face of the radiating surface that could alter the radiated power. From [18] the frequency where diffraction effects start to occur can be estimated by equating the radiating surface to an equivalent piston. When the acoustic wavelength is shorter than the circumference of the piston diffraction effects can occur. For this plate, 4' x 4', diffraction effects should start occurring at about 390 Hz. A close investigation of the calculated sound intensity



distribution on the plate in Run # 2 shows a significant increase in intensity (about five times the average intensity) at only two locations. These locations are illustrated on the boundary element model in Figure [21].

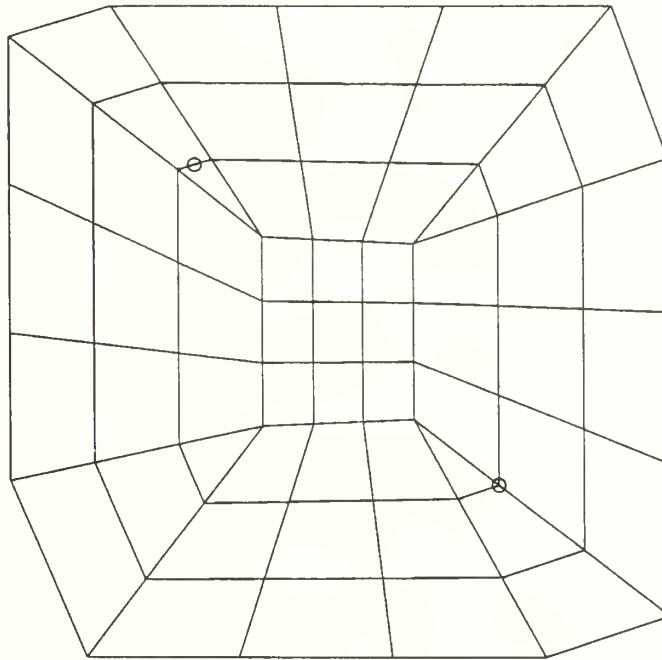


Figure 21. Location of Increased Sound Intensity in Run # 2

This is evidently the primary source of the power peak. Closer scrutinization of the results show that the plate velocity at these locations is not increased significantly over the velocities at other points, but the pressure at these nodes is higher than the average pressure. This gives the indication that the nonresonant peak at 462 Hz could be due to diffraction effects.



Modal overlap occurs when the effective bandwidth of a mode approaches the average frequency separation. When this occurs the effects of individual modes may be masked by the effects of another mode that overlaps it in frequency. The theoretical frequency above which modal overlap occurs in a simple resonator given in [6] is  $2\delta\bar{f}/\pi\eta$ , for a modal separation of 8 Hz and a loss factor of .02 it should occur above 255 Hz, therefore, modal interactions could be causing the greater number of peaks in the calculated radiated power spectrum.

Modal overlap, diffraction effects, and possibly other nonresonant effects occurring in this model (which are discussed in [19]) could be masking the increase in radiated power when a global mode pair is formed.

### 5.3 Validation With Analytical Calculations

In Section 2.6 the analytical calculations for the average modal separation in frequency for a freely vibrating plate were presented. In the computer analysis the average modal separation from 400 to 600 Hz is 8.0 Hz the expected modal separation from equation (2.54) is 13.1 Hz. The computer analysis done in [3] resulted in an average modal separation of 9.8 Hz where the model was not fluid loaded. The increased modal density in the computer model is due to the added stiffness provided by the attached foundation, and the difference from [3] is the result of the added mass fluid loading of the plate. This data gives credibility to the computer modal analysis.





Also in Section 2.6 the radiation efficiency of a plate with a point Attachment was estimated. The boundary element program calculated an average radiation efficiency for the plate with the foundation attached of approximately  $10^{-10}$ . Analytically the predicted radiation efficiency of a plate of the same dimensions with one mass like obstruction of 2 Kg (the mass of one leg of the foundation) was on the order of  $10^{-6}$ . Also, the foundation mode in the composite model is very close in frequency to the simply supported foundation model mode # 6 (489 Hz). This implies that the condition at the junction for the joined model is more like a simple support than fixed support. In Section 2.6 the theoretical reasons for the sound radiation from a plate with an attached foundation are discussed, and the mobility of the foundation is assumed to be mass like. This appears to be a valid assumption based on the type of support.

Further comparisons and validation of the computer analysis will be done with the experimental data in the next section.



## 6 EXPERIMENTAL MEASUREMENTS AND RESULTS

### 6.1 Equipment Setup

The foundation and hull model depicted in Figure [1] is floated on the surface of the reverberant water tank at BBN Inc. to make the radiated sound measurements. The model is instrumented as shown in Figure [22].

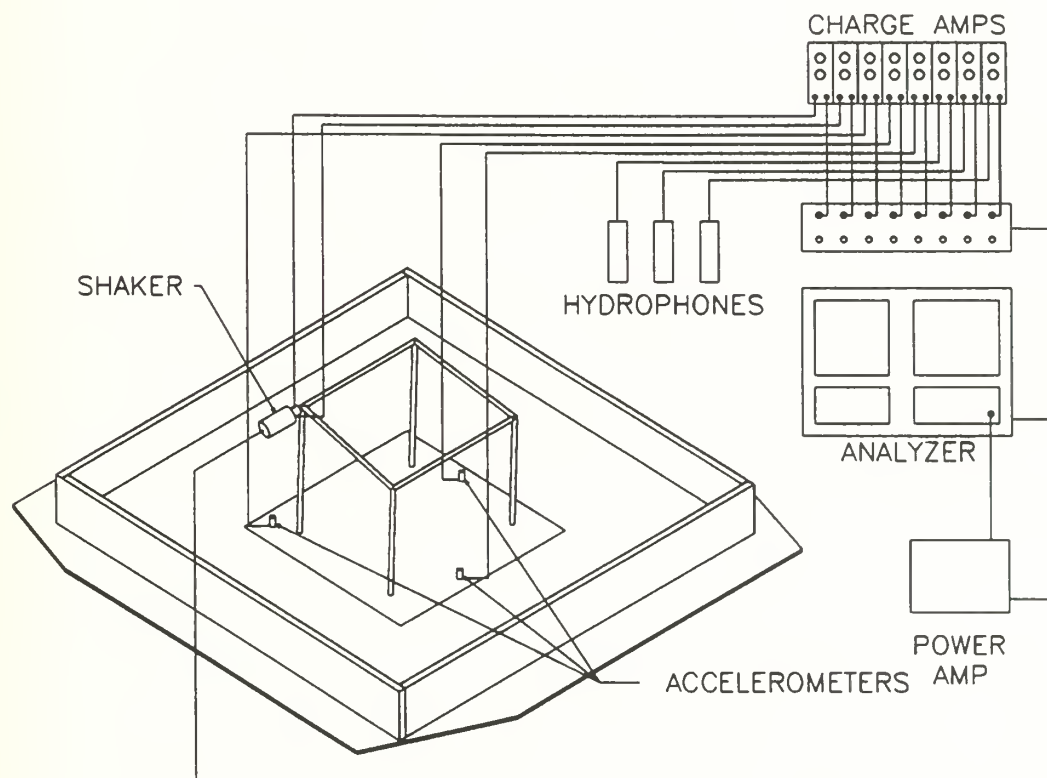


Figure 22. Experimental instrumentation Setup



The frequency analyzer used to make the measurements in these experiments is the General Radio 2515 Multi-Channel analyzer. It can receive, process, and store data for 16 channels. It also has programming capability that is useful for data display.

The waterborne model is excited with a Wilcoxon Research model F1 piezoelectric shaker attached through an impedance head to a mounting stud fixed onto the model in the location shown (the same location used in the computer model). The shaker is powered by an amplified pseudo random noise signal from the General Radio (Gen Rad) analyzer and produces a nominal .75 lb rms force. Pseudo random noise is random noise that is periodic with respect to each sampling period. The impedance head is a Wilcoxon Research model Z602 that senses the force and acceleration at the drive point. These signals are fed into ENDEVCO 2721B charge amplifiers and into the analyzer where they are averaged over time and divided to give the average drive point acceleration spectrum.

Three Wilcoxon Research M408 accelerometers are mounted on studs epoxied to the steel plate. The accelerometers send their signals through ENDEVCO charge amplifiers into the Gen Rad analyzer. The signals from the accelerometers are averaged in space and time and squared to give the average plate acceleration squared spectrum. The nominal sensitivity of the accelerometers is 50 mv/g.

The acoustic pressure in the reverberant sound tank is sensed by three ITC model 6050C hydrophones. Their output is amplified and sent to the analyzer. The pressure is averaged in space and time to give the average acoustic sound pressure spectrum. Table [7] lists the sensitivity of the three hydrophone.



The lowest practical frequency for using the BBN reverberant sound tank is the 1/3 octave band centered at 315 Hz. For this research a lower limit was set at 400 Hz with a corresponding acoustic wavelength of 12.2 feet. To allow at least one wavelength between the model and hydrophones each was placed at least 12.2 feet from the center of the model. The coordinates of each hydrophone referenced to an origin at the center of the model are listed in Table [7].

Hydrophone	X (feet)	Y (feet)	Z (feet)	Distance (feet)	Sensitivity (dB//1V/ $\mu$ Pa)
607	8.5	0.0	9.0	12.4	-157
612	-6.0	-4.0	10.0	12.3	-158
720	-6.0	4.0	10.0	12.3	-158

Table 7. Hydrophone Placement in the Reverberant Sound Tank

The following list summarizes the equipment used.

Accelerometers	- Wilcoxon Research M408
Impedance Head	- Wilcoxon Research Z602
Shaker	- Wilcoxon Research F1
Charge Amps	- Endevco 2721B
Hydrophones	- ITC 6050C
Analyzer	- GenRad 2515 (16 Channel)
Power Amplifier	- Macintosh 40 W





## 6.2 Measurements

A series of five experiments were run to closely follow the computer analyses performed.

- Exp 1 - Model without modification set in the center of the reverberant tank
- Exp 2 - 0.75 lb weight added to the midpoint of the cross beam as in Run # 2
- Exp 3 - 1.50 lb weight added to the mid point of the cross beam as in Run # 3
- Exp 4 - 0.75 lb weight added to the 1/4 point of the same cross beam as in Run # 4
- Exp 5 - Two 0.75 lb weights added to opposite cross beams as in Run # 5

In each of the experiments the time averaged drive point acceleration, time and space averaged plate acceleration squared and time and space averaged pressure in the reverberant tank were measured. The signal sampling time is set in the analyzer to give a frequency resolution of 1 Hz.



### 6.3 Drive Point Accelerance

Figure 23 is the combined spectra of the drive point acceleration divided by the drive point force (drive point accelerance) from 450 Hz to 500 Hz for experiments 1 through 5, where the top spectrum is experiment 1, and the bottom is experiment 5. Each spectrum is of the same scale but shifted up or down so five spectra could be plotted. The vertical scale is in dB(g/lb) and the horizontal scale is linear in Hz.

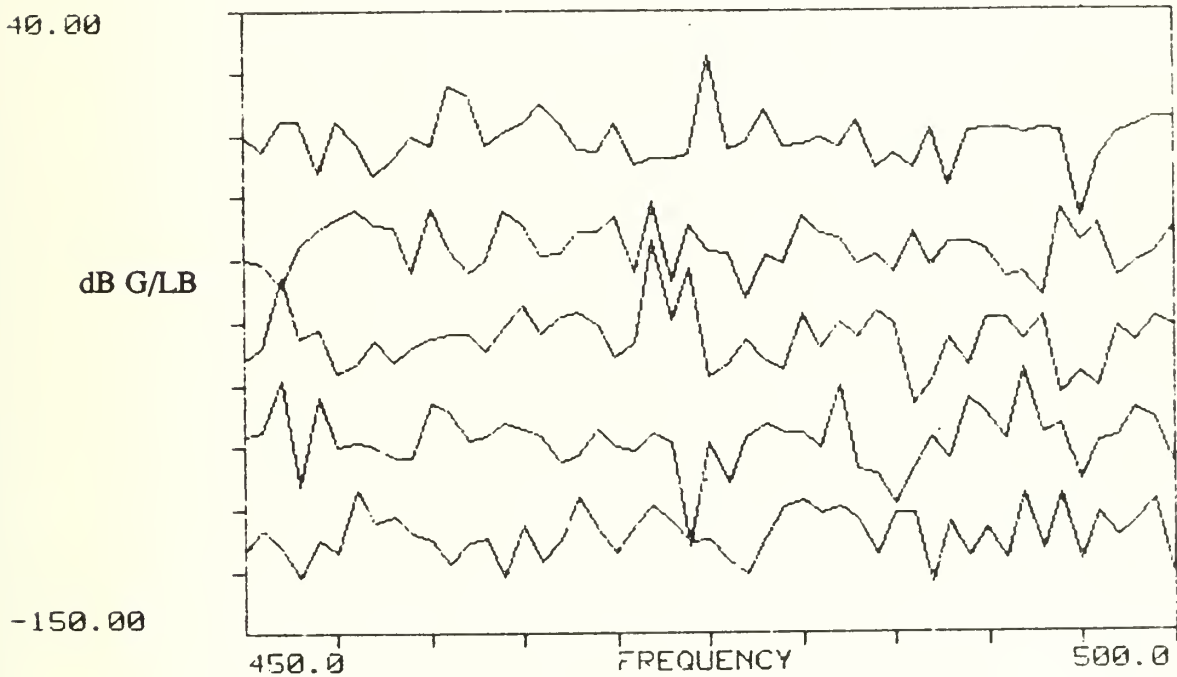


Figure 23. Drive Point Accelerance for Experiments 1 - 5



## 6.4 Plate Acceleration

Figure 24 is the combined spectra of the plate acceleration squared from 450 Hz to 500 Hz for experiments 1 through 5, where the top spectrum is experiment 1, and the bottom is experiment 5. Each spectrum is of the same scale but shifted up or down so five spectra could be plotted. The vertical scale is in dB Volts (re  $g^2$ ) and the horizontal scale is linear in Hz.

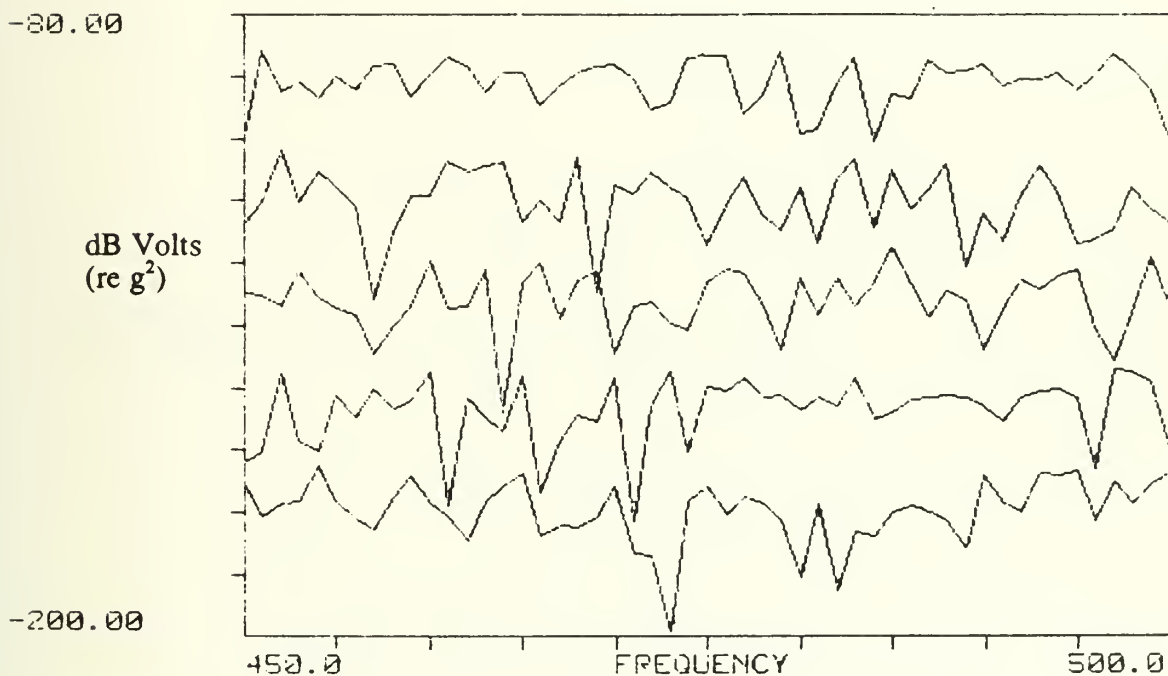


Figure 24. Plate Acceleration for Experiments 1 - 5



## 6.5 Waterborne Sound Pressure Level

Figure 25 is the combined spectra of the sound pressure level in the reverberant sound tank from 450 Hz to 500 Hz for experiments 1 through 5, where the top spectra is experiment 1, and the bottom is experiment 5. Each spectra is of the same scale but shifted up or down so five spectra could be plotted. The vertical scale is in dB Volts (re 1 volt) and the horizontal scale is linear in Hz.

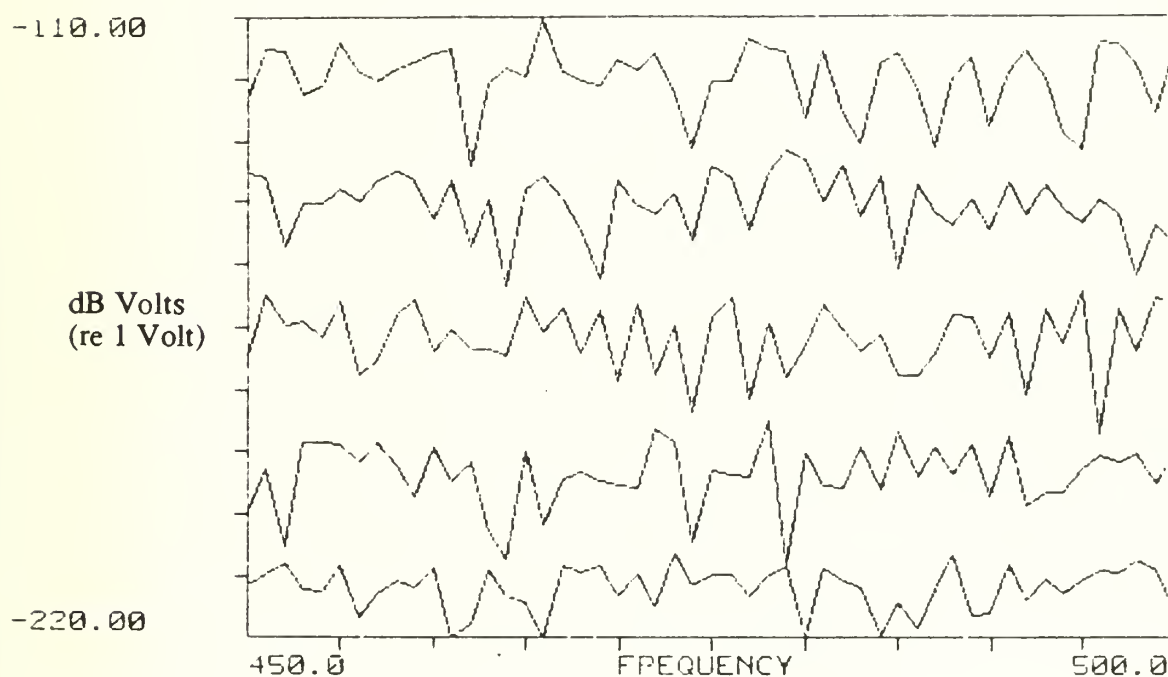


Figure 25. Sound Pressure Level for Experiments 1 - 5





## 6.6 Analysis

### 6.6.1 Experiment 1

The plate acceleration squared spectrum and accelerance spectrum show 14 - 15 peaks in the 50 Hz band. This is a modal separation of about 3.5 Hz. Also, the definition of the peaks as individual peaks is poor and could be the result of modal overlap. The sound pressure spectrum also shows 14 - 15 peaks giving the same modal separation as the plate modes.

### 6.6.2 Experiment 2

The drive point accelerance shows a broad peak at 456 Hz and the pressure spectrum shows a relatively large broad peak centered at 458 Hz. This may relate to the peak in the calculated radiated power spectrum at 462 Hz from Run # 2. The radiated power spectrum also shows a general increase of the peaks from 475 Hz to 485 Hz where the drive point accelerance shows a increase and coupling of the peaks at 480 Hz. From the modal analysis the foundation mode shifted down in frequency to 479 Hz in Run # 2 which may have caused coupling to occur that did not show in the computer analysis.



### 6.6.3 Experiment 3

The broad peak in the drive point accelerance at 456 Hz in Exp 2 is uncoupled and there are two sharp peaks at 452 Hz and 455 Hz, also the relatively large broad peak that was at 458 Hz in Exp 2 decreased. Compared to Exp 1 the sound pressure levels are relatively the same. The relative changes in this experiment correlate with computer Run # 3.

### 6.6.4 Experiment 4

In the drive point accelerance spectrum there is a shift of the sharp peak at 475 Hz from Exp 1 to a sharp doublet at 472 Hz and 474 Hz, but there is no significant change in the pressure spectrum at these frequencies.

### 6.6.5 Experiment 5

The changes in the drive point accelerance from Exp 1 are a broad peak at 456 Hz and one at 480 Hz, but there is no significant change in the pressure spectrum that would be expected if coupling had occurred.



## 6.7 Validation of Results

In Section 5.3 the average modal separation of the modal analysis was compared to analytical results. The drive point accelerance from 450 Hz to 500 Hz in the experiments shows an average peak separation of 4 Hz. This does not correlate well with the calculated modal separation of 13.1 Hz or the modal separation from the computer analysis of 8 Hz. Although the reasons are unclear it is thought that modal overlap, coupling with tank resonances or diffraction effects are influencing the plate vibrations. Both the calculated power and measured power spectrums showed 14 - 15 peaks in the 50 Hz band, and since the computer model of the tank was a semi-infinite pressure release surface the coupling of tank and plate modes is unlikely to be the reason for the increase in modal density. The estimated frequency for modal overlap to occur was 255 Hz, and the indications in the plate acceleration and accelerance measurements are that modal overlap may be occurring. Also, there was a peak in the calculated radiated sound power in section 5 that could be due to diffraction effects, which gives some weight to the argument that diffraction effects may be causing this discrepancy. Other less likely reasons for this discrepancy in experimental measurements are discussed in [19].

In Section 2.6 it was shown that the radiation efficiency can be calculated from experimental measurement of  $\Pi_{\text{rad}}$  and  $\langle v_p^2 \rangle$ . For experiment 1 the average pressure measurement was about -124 dB re 1 Volt and the average mean squared acceleration



was about -94 dB re  $1 \text{ g}^2$ . Using equations (2.36) - (2.39), (2.42), and (2.52) and  $\langle v_p^2 \rangle = \langle a_p^2 \rangle / \omega^2$  the radiation efficiency can be calculated:  $\sigma_{\text{rad}} = 5.6 \times 10^{-13}$ . This correlates well with the boundary element average  $\sigma_{\text{rad}}$  of  $10^{-10}$ .

The calculation of radiation efficiency and modal separation for the boundary element model indicate that the model is accurate. The modal density difference between the finite element and experimental models appear to be due to an inadequate model of the fluid plate interface. A similar finite element model predicted the modal density accurately in [3] when the model was evaluated in air, but when the model is given a fluid loading a discrepancy exists.





## 7 CONCLUSIONS AND RECOMMENDATIONS

In a structure more complex than a simple plate and beam where fluid loading has a significant effect on the vibration of the plate it is difficult to identify the vibrational modes and classify them. Modal analysis using a finite element model results in mode shapes that can be identified as foundation, plate or global. The numerical analysis shows the shifting of resonant frequencies when mass is added to a structure, and also the expected increase in radiated power when a global mode is formed.

The modal analysis demonstrates the difficulties in identifying global modes experimentally in that most modes are shifted by the addition of a mass to the structure. The finite element modal analysis in Run # 0 showed that of the seven mode shapes between 450 Hz and 500 Hz, five indicated both foundation and plate motion, one could be classified as a plate mode, and one could be classified as a foundation mode. When mass was added to shift the foundation mode it effected all of the modes with foundation motion (6 modes in a 50 Hz band). It is also expected that addition of a mass at the junction of the foundation and plate would shift all of the modes with plate motion (6 modes). It is shown here that the foundation mode shift is greatest which makes it stand out from the rest, and as the other modes shift their coupling is apparently changed because radiated power is decreased. When the foundation mode is coupled there is an increase in radiated power which aides in its classification, but another factor that must be considered is an increase in radiated power could be due to other, nonresonant, effects.



The experimental results did not allow direct correlation between the calculated structural resonances and peaks in the plate acceleration or drive point acceleration. The modal density of the plate was almost two times the predicted value. The difference in the modal density is thought to be due to the fluid structure interaction. Previous experiments with the model in air had good agreement with the finite element model and theoretical calculations. The computer model in this research used an added mass approximation of the fluid loading on the plate and the agreement between theoretical calculations, numerical calculations, and experimental results do not agree. This implies that the fluid structure interface in this model is not adequately defined. It is thought that modal overlap and/or diffraction effects could be causing an increase in the modal density of the structure that is not accounted for in the finite element modal analysis.

Continuation of this research using the same methods would be beneficial and would involve trying to improve the fluid loading approximation and using different masses and locations on the foundation and the foundation plate junction. Reducing the modal overlap and diffraction effects by using a larger model and less damping should also be investigated.

An improvement in the results could be achieved in future research by more accurately predicting the fluid structure interaction. This could be done in the computer model by either modeling both the structure and fluid with finite elements or using an integrated program that combines a finite element method with a boundary element method and iterates on the fluid structure interaction. Finite element programs are available that have acoustic elements, and there are also combined programs. This research used commercially available software with a relatively inexpensive personal



computer which makes the method appealing because of the expense and accessibility.

Programs that can better model the fluid structure interaction would require more elements and would require a higher capacity and faster computer.



## Referencess

- 1 Song, J. B. and Lyon, R. H., "Determination of Foundation/Hull Coupling from Foundation Mobility Functions", RH Lyon Corp. Report LC-122, Project No. N6153387M2193, 1 November 1987.
- 2 McCoy, K. M., "Identification and Alteration of Global Resonance Modes in Ship Structures to Reduce Sound Radiation", Naval Engineer Thesis MIT, May 1989.
- 3 Bowen, D. L., Gardner, C. M., and Lyon, R. H., "Foundation and Hull Strong Coupling: Detection and Avoidance", RH Lyon Corp Report project No. N6153389M3060, 28 February 1990.
- 4 Rao, S. S., Mechanical Vibrations, Addison-Wesley Publishing Co. Reading, MA, 1986.
- 5 ALGOR Processor Reference Manual, ALGOR Interactive Systems Inc., Pittsburgh, PA, 1989.
- 6 Lyon, R. H., Machinery Noise and Diagnostics, Butterworths, Boston, MA, 1987.
- 7 Schenk, H. A., "Improved Integral Formulation for Acoustic Radiation Problems", J. Acoust. Soc. Amer. 44, pp 41-58, 1968.
- 8 Cheng, C. Y. R. and Seybert, A. F., "Recent Applications of the Boundary Element Methods to Problems in Acoustics", Presented at SAE Noise and Vibration Conference, April 1987.
- 9 Junger, M. C., "Approaches to Acoustic Fluid - Elastic Structure Interactions", J. Acoust. Soc. Amer., 82 (4), October 1987.
- 10 Geers, T. L., "Residual Potential and Approximate Methods for Three Dimensional Fluid Structure Interaction Problems", J. Acoust. Soc. Amer. 49 pp 1505-1570, 1971.
- 11 Huang, H. and Wang, Y. F., "Asymptotic Fluid-Structure Interaction Theories for Acoustic Radiation Prediction", J. Acoust. Soc. Amer. 77(4), 1985.



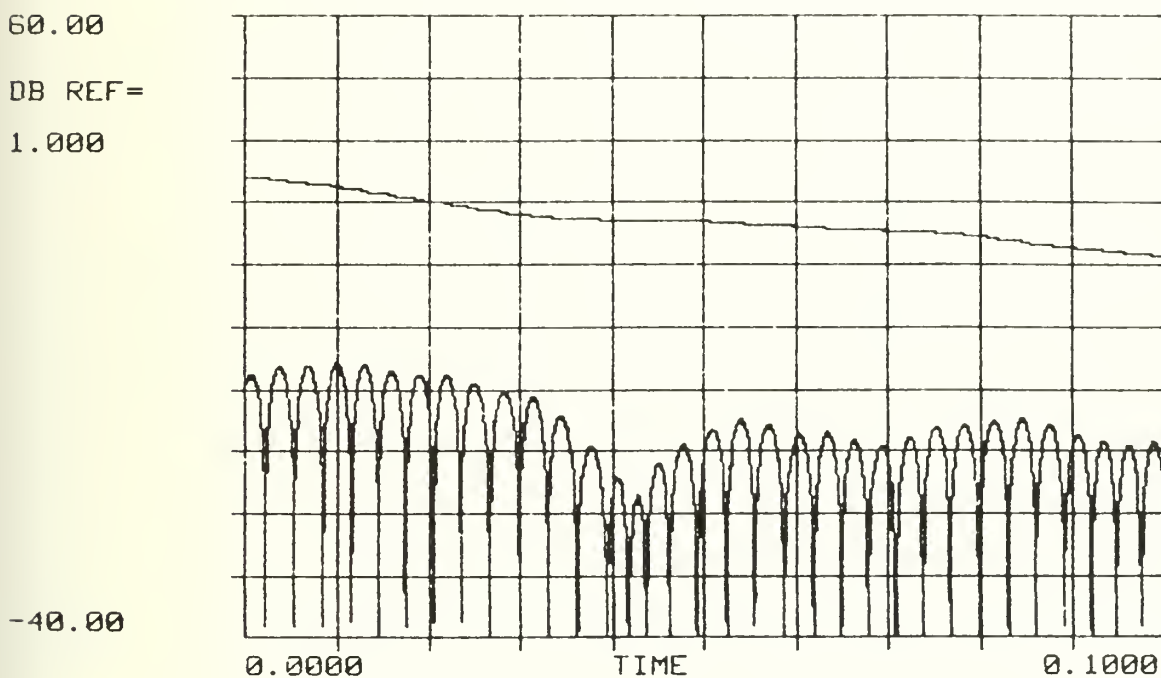


- 12 Everstein, G. C., "Calculation of Low Frequency Vibration Resonances of submerged Structures", NASA CP-3029, Washington D.C., April 1989.
- 13 Marcus, M. S., "A Finite Element Method Applied to the Vibration of Submerged PLates", J. of Ship Res. Vol. 22, No. 2, June 1978.
- 14 Junger, M. C. and Feit, D., Sound, Structures, and Their Interaction, MIT Press Cambridge, MA, 1972.
- 15 Smith, P. W. Jr. and Lyon, Richard H., "Sound and Structural Vibration", NASA Contractor Report CR-160, March 1961.
- 16 Schoeder M. R., "New Method of Measuring Reverberation Time", J. Acoust. Soc. Am., Vol. 37, No. 3, 409-412, March 1965.
- 17 Sebert, A. F., Wu, T. W., and Wan, G. C., User's Manual Computer Program BEMAP, Version 2.43, Spectronics Inc., Lexington, KY, September 1990.
- 18 Morse, P. M., Vibration and Sound, McGraw-Hill Book Co. Inc, 1948.
- 19 Muhlenkamp, W. S., "Vibration Analysis in Waterborne Structures", Bachelor's Thesis, MIT, June 1991.



## APPENDIX A. DAMPING MEASUREMENTS

The damping loss factor of the model was measured in 1/3 octave frequency bands from 200 Hz to 1000 Hz. These graphs show the acceleration amplitude referenced to 1g versus time after a single impact to the model as it floated in the BBN reverberant water tank. Also, plotted on each graph is the area under the acceleration squared curve from which the plate damping loss factor was calculated.



1/3 octave frequency band = 200 Hz, DR = 140 dB/sec,  $\eta = .026$ .

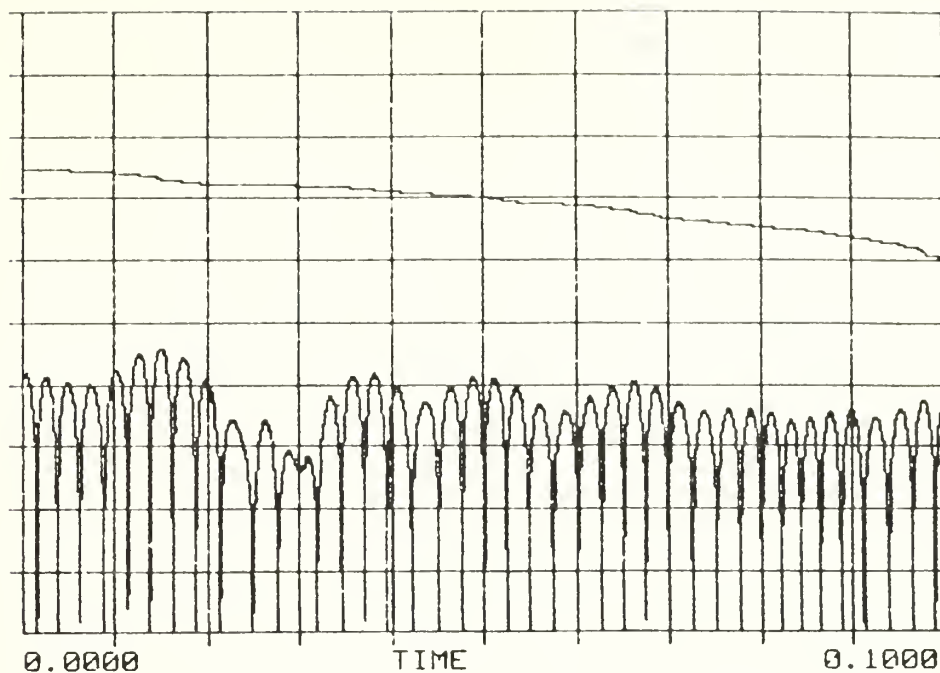


60.00

DB REF =

1.000

-40.00



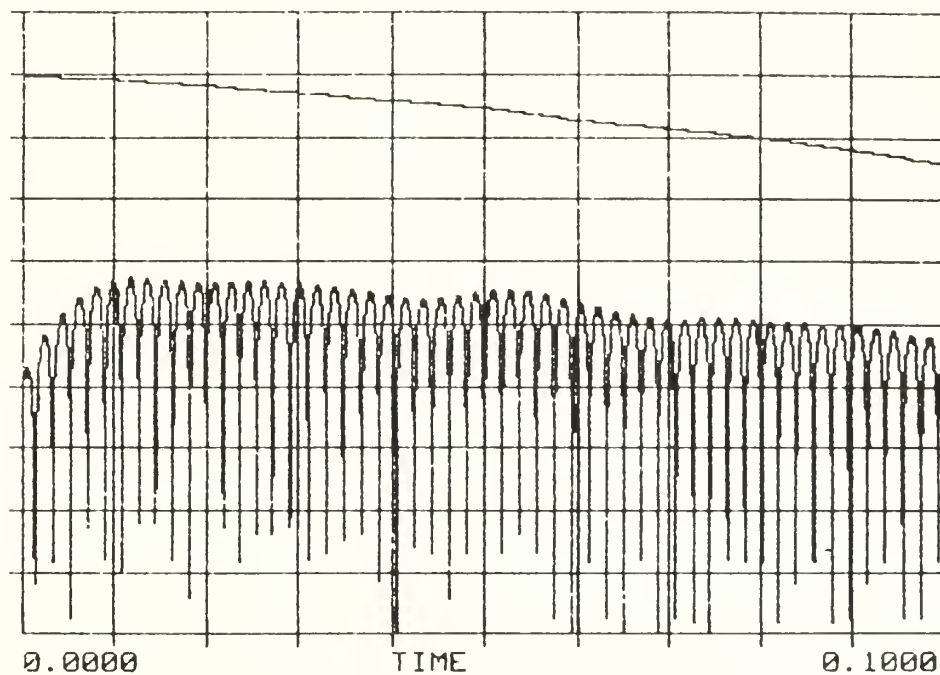
1/3 octave frequency band = 250 Hz, DR = 190 dB/sec,  $\eta = .028$ .

60.00

DB REF =

1.000

-40.00



1/3 octave frequency band = 315 Hz, DR = 200 dB/sec,  $\eta = .023$ .

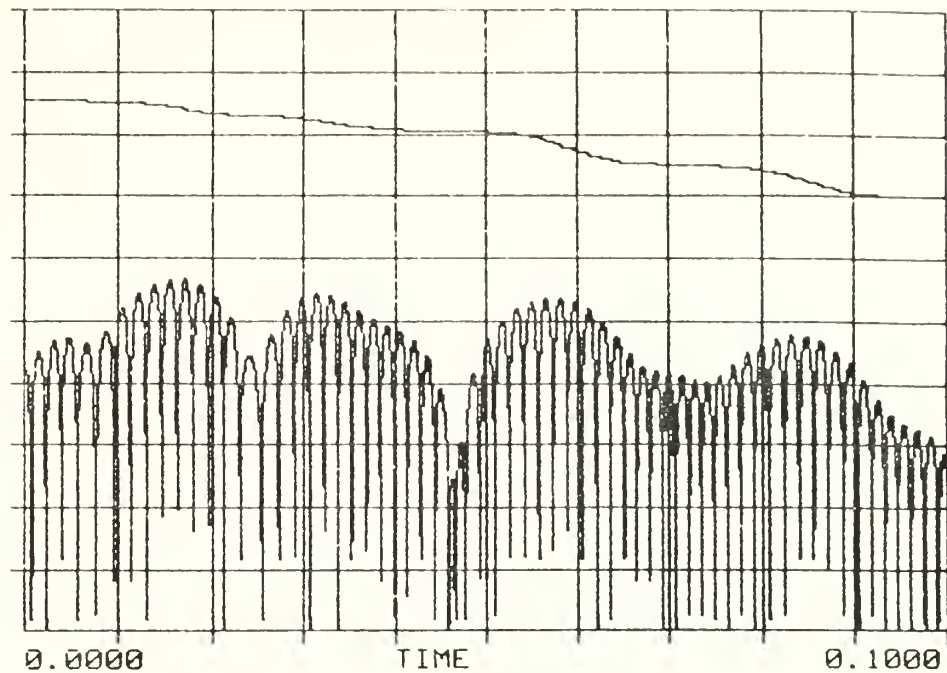


60.00

DB REF =

1.000

-40.00



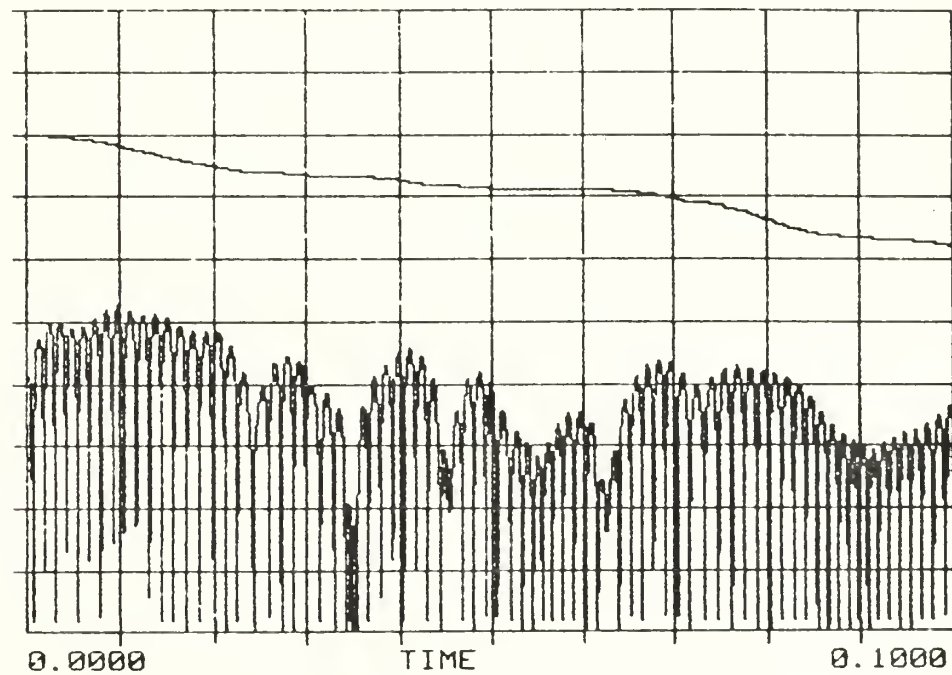
1/3 octave frequency band = 400 Hz, DR = 240 dB/sec,  $\eta = .022$ .

60.00

DB REF =

1.000

-40.00



1/3 octave frequency band = 500 Hz, DR = 330 dB/sec,  $\eta = .024$ .



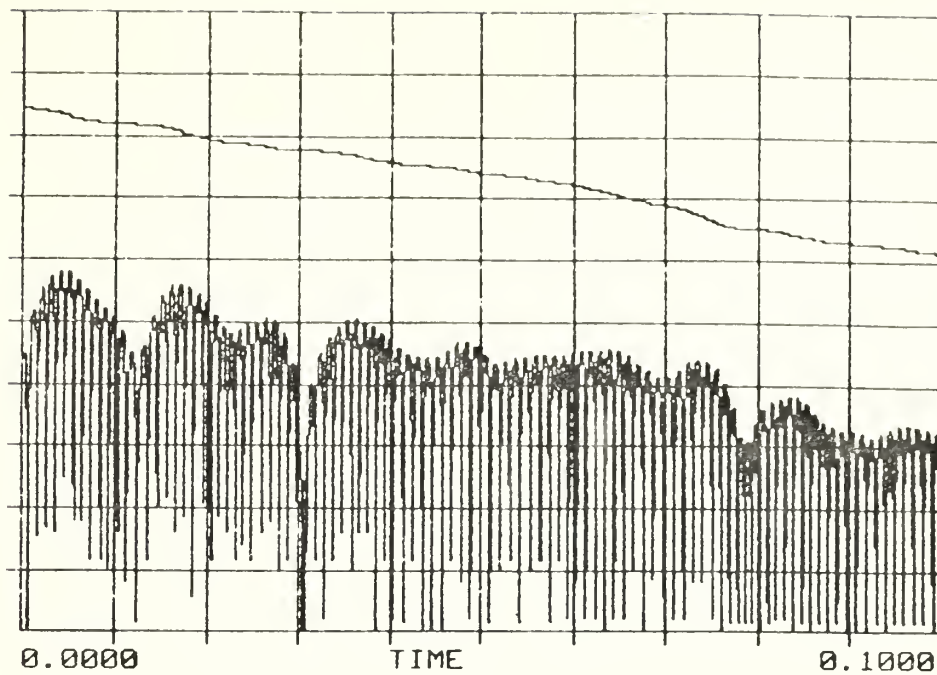


60.00

DB REF=

1.000

-40.00



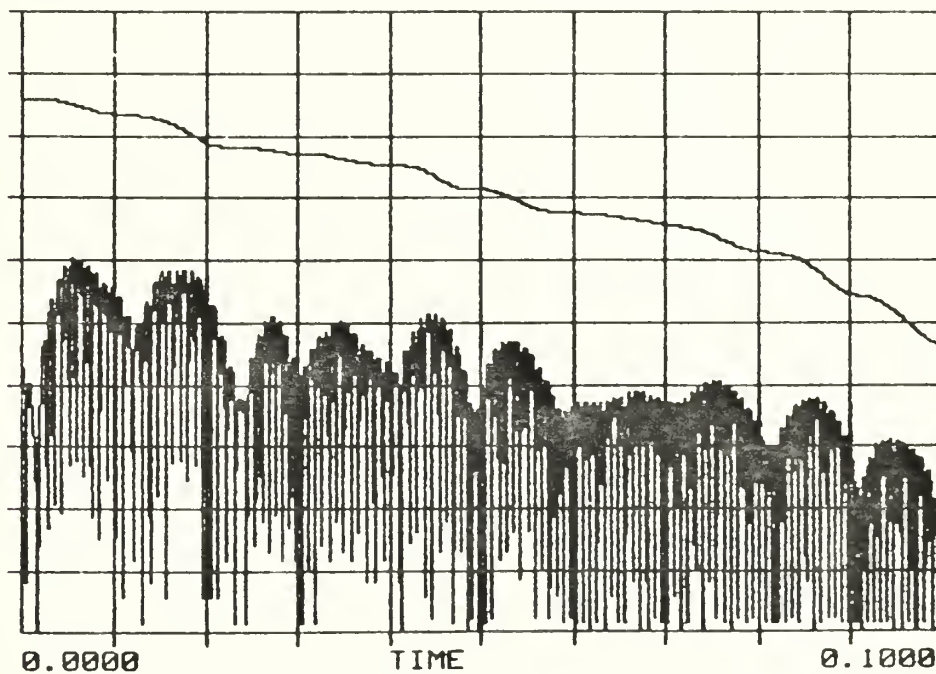
1/3 octave frequency band = 630 Hz, DR = 330 dB/sec,  $\eta = .019$ .

60.00

DB REF=

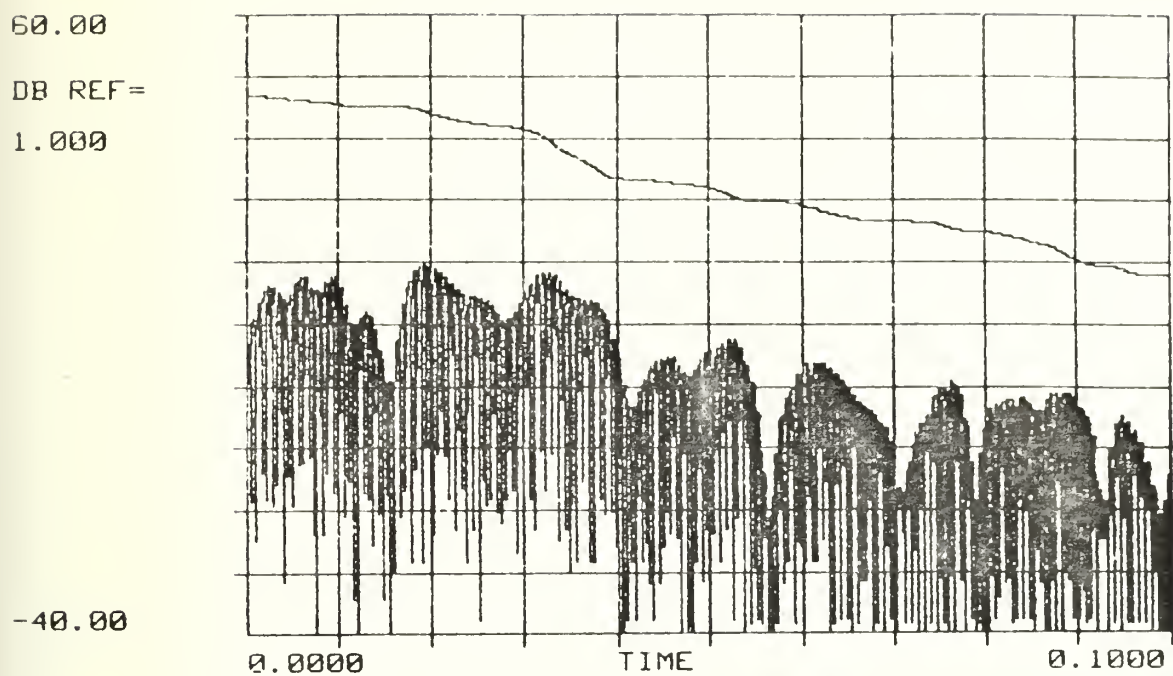
1.000

-40.00



1/3 octave frequency band = 800 Hz, DR = 350 dB/sec,  $\eta = .016$ .





1/3 octave frequency band = 1000 Hz, DR = 330 dB/sec,  $\eta = .012$ .



## APPENDIX B. FINITE ELEMENT PROGRAM INPUT FILES

Example input file for the ALGOR modal analysis program, SSAP1H, the structure of the file is as follows: the first section contains the nodal coordinates and boundary conditions, next is the plate element material properties and connectivity data, then the beam element material properties and connectivity data, followed by the nodal loads (fluid loading), and the last line contains the frequency analysis data.

FILE PREPARED BY DECODER (Type 6)

323 2 0 100 0 1 0 0 0 0 000 0 0 0 0 386.1

(Node #, boundary conditions, and coordinates x,y,z)

1	0	0	0	0	0	.0000000E+00	.5500000E+01	.0000000E+00	0	.00000E+00	0	0
2	0	0	0	0	0	.0000000E+00	.1108333E+02	.0000000E+00	0	.00000E+00		
3	0	0	0	0	0	.0000000E+00	.1666667E+02	.0000000E+00	0	.00000E+00		
4	0	0	0	0	0	.0000000E+00	.2225000E+02	.0000000E+00	0	.00000E+00		
5	0	0	0	0	0	.0000000E+00	.2783334E+02	.0000000E+00	0	.00000E+00		
6	0	0	0	0	0	.0000000E+00	.3341667E+02	.0000000E+00	0	.00000E+00		
7	0	0	0	0	0	.0000000E+00	.3900000E+02	.0000000E+00	0	.00000E+00		
8	0	0	0	0	0	.0000000E+00	.4350000E+02	.1500000E+01	0	.00000E+00		
9	0	0	0	0	0	.0000000E+00	.7666667E+01	.2833333E+01	0	.00000E+00		
10	0	0	0	0	0	.0000000E+00	.1263585E+02	.2847253E+01	0	.00000E+00		
11	0	0	0	0	0	.0000000E+00	.1758881E+02	.2861126E+01	0	.00000E+00		
12	0	0	0	0	0	.0000000E+00	.2254167E+02	.2875000E+01	0	.00000E+00		
13	0	0	0	0	0	.0000000E+00	.2749442E+02	.2888873E+01	0	.00000E+00		
14	0	0	0	0	0	.0000000E+00	.3244706E+02	.2902746E+01	0	.00000E+00		
15	0	0	0	0	0	.0000000E+00	.3741667E+02	.2916667E+01	0	.00000E+00		
16	0	0	0	0	0	.0000000E+00	.4800000E+02	.3000000E+01	0	.00000E+00		
17	0	0	0	0	0	.0000000E+00	.4116667E+02	.4166666E+01	0	.00000E+00		
18	0	0	0	0	0	.0000000E+00	.4491667E+02	.5416667E+01	0	.00000E+00		
19	0	0	0	0	0	.0000000E+00	.9833334E+01	.5666666E+01	0	.00000E+00		
20	0	0	0	0	0	.0000000E+00	.1418841E+02	.5694584E+01	0	.00000E+00		
21	0	0	0	0	0	.0000000E+00	.1851097E+02	.5722292E+01	0	.00000E+00		
22	0	0	0	0	0	.0000000E+00	.2283333E+02	.5750000E+01	0	.00000E+00		
23	0	0	0	0	0	.0000000E+00	.2715551E+02	.5777706E+01	0	.00000E+00		
24	0	0	0	0	0	.0000000E+00	.3147749E+02	.5805411E+01	0	.00000E+00		
25	0	0	0	0	0	.0000000E+00	.3583333E+02	.5833333E+01	0	.00000E+00		
26	0	0	0	0	0	.0000000E+00	.2750000E+01	.6500000E+01	0	.00000E+00		
27	0	0	0	0	0	.0000000E+00	.3883333E+02	.6833333E+01	0	.00000E+00		
28	0	0	0	0	0	.0000000E+00	.4183333E+02	.7833334E+01	0	.00000E+00		
29	0	0	0	0	0	.0000000E+00	.5375000E+01	.8250000E+01	0	.00000E+00		
30	0	0	0	0	0	.0000000E+00	.1200000E+02	.8500000E+01	0	.00000E+00		





31 0 0 0 0 0 0	.0000000E+00	.1574104E+02	.8542035E+01	0	.00000E+00
32 0 0 0 0 0 0	.0000000E+00	.1943315E+02	.8583519E+01	0	.00000E+00
33 0 0 0 0 0 0	.0000000E+00	.2312500E+02	.8625000E+01	0	.00000E+00
34 0 0 0 0 0 0	.0000000E+00	.2681660E+02	.8666479E+01	0	.00000E+00
35 0 0 0 0 0 0	.0000000E+00	.4800000E+02	.8625000E+01	0	.00000E+00
36 0 0 0 0 0 0	.0000000E+00	.3050796E+02	.8707955E+01	0	.00000E+00
37 0 0 0 0 0 0	.0000000E+00	.3425000E+02	.8750000E+01	0	.00000E+00
38 0 0 0 0 0 0	.0000000E+00	.3650000E+02	.9500000E+01	0	.00000E+00
39 0 0 0 0 0 0	.0000000E+00	.8000000E+01	.1000000E+02	0	.00000E+00
40 0 0 0 0 0 0	.0000000E+00	.3875000E+02	.1025000E+02	0	.00000E+00
41 0 0 0 0 0 0	.0000000E+00	.4491667E+02	.1045417E+02	0	.00000E+00
42 0 0 0 0 0 0	.0000000E+00	.1416667E+02	.1133333E+02	0	.00000E+00
43 0 0 0 0 0 0	.0000000E+00	.1729377E+02	.1138968E+02	0	.00000E+00
44 0 0 0 0 0 0	.0000000E+00	.2035536E+02	.1144484E+02	0	.00000E+00
45 0 0 0 0 0 0	.0000000E+00	.2341667E+02	.1150000E+02	0	.00000E+00
46 0 0 0 0 0 0	.0000000E+00	.2647771E+02	.1155515E+02	0	.00000E+00
47 0 0 0 0 0 0	.0000000E+00	.2953848E+02	.1161030E+02	0	.00000E+00
48 0 0 0 0 0 0	.0000000E+00	.3266667E+02	.1166667E+02	0	.00000E+00
49 0 0 0 0 0 0	.0000000E+00	.1062500E+02	.1175000E+02	0	.00000E+00
50 0 0 0 0 0 0	.0000000E+00	.3416667E+02	.1216667E+02	0	.00000E+00
51 0 0 0 0 0 0	.0000000E+00	.4183333E+02	.1228333E+02	0	.00000E+00
52 0 0 0 0 0 0	.0000000E+00	.3566667E+02	.1266667E+02	0	.00000E+00
53 0 0 0 0 0 0	.0000000E+00	.0000000E+00	.1300000E+02	0	.00000E+00
54 0 0 0 0 0 0	.0000000E+00	.1325000E+02	.1350000E+02	0	.00000E+00
55 0 0 0 0 0 0	.0000000E+00	.3083333E+01	.1366667E+02	0	.00000E+00
56 0 0 0 0 0 0	.0000000E+00	.1633333E+02	.1416667E+02	0	.00000E+00
57 0 0 0 0 0 0	.0000000E+00	.3875000E+02	.1411250E+02	0	.00000E+00
58 0 0 0 0 0 0	.0000000E+00	.1884669E+02	.1423766E+02	0	.00000E+00
59 0 0 0 0 0 0	.0000000E+00	.6166666E+01	.1433333E+02	0	.00000E+00
60 0 0 0 0 0 0	.0000000E+00	.2127762E+02	.1430634E+02	0	.00000E+00
61 0 0 0 0 0 0	.0000000E+00	.4800000E+02	.1425000E+02	0	.00000E+00
62 0 0 0 0 0 0	.0000000E+00	.2370833E+02	.1437500E+02	0	.00000E+00
63 0 0 0 0 0 0	.0000000E+00	.2613883E+02	.1444366E+02	0	.00000E+00
64 0 0 0 0 0 0	.0000000E+00	.2856913E+02	.1451231E+02	0	.00000E+00
65 0 0 0 0 0 0	.0000000E+00	.3108334E+02	.1458333E+02	0	.00000E+00
66 0 0 0 0 0 0	.0000000E+00	.3183333E+02	.1483333E+02	0	.00000E+00
67 0 0 0 0 0 0	.0000000E+00	.9250000E+01	.1500000E+02	0	.00000E+00
68 0 0 0 0 0 0	.0000000E+00	.3258334E+02	.1508333E+02	0	.00000E+00
69 0 0 0 0 0 0	.0000000E+00	.1587500E+02	.1525000E+02	0	.00000E+00
70 0 0 0 0 0 0	.0000000E+00	.4491667E+02	.1550833E+02	0	.00000E+00
71 0 0 0 0 0 0	.0000000E+00	.1233333E+02	.1566667E+02	0	.00000E+00
72 0 0 0 0 0 0	.0000000E+00	.3566667E+02	.1594166E+02	0	.00000E+00
73 0 0 0 0 0 0	.0000000E+00	.1541667E+02	.1633333E+02	0	.00000E+00
74 0 0 0 0 0 0	.0000000E+00	.4183333E+02	.1676666E+02	0	.00000E+00
75 0 0 0 0 0 0	.0000000E+00	.1850000E+02	.1700000E+02	0	.00000E+00
76 0 0 0 0 0 0	.0000000E+00	.2040000E+02	.1708636E+02	0	.00000E+00
77 0 0 0 0 0 0	.0000000E+00	.2220000E+02	.1716818E+02	0	.00000E+00
78 0 0 0 0 0 0	.0000000E+00	.2400000E+02	.1725000E+02	0	.00000E+00
79 0 0 0 0 0 0	.0000000E+00	.2580000E+02	.1733182E+02	0	.00000E+00
80 0 0 0 0 0 0	.0000000E+00	.2760000E+02	.1741364E+02	0	.00000E+00
81 0 0 0 0 0 0	.0000000E+00	.2950000E+02	.1750000E+02	0	.00000E+00
82 0 0 0 0 0 0	.0000000E+00	.3258334E+02	.1777083E+02	0	.00000E+00
83 0 0 0 0 0 0	.0000000E+00	.3875000E+02	.1802500E+02	0	.00000E+00
84 0 0 0 0 0 0	.0000000E+00	.0000000E+00	.1845833E+02	0	.00000E+00
85 0 0 0 0 0 0	.0000000E+00	.3083333E+01	.1861528E+02	0	.00000E+00





86 0 0 0 0 0 0	.0000000E+00	.6166666E+01	.1877222E+02	0	.00000E+00
87 0 0 0 0 0 0	.0000000E+00	.9250000E+01	.1892917E+02	0	.00000E+00
88 0 0 0 0 0 0	.0000000E+00	.1233333E+02	.1908611E+02	0	.00000E+00
89 0 0 0 0 0 0	.0000000E+00	.1541667E+02	.1924306E+02	0	.00000E+00
90 0 0 0 0 0 0	.0000000E+00	.3566667E+02	.1928333E+02	0	.00000E+00
91 0 0 0 0 0 0	.0000000E+00	.1850000E+02	.1940000E+02	0	.00000E+00
92 0 0 0 0 0 0	.0000000E+00	.2040000E+02	.1943454E+02	0	.00000E+00
93 0 0 0 0 0 0	.0000000E+00	.2220000E+02	.1946727E+02	0	.00000E+00
94 0 0 0 0 0 0	.0000000E+00	.2400000E+02	.1950000E+02	0	.00000E+00
95 0 0 0 0 0 0	.0000000E+00	.2580000E+02	.1953273E+02	0	.00000E+00
96 0 0 0 0 0 0	.0000000E+00	.2760000E+02	.1956545E+02	0	.00000E+00
97 0 0 0 0 0 0	.0000000E+00	.2950000E+02	.1960000E+02	0	.00000E+00
98 0 0 0 0 0 0	.0000000E+00	.4800000E+02	.1987500E+02	0	.00000E+00
99 0 0 0 0 0 0	.0000000E+00	.3258334E+02	.2054166E+02	0	.00000E+00
100 0 0 0 0 0 0	.0000000E+00	.4491667E+02	.2056250E+02	0	.00000E+00
101 0 0 0 0 0 0	.0000000E+00	.4183333E+02	.2125000E+02	0	.00000E+00
102 0 0 0 0 0 0	.0000000E+00	.1850000E+02	.2170000E+02	0	.00000E+00
103 0 0 0 0 0 0	.0000000E+00	.2040000E+02	.2171727E+02	0	.00000E+00
104 0 0 0 0 0 0	.0000000E+00	.2220000E+02	.2173364E+02	0	.00000E+00
105 0 0 0 0 0 0	.0000000E+00	.2400000E+02	.2175000E+02	0	.00000E+00
106 0 0 0 0 0 0	.0000000E+00	.2580000E+02	.2176636E+02	0	.00000E+00
107 0 0 0 0 0 0	.0000000E+00	.2760000E+02	.2178273E+02	0	.00000E+00
108 0 0 0 0 0 0	.0000000E+00	.2950000E+02	.2180000E+02	0	.00000E+00
109 0 0 0 0 0 0	.0000000E+00	.3875000E+02	.2193750E+02	0	.00000E+00
110 0 0 0 0 0 0	.0000000E+00	.1541667E+02	.2206944E+02	0	.00000E+00
111 0 0 0 0 0 0	.0000000E+00	.1233333E+02	.2243889E+02	0	.00000E+00
112 0 0 0 0 0 0	.0000000E+00	.3566667E+02	.2262500E+02	0	.00000E+00
113 0 0 0 0 0 0	.0000000E+00	.9250000E+01	.2280833E+02	0	.00000E+00
114 0 0 0 0 0 0	.0000000E+00	.6166666E+01	.2317778E+02	0	.00000E+00
115 0 0 0 0 0 0	.0000000E+00	.3258334E+02	.2331250E+02	0	.00000E+00
116 0 0 0 0 0 0	.0000000E+00	.3083333E+01	.2354722E+02	0	.00000E+00
117 0 0 0 0 0 0	.0000000E+00	.0000000E+00	.2391667E+02	0	.00000E+00
118 0 0 0 0 0 0	.0000000E+00	.1850000E+02	.2400000E+02	0	.00000E+00
119 0 0 0 0 0 0	.0000000E+00	.2040000E+02	.2400000E+02	0	.00000E+00
120 0 0 0 0 0 0	.0000000E+00	.2220000E+02	.2400000E+02	0	.00000E+00
121 0 0 0 0 0 0	.0000000E+00	.2400000E+02	.2400000E+02	0	.00000E+00
122 0 0 0 0 0 0	.0000000E+00	.2580000E+02	.2400000E+02	0	.00000E+00
123 0 0 0 0 0 0	.0000000E+00	.2760000E+02	.2400000E+02	0	.00000E+00
124 0 0 0 0 0 0	.0000000E+00	.2950000E+02	.2400000E+02	0	.00000E+00
125 0 0 0 0 0 0	.0000000E+00	.1541667E+02	.2489583E+02	0	.00000E+00
126 0 0 0 0 0 0	.0000000E+00	.4800000E+02	.2550000E+02	0	.00000E+00
127 0 0 0 0 0 0	.0000000E+00	.4491667E+02	.2561667E+02	0	.00000E+00
128 0 0 0 0 0 0	.0000000E+00	.1233333E+02	.2579167E+02	0	.00000E+00
129 0 0 0 0 0 0	.0000000E+00	.4183333E+02	.2573333E+02	0	.00000E+00
130 0 0 0 0 0 0	.0000000E+00	.3875000E+02	.2585000E+02	0	.00000E+00
131 0 0 0 0 0 0	.0000000E+00	.3566667E+02	.2596667E+02	0	.00000E+00
132 0 0 0 0 0 0	.0000000E+00	.3258334E+02	.2608333E+02	0	.00000E+00
133 0 0 0 0 0 0	.0000000E+00	.1850000E+02	.2630000E+02	0	.00000E+00
134 0 0 0 0 0 0	.0000000E+00	.2040000E+02	.2628273E+02	0	.00000E+00
135 0 0 0 0 0 0	.0000000E+00	.2220000E+02	.2626636E+02	0	.00000E+00
136 0 0 0 0 0 0	.0000000E+00	.2400000E+02	.2625000E+02	0	.00000E+00
137 0 0 0 0 0 0	.0000000E+00	.2580000E+02	.2623364E+02	0	.00000E+00
138 0 0 0 0 0 0	.0000000E+00	.2760000E+02	.2621727E+02	0	.00000E+00
139 0 0 0 0 0 0	.0000000E+00	.2950000E+02	.2620000E+02	0	.00000E+00
140 0 0 0 0 0 0	.0000000E+00	.9250000E+01	.2668750E+02	0	.00000E+00



141 0 0 0 0 0	.0000000E+00	.6166666E+01	.2758333E+02	0	.00000E+00
142 0 0 0 0 0	.0000000E+00	.1541667E+02	.2772222E+02	0	.00000E+00
143 0 0 0 0 0	.0000000E+00	.3083333E+01	.2847917E+02	0	.00000E+00
144 0 0 0 0 0	.0000000E+00	.2580000E+02	.2846727E+02	0	.00000E+00
145 0 0 0 0 0	.0000000E+00	.2760000E+02	.2843455E+02	0	.00000E+00
146 0 0 0 0 0	.0000000E+00	.2950000E+02	.2840000E+02	0	.00000E+00
147 0 0 0 0 0	.0000000E+00	.2400000E+02	.2850000E+02	0	.00000E+00
148 0 0 0 0 0	.0000000E+00	.1850000E+02	.2860000E+02	0	.00000E+00
149 0 0 0 0 0	.0000000E+00	.2040000E+02	.2856545E+02	0	.00000E+00
150 0 0 0 0 0	.0000000E+00	.2220000E+02	.2853273E+02	0	.00000E+00
151 0 0 0 0 0	.0000000E+00	.3258334E+02	.2885417E+02	0	.00000E+00
152 0 0 0 0 0	.0000000E+00	.1233333E+02	.2914444E+02	0	.00000E+00
153 0 0 0 0 0	.0000000E+00	.3566667E+02	.2930833E+02	0	.00000E+00
154 0 0 0 0 0	.0000000E+00	.0000000E+00	.2937500E+02	0	.00000E+00
155 0 0 0 0 0	.0000000E+00	.3875000E+02	.2976250E+02	0	.00000E+00
156 0 0 0 0 0	.0000000E+00	.4183333E+02	.3021667E+02	0	.00000E+00
157 0 0 0 0 0	.0000000E+00	.2950000E+02	.3050000E+02	0	.00000E+00
158 0 0 0 0 0	.0000000E+00	.9250000E+01	.3056667E+02	0	.00000E+00
159 0 0 0 0 0	.0000000E+00	.1541667E+02	.3054861E+02	0	.00000E+00
160 0 0 0 0 0	.0000000E+00	.2760000E+02	.3058636E+02	0	.00000E+00
161 0 0 0 0 0	.0000000E+00	.2580000E+02	.3066818E+02	0	.00000E+00
162 0 0 0 0 0	.0000000E+00	.4491667E+02	.3067083E+02	0	.00000E+00
163 0 0 0 0 0	.0000000E+00	.2400000E+02	.3075000E+02	0	.00000E+00
164 0 0 0 0 0	.0000000E+00	.2220000E+02	.3083182E+02	0	.00000E+00
165 0 0 0 0 0	.0000000E+00	.2040000E+02	.3091364E+02	0	.00000E+00
166 0 0 0 0 0	.0000000E+00	.1850000E+02	.3100000E+02	0	.00000E+00
167 0 0 0 0 0	.0000000E+00	.4800000E+02	.3112500E+02	0	.00000E+00
168 0 0 0 0 0	.0000000E+00	.3258334E+02	.3154166E+02	0	.00000E+00
169 0 0 0 0 0	.0000000E+00	.6166666E+01	.3198889E+02	0	.00000E+00
170 0 0 0 0 0	.0000000E+00	.1233333E+02	.3249722E+02	0	.00000E+00
171 0 0 0 0 0	.0000000E+00	.3225000E+02	.3247917E+02	0	.00000E+00
172 0 0 0 0 0	.0000000E+00	.3566667E+02	.3258333E+02	0	.00000E+00
173 0 0 0 0 0	.0000000E+00	.3083333E+01	.3341111E+02	0	.00000E+00
174 0 0 0 0 0	.0000000E+00	.1541667E+02	.3345834E+02	0	.00000E+00
175 0 0 0 0 0	.0000000E+00	.3191666E+02	.3341666E+02	0	.00000E+00
176 0 0 0 0 0	.0000000E+00	.2931885E+02	.3348764E+02	0	.00000E+00
177 0 0 0 0 0	.0000000E+00	.2680538E+02	.3355632E+02	0	.00000E+00
178 0 0 0 0 0	.0000000E+00	.1604166E+02	.3364584E+02	0	.00000E+00
179 0 0 0 0 0	.0000000E+00	.2429167E+02	.3362500E+02	0	.00000E+00
180 0 0 0 0 0	.0000000E+00	.3875000E+02	.3362500E+02	0	.00000E+00
181 0 0 0 0 0	.0000000E+00	.2177770E+02	.3369369E+02	0	.00000E+00
182 0 0 0 0 0	.0000000E+00	.1926348E+02	.3376239E+02	0	.00000E+00
183 0 0 0 0 0	.0000000E+00	.1666667E+02	.3383334E+02	0	.00000E+00
184 0 0 0 0 0	.0000000E+00	.9250000E+01	.3444583E+02	0	.00000E+00
185 0 0 0 0 0	.0000000E+00	.3500000E+02	.3445833E+02	0	.00000E+00
186 0 0 0 0 0	.0000000E+00	.4183333E+02	.3466666E+02	0	.00000E+00
187 0 0 0 0 0	.0000000E+00	.0000000E+00	.3483334E+02	0	.00000E+00
188 0 0 0 0 0	.0000000E+00	.4491667E+02	.3570833E+02	0	.00000E+00
189 0 0 0 0 0	.0000000E+00	.1233333E+02	.3591667E+02	0	.00000E+00
190 0 0 0 0 0	.0000000E+00	.1358333E+02	.3629167E+02	0	.00000E+00
191 0 0 0 0 0	.0000000E+00	.6166666E+01	.3639445E+02	0	.00000E+00
192 0 0 0 0 0	.0000000E+00	.3433333E+02	.3633333E+02	0	.00000E+00
193 0 0 0 0 0	.0000000E+00	.2781089E+02	.3644483E+02	0	.00000E+00
194 0 0 0 0 0	.0000000E+00	.3103815E+02	.3638966E+02	0	.00000E+00
195 0 0 0 0 0	.0000000E+00	.3775000E+02	.3643750E+02	0	.00000E+00





196 0 0 0 0 0 0	.0000000E+00	.2135546E+02	.3655518E+02	0	.00000E+00
197 0 0 0 0 0 0	.0000000E+00	.2458333E+02	.3650000E+02	0	.00000E+00
198 0 0 0 0 0 0	.0000000E+00	.1483333E+02	.3666667E+02	0	.00000E+00
199 0 0 0 0 0 0	.0000000E+00	.1812727E+02	.3661036E+02	0	.00000E+00
200 0 0 0 0 0 0	.0000000E+00	.4800000E+02	.3675000E+02	0	.00000E+00
201 0 0 0 0 0 0	.0000000E+00	.3083333E+01	.3834305E+02	0	.00000E+00
202 0 0 0 0 0 0	.0000000E+00	.9250000E+01	.3837500E+02	0	.00000E+00
203 0 0 0 0 0 0	.0000000E+00	.4050000E+02	.3841667E+02	0	.00000E+00
204 0 0 0 0 0 0	.0000000E+00	.1112500E+02	.3893750E+02	0	.00000E+00
205 0 0 0 0 0 0	.0000000E+00	.3675000E+02	.3925000E+02	0	.00000E+00
206 0 0 0 0 0 0	.0000000E+00	.2487500E+02	.3937500E+02	0	.00000E+00
207 0 0 0 0 0 0	.0000000E+00	.2881646E+02	.3933351E+02	0	.00000E+00
208 0 0 0 0 0 0	.0000000E+00	.3275765E+02	.3929202E+02	0	.00000E+00
209 0 0 0 0 0 0	.0000000E+00	.1699120E+02	.3945799E+02	0	.00000E+00
210 0 0 0 0 0 0	.0000000E+00	.2093325E+02	.3941649E+02	0	.00000E+00
211 0 0 0 0 0 0	.0000000E+00	.1300000E+02	.3950000E+02	0	.00000E+00
212 0 0 0 0 0 0	.0000000E+00	.0000000E+00	.4029167E+02	0	.00000E+00
213 0 0 0 0 0 0	.0000000E+00	.4325000E+02	.4039583E+02	0	.00000E+00
214 0 0 0 0 0 0	.0000000E+00	.6166666E+01	.4083333E+02	0	.00000E+00
215 0 0 0 0 0 0	.0000000E+00	.8666666E+01	.4158334E+02	0	.00000E+00
216 0 0 0 0 0 0	.0000000E+00	.3447726E+02	.4219458E+02	0	.00000E+00
217 0 0 0 0 0 0	.0000000E+00	.3916666E+02	.4216666E+02	0	.00000E+00
218 0 0 0 0 0 0	.0000000E+00	.1116667E+02	.4233334E+02	0	.00000E+00
219 0 0 0 0 0 0	.0000000E+00	.1585520E+02	.4230543E+02	0	.00000E+00
220 0 0 0 0 0 0	.0000000E+00	.2051105E+02	.4227771E+02	0	.00000E+00
221 0 0 0 0 0 0	.0000000E+00	.2516667E+02	.4225000E+02	0	.00000E+00
222 0 0 0 0 0 0	.0000000E+00	.2982207E+02	.4222229E+02	0	.00000E+00
223 0 0 0 0 0 0	.0000000E+00	.4600000E+02	.4237500E+02	0	.00000E+00
224 0 0 0 0 0 0	.0000000E+00	.3083333E+01	.4329167E+02	0	.00000E+00
225 0 0 0 0 0 0	.0000000E+00	.6208333E+01	.4422917E+02	0	.00000E+00
226 0 0 0 0 0 0	.0000000E+00	.9333333E+01	.4516667E+02	0	.00000E+00
227 0 0 0 0 0 0	.0000000E+00	.1471925E+02	.4515275E+02	0	.00000E+00
228 0 0 0 0 0 0	.0000000E+00	.2008885E+02	.4513887E+02	0	.00000E+00
229 0 0 0 0 0 0	.0000000E+00	.2545833E+02	.4512500E+02	0	.00000E+00
230 0 0 0 0 0 0	.0000000E+00	.3082770E+02	.4511113E+02	0	.00000E+00
231 0 0 0 0 0 0	.0000000E+00	.3619694E+02	.4509725E+02	0	.00000E+00
232 0 0 0 0 0 0	.0000000E+00	.4158333E+02	.4508333E+02	0	.00000E+00
233 0 0 0 0 0 0	.0000000E+00	.0000000E+00	.4575000E+02	0	.00000E+00
234 0 0 0 0 0 0	.0000000E+00	.3750000E+01	.4687500E+02	0	.00000E+00
235 0 0 0 0 0 0	.0000000E+00	.7500000E+01	.4800000E+02	0	.00000E+00
236 0 0 0 0 0 0	.0000000E+00	.1358333E+02	.4800000E+02	0	.00000E+00
237 0 0 0 0 0 0	.0000000E+00	.1966667E+02	.4800000E+02	0	.00000E+00
238 0 0 0 0 0 0	.0000000E+00	.2575000E+02	.4800000E+02	0	.00000E+00
239 0 0 0 0 0 0	.0000000E+00	.3183333E+02	.4800000E+02	0	.00000E+00
240 0 0 0 0 0 0	.0000000E+00	.3791667E+02	.4800000E+02	0	.00000E+00
241 0 0 0 0 0 0	.0000000E+00	.4400000E+02	.4800000E+02	0	.00000E+00
242 1 1 1 1 1 1	.0000000E+00	.0000000E+00	-.1000000E+15	0	.00000E+00
243 1 1 1 1 1 1	.0000000E+00	-.1000000E+15	.0000000E+00	0	.00000E+00
244 1 1 1 1 1 1	-.1000000E+15	.0000000E+00	.0000000E+00	0	.00000E+00
245 1 1 1 1 1 1	.1000000E+15	.0000000E+00	.0000000E+00	0	.00000E+00
246 1 1 1 1 1 1	.0000000E+00	.1000000E+15	.0000000E+00	0	.00000E+00
247 0 0 0 0 0 0	.1100000E+01	.1850000E+02	.1700000E+02	0	.00000E+00
248 0 0 0 0 0 0	.2200000E+01	.1850000E+02	.1700000E+02	0	.00000E+00
249 0 0 0 0 0 0	.3300000E+01	.1850000E+02	.1700000E+02	0	.00000E+00
250 0 0 0 0 0 0	.4400000E+01	.1850000E+02	.1700000E+02	0	.00000E+00



251 0 0 0 0 0	.5500000E+01	.1850000E+02	.1700000E+02	0	.00000E+00
252 0 0 0 0 0	.6600000E+01	.1850000E+02	.1700000E+02	0	.00000E+00
253 0 0 0 0 0	.7700000E+01	.1850000E+02	.1700000E+02	0	.00000E+00
254 0 0 0 0 0	.8800000E+01	.1850000E+02	.1700000E+02	0	.00000E+00
255 0 0 0 0 0	.9900000E+01	.1850000E+02	.1700000E+02	0	.00000E+00
256 0 0 0 0 0	.1100000E+02	.1850000E+02	.1700000E+02	0	.00000E+00
257 0 0 0 0 0	.1120000E+02	.1960000E+02	.1705000E+02	0	.00000E+00
258 0 0 0 0 0	.1140000E+02	.2070000E+02	.1710000E+02	0	.00000E+00
259 0 0 0 0 0	.1160000E+02	.2180000E+02	.1715000E+02	0	.00000E+00
260 0 0 0 0 0	.1180000E+02	.2290000E+02	.1720000E+02	0	.00000E+00
261 0 0 0 0 0	.1200000E+02	.2400000E+02	.1725000E+02	0	.00000E+00
262 0 0 0 0 0	.1220000E+02	.2510000E+02	.1730000E+02	0	.00000E+00
263 0 0 0 0 0	.1240000E+02	.2620000E+02	.1735000E+02	0	.00000E+00
264 0 0 0 0 0	.1260000E+02	.2730000E+02	.1740000E+02	0	.00000E+00
265 0 0 0 0 0	.1280000E+02	.2840000E+02	.1745000E+02	0	.00000E+00
266 0 0 0 0 0	.1300000E+01	.2950000E+02	.1750000E+02	0	.00000E+00
267 0 0 0 0 0	.2600000E+01	.2950000E+02	.1750000E+02	0	.00000E+00
268 0 0 0 0 0	.3900000E+01	.2950000E+02	.1750000E+02	0	.00000E+00
269 0 0 0 0 0	.5200000E+01	.2950000E+02	.1750000E+02	0	.00000E+00
270 0 0 0 0 0	.6500000E+01	.2950000E+02	.1750000E+02	0	.00000E+00
271 0 0 0 0 0	.7800000E+01	.2950000E+02	.1750000E+02	0	.00000E+00
272 0 0 0 0 0	.9100000E+01	.2950000E+02	.1750000E+02	0	.00000E+00
273 0 0 0 0 0	.1040000E+02	.2950000E+02	.1750000E+02	0	.00000E+00
274 0 0 0 0 0	.1170000E+02	.2950000E+02	.1750000E+02	0	.00000E+00
275 0 0 0 0 0	.1300000E+02	.2950000E+02	.1750000E+02	0	.00000E+00
276 0 0 0 0 0	.1100000E+02	.1850000E+02	.1840000E+02	0	.00000E+00
277 0 0 0 0 0	.1300000E+02	.2950000E+02	.1880000E+02	0	.00000E+00
278 0 0 0 0 0	.1100000E+02	.1850000E+02	.1980000E+02	0	.00000E+00
279 0 0 0 0 0	.1300000E+02	.2950000E+02	.2010000E+02	0	.00000E+00
280 0 0 0 0 0	.1100000E+02	.1850000E+02	.2120000E+02	0	.00000E+00
281 0 0 0 0 0	.1300000E+02	.2950000E+02	.2140000E+02	0	.00000E+00
282 0 0 0 0 0	.1100000E+02	.1850000E+02	.2260000E+02	0	.00000E+00
283 0 0 0 0 0	.1300000E+02	.2950000E+02	.2270000E+02	0	.00000E+00
284 0 0 0 0 0	.1100000E+02	.1850000E+02	.2400000E+02	0	.00000E+00
285 0 0 0 0 0	.1300000E+02	.2950000E+02	.2400000E+02	0	.00000E+00
286 0 0 0 0 0	.1300000E+02	.2950000E+02	.2530000E+02	0	.00000E+00
287 0 0 0 0 0	.1100000E+02	.1850000E+02	.2540000E+02	0	.00000E+00
288 0 0 0 0 0	.1300000E+02	.2950000E+02	.2660000E+02	0	.00000E+00
289 0 0 0 0 0	.1100000E+02	.1850000E+02	.2680000E+02	0	.00000E+00
290 0 0 0 0 0	.1300000E+02	.2950000E+02	.2790000E+02	0	.00000E+00
291 0 0 0 0 0	.1100000E+02	.1850000E+02	.2820000E+02	0	.00000E+00
292 0 0 0 0 0	.1300000E+02	.2950000E+02	.2920000E+02	0	.00000E+00
293 0 0 0 0 0	.1100000E+02	.1850000E+02	.2960000E+02	0	.00000E+00
294 0 0 0 0 0	.1300000E+01	.2950000E+02	.3050000E+02	0	.00000E+00
295 0 0 0 0 0	.2600000E+01	.2950000E+02	.3050000E+02	0	.00000E+00
296 0 0 0 0 0	.3900000E+01	.2950000E+02	.3050000E+02	0	.00000E+00
297 0 0 0 0 0	.5200000E+01	.2950000E+02	.3050000E+02	0	.00000E+00
298 0 0 0 0 0	.6500000E+01	.2950000E+02	.3050000E+02	0	.00000E+00
299 0 0 0 0 0	.7800000E+01	.2950000E+02	.3050000E+02	0	.00000E+00
300 0 0 0 0 0	.9100000E+01	.2950000E+02	.3050000E+02	0	.00000E+00
301 0 0 0 0 0	.1040000E+02	.2950000E+02	.3050000E+02	0	.00000E+00
302 0 0 0 0 0	.1170000E+02	.2950000E+02	.3050000E+02	0	.00000E+00
303 0 0 0 0 0	.1300000E+02	.2950000E+02	.3050000E+02	0	.00000E+00
304 0 0 0 0 0	.1280000E+02	.2840000E+02	.3055000E+02	0	.00000E+00
305 0 0 0 0 0	.1260000E+02	.2730000E+02	.3060000E+02	0	.00000E+00





306	0	0	0	0	0	.1240000E+02	.2620000E+02	.3065000E+02	0	.00000E+00
307	0	0	0	0	0	.1220000E+02	.2510000E+02	.3070000E+02	0	.00000E+00
308	0	0	0	0	0	.1200000E+02	.2400000E+02	.3075000E+02	0	.00000E+00
309	0	0	0	0	0	.1180000E+02	.2290000E+02	.3080000E+02	0	.00000E+00
310	0	0	0	0	0	.1160000E+02	.2180000E+02	.3085000E+02	0	.00000E+00
311	0	0	0	0	0	.1140000E+02	.2070000E+02	.3090000E+02	0	.00000E+00
312	0	0	0	0	0	.1120000E+02	.1960000E+02	.3095000E+02	0	.00000E+00
313	0	0	0	0	0	.1100000E+01	.1850000E+02	.3100000E+02	0	.00000E+00
314	0	0	0	0	0	.2200000E+01	.1850000E+02	.3100000E+02	0	.00000E+00
315	0	0	0	0	0	.3300000E+01	.1850000E+02	.3100000E+02	0	.00000E+00
316	0	0	0	0	0	.4400000E+01	.1850000E+02	.3100000E+02	0	.00000E+00
317	0	0	0	0	0	.5500000E+01	.1850000E+02	.3100000E+02	0	.00000E+00
318	0	0	0	0	0	.6600000E+01	.1850000E+02	.3100000E+02	0	.00000E+00
319	0	0	0	0	0	.7700000E+01	.1850000E+02	.3100000E+02	0	.00000E+00
320	0	0	0	0	0	.8800000E+01	.1850000E+02	.3100000E+02	0	.00000E+00
321	0	0	0	0	0	.9900000E+01	.1850000E+02	.3100000E+02	0	.00000E+00
322	0	0	0	0	0	.1100000E+02	.1850000E+02	.3100000E+02	0	.00000E+00
323	1	1	1	1	1	.0000000E+00	.0000000E+00	.1000000E+15	0	.00000E+00

(Plate element material properties and connectivity table.)

6	228	1	0	0	0	0	0	0	0	0
1		.2840E+00	.0000E+00	.6500E-05	.6500E-05	.0000E+00	.3297E+08	.9890E+07	.0000E+00	.3297E+08
		.1154E+08	.1000E+01	.0000E+00	.0000E+00	.0000E+00	.1000E+01	.0000E+00	.0000E+00	.0000E+00
		.0000E+00	.0000E+00	.0000E+00	.0000E+00	.0000E+00	.0000E+00	.0000E+00	.0000E+00	.0000E+00
		.0000E+00	.0000E+00	.0000E+00	.0000E+00	.0000E+00	.0000E+00	.0000E+00	.0000E+00	.0000E+00
		.0000E+00	.0000E+00	.0000E+00	.0000E+00	.0000E+00	.0000E+00	.0000E+00	.0000E+00	.0000E+00
1	1	2	10	9	0	1	0	.2500E+00	.0000E+00	.0000E+00
2	2	3	11	10	0	1	0	.2500E+00	.0000E+00	.0000E+00
3	3	4	12	11	0	1	0	.2500E+00	.0000E+00	.0000E+00
4	4	5	13	12	0	1	0	.2500E+00	.0000E+00	.0000E+00
5	5	6	14	13	0	1	0	.2500E+00	.0000E+00	.0000E+00
6	6	7	15	14	0	1	0	.2500E+00	.0000E+00	.0000E+00
7	7	8	17	15	0	1	0	.2500E+00	.0000E+00	.0000E+00
8	8	16	18	17	0	1	0	.2500E+00	.0000E+00	.0000E+00
9	19	9	10	20	0	1	0	.2500E+00	.0000E+00	.0000E+00
10	20	10	11	21	0	1	0	.2500E+00	.0000E+00	.0000E+00
11	21	11	12	22	0	1	0	.2500E+00	.0000E+00	.0000E+00
12	22	12	13	23	0	1	0	.2500E+00	.0000E+00	.0000E+00
13	26	1	9	29	0	1	0	.2500E+00	.0000E+00	.0000E+00
14	23	13	14	24	0	1	0	.2500E+00	.0000E+00	.0000E+00
15	15	25	24	14	0	1	0	.2500E+00	.0000E+00	.0000E+00
16	25	15	17	27	0	1	0	.2500E+00	.0000E+00	.0000E+00
17	18	28	27	17	0	1	0	.2500E+00	.0000E+00	.0000E+00
18	9	19	39	29	0	1	0	.2500E+00	.0000E+00	.0000E+00
19	16	35	41	18	0	1	0	.2500E+00	.0000E+00	.0000E+00
20	30	19	20	31	0	1	0	.2500E+00	.0000E+00	.0000E+00
21	31	20	21	32	0	1	0	.2500E+00	.0000E+00	.0000E+00
22	32	21	22	33	0	1	0	.2500E+00	.0000E+00	.0000E+00
23	33	22	23	34	0	1	0	.2500E+00	.0000E+00	.0000E+00
24	34	23	24	36	0	1	0	.2500E+00	.0000E+00	.0000E+00
25	25	37	36	24	0	1	0	.2500E+00	.0000E+00	.0000E+00



26	37	25	27	38	0	1	0	.2500E+00	.0000E+00	.0000E+00	.0000E+00
27	28	40	38	27	0	1	0	.2500E+00	.0000E+00	.0000E+00	.0000E+00
28	19	30	49	39	0	1	0	.2500E+00	.0000E+00	.0000E+00	.0000E+00
29	28	18	41	51	0	1	0	.2500E+00	.0000E+00	.0000E+00	.0000E+00
30	42	30	31	43	0	1	0	.2500E+00	.0000E+00	.0000E+00	.0000E+00
31	43	31	32	44	0	1	0	.2500E+00	.0000E+00	.0000E+00	.0000E+00
32	44	32	33	45	0	1	0	.2500E+00	.0000E+00	.0000E+00	.0000E+00
33	45	33	34	46	0	1	0	.2500E+00	.0000E+00	.0000E+00	.0000E+00
34	46	34	36	47	0	1	0	.2500E+00	.0000E+00	.0000E+00	.0000E+00
35	37	48	47	36	0	1	0	.2500E+00	.0000E+00	.0000E+00	.0000E+00
36	53	26	29	55	0	1	0	.2500E+00	.0000E+00	.0000E+00	.0000E+00
37	48	37	38	50	0	1	0	.2500E+00	.0000E+00	.0000E+00	.0000E+00
38	40	52	50	38	0	1	0	.2500E+00	.0000E+00	.0000E+00	.0000E+00
39	40	28	51	57	0	1	0	.2500E+00	.0000E+00	.0000E+00	.0000E+00
40	30	42	54	49	0	1	0	.2500E+00	.0000E+00	.0000E+00	.0000E+00
41	59	55	29	39	0	1	0	.2500E+00	.0000E+00	.0000E+00	.0000E+00
42	35	61	70	41	0	1	0	.2500E+00	.0000E+00	.0000E+00	.0000E+00
43	67	59	39	49	0	1	0	.2500E+00	.0000E+00	.0000E+00	.0000E+00
44	56	42	43	58	0	1	0	.2500E+00	.0000E+00	.0000E+00	.0000E+00
45	58	43	44	60	0	1	0	.2500E+00	.0000E+00	.0000E+00	.0000E+00
46	60	44	45	62	0	1	0	.2500E+00	.0000E+00	.0000E+00	.0000E+00
47	62	45	46	63	0	1	0	.2500E+00	.0000E+00	.0000E+00	.0000E+00
48	63	46	47	64	0	1	0	.2500E+00	.0000E+00	.0000E+00	.0000E+00
49	48	65	64	47	0	1	0	.2500E+00	.0000E+00	.0000E+00	.0000E+00
50	52	40	57	72	0	1	0	.2500E+00	.0000E+00	.0000E+00	.0000E+00
51	65	48	50	66	0	1	0	.2500E+00	.0000E+00	.0000E+00	.0000E+00
52	42	56	69	54	0	1	0	.2500E+00	.0000E+00	.0000E+00	.0000E+00
53	52	68	66	50	0	1	0	.2500E+00	.0000E+00	.0000E+00	.0000E+00
54	51	41	70	74	0	1	0	.2500E+00	.0000E+00	.0000E+00	.0000E+00
55	71	67	49	54	0	1	0	.2500E+00	.0000E+00	.0000E+00	.0000E+00
56	73	71	54	69	0	1	0	.2500E+00	.0000E+00	.0000E+00	.0000E+00
57	57	51	74	83	0	1	0	.2500E+00	.0000E+00	.0000E+00	.0000E+00
58	68	52	72	82	0	1	0	.2500E+00	.0000E+00	.0000E+00	.0000E+00
59	56	75	69	0	0	1	0	.2500E+00	.0000E+00	.0000E+00	.0000E+00
60	76	75	56	58	0	1	0	.2500E+00	.0000E+00	.0000E+00	.0000E+00
61	77	76	58	60	0	1	0	.2500E+00	.0000E+00	.0000E+00	.0000E+00
62	81	65	66	0	0	1	0	.2500E+00	.0000E+00	.0000E+00	.0000E+00
63	78	77	60	62	0	1	0	.2500E+00	.0000E+00	.0000E+00	.0000E+00
64	79	78	62	63	0	1	0	.2500E+00	.0000E+00	.0000E+00	.0000E+00
65	68	81	66	0	0	1	0	.2500E+00	.0000E+00	.0000E+00	.0000E+00
66	84	53	55	85	0	1	0	.2500E+00	.0000E+00	.0000E+00	.0000E+00
67	80	79	63	64	0	1	0	.2500E+00	.0000E+00	.0000E+00	.0000E+00
68	65	81	80	64	0	1	0	.2500E+00	.0000E+00	.0000E+00	.0000E+00
69	75	73	69	0	0	1	0	.2500E+00	.0000E+00	.0000E+00	.0000E+00
70	55	59	86	85	0	1	0	.2500E+00	.0000E+00	.0000E+00	.0000E+00
71	59	67	87	86	0	1	0	.2500E+00	.0000E+00	.0000E+00	.0000E+00
72	72	57	83	90	0	1	0	.2500E+00	.0000E+00	.0000E+00	.0000E+00
73	67	71	88	87	0	1	0	.2500E+00	.0000E+00	.0000E+00	.0000E+00
74	97	81	68	82	0	1	0	.2500E+00	.0000E+00	.0000E+00	.0000E+00
75	71	73	89	88	0	1	0	.2500E+00	.0000E+00	.0000E+00	.0000E+00
76	61	98	100	70	0	1	0	.2500E+00	.0000E+00	.0000E+00	.0000E+00
77	73	75	91	89	0	1	0	.2500E+00	.0000E+00	.0000E+00	.0000E+00
78	75	76	92	91	0	1	0	.2500E+00	.0000E+00	.0000E+00	.0000E+00
79	77	93	92	76	0	1	0	.2500E+00	.0000E+00	.0000E+00	.0000E+00
80	93	77	78	94	0	1	0	.2500E+00	.0000E+00	.0000E+00	.0000E+00



81	78	79	95	94	0	1	0	.2500E+00	.0000E+00	.0000E+00	.0000E+00
82	82	72	90	99	0	1	0	.2500E+00	.0000E+00	.0000E+00	.0000E+00
83	80	96	95	79	0	1	0	.2500E+00	.0000E+00	.0000E+00	.0000E+00
84	81	97	96	80	0	1	0	.2500E+00	.0000E+00	.0000E+00	.0000E+00
85	74	70	100	101	0	1	0	.2500E+00	.0000E+00	.0000E+00	.0000E+00
86	83	74	101	109	0	1	0	.2500E+00	.0000E+00	.0000E+00	.0000E+00
87	108	97	82	99	0	1	0	.2500E+00	.0000E+00	.0000E+00	.0000E+00
88	90	83	109	112	0	1	0	.2500E+00	.0000E+00	.0000E+00	.0000E+00
89	91	102	110	89	0	1	0	.2500E+00	.0000E+00	.0000E+00	.0000E+00
90	103	102	91	92	0	1	0	.2500E+00	.0000E+00	.0000E+00	.0000E+00
91	104	103	92	93	0	1	0	.2500E+00	.0000E+00	.0000E+00	.0000E+00
92	94	105	104	93	0	1	0	.2500E+00	.0000E+00	.0000E+00	.0000E+00
93	105	94	95	106	0	1	0	.2500E+00	.0000E+00	.0000E+00	.0000E+00
94	110	111	88	89	0	1	0	.2500E+00	.0000E+00	.0000E+00	.0000E+00
95	107	106	95	96	0	1	0	.2500E+00	.0000E+00	.0000E+00	.0000E+00
96	97	108	107	96	0	1	0	.2500E+00	.0000E+00	.0000E+00	.0000E+00
97	111	113	87	88	0	1	0	.2500E+00	.0000E+00	.0000E+00	.0000E+00
98	113	114	86	87	0	1	0	.2500E+00	.0000E+00	.0000E+00	.0000E+00
99	114	116	85	86	0	1	0	.2500E+00	.0000E+00	.0000E+00	.0000E+00
100	117	84	85	116	0	1	0	.2500E+00	.0000E+00	.0000E+00	.0000E+00
101	99	90	112	115	0	1	0	.2500E+00	.0000E+00	.0000E+00	.0000E+00
102	124	108	99	115	0	1	0	.2500E+00	.0000E+00	.0000E+00	.0000E+00
103	118	102	103	119	0	1	0	.2500E+00	.0000E+00	.0000E+00	.0000E+00
104	120	119	103	104	0	1	0	.2500E+00	.0000E+00	.0000E+00	.0000E+00
105	105	121	120	104	0	1	0	.2500E+00	.0000E+00	.0000E+00	.0000E+00
106	121	105	106	122	0	1	0	.2500E+00	.0000E+00	.0000E+00	.0000E+00
107	123	122	106	107	0	1	0	.2500E+00	.0000E+00	.0000E+00	.0000E+00
108	108	124	123	107	0	1	0	.2500E+00	.0000E+00	.0000E+00	.0000E+00
109	98	126	127	100	0	1	0	.2500E+00	.0000E+00	.0000E+00	.0000E+00
110	102	118	125	110	0	1	0	.2500E+00	.0000E+00	.0000E+00	.0000E+00
111	101	100	127	129	0	1	0	.2500E+00	.0000E+00	.0000E+00	.0000E+00
112	109	101	129	130	0	1	0	.2500E+00	.0000E+00	.0000E+00	.0000E+00
113	125	128	111	110	0	1	0	.2500E+00	.0000E+00	.0000E+00	.0000E+00
114	112	109	130	131	0	1	0	.2500E+00	.0000E+00	.0000E+00	.0000E+00
115	128	140	113	111	0	1	0	.2500E+00	.0000E+00	.0000E+00	.0000E+00
116	115	112	131	132	0	1	0	.2500E+00	.0000E+00	.0000E+00	.0000E+00
117	139	124	115	132	0	1	0	.2500E+00	.0000E+00	.0000E+00	.0000E+00
118	140	141	114	113	0	1	0	.2500E+00	.0000E+00	.0000E+00	.0000E+00
119	134	133	118	119	0	1	0	.2500E+00	.0000E+00	.0000E+00	.0000E+00
120	119	120	135	134	0	1	0	.2500E+00	.0000E+00	.0000E+00	.0000E+00
121	121	136	135	120	0	1	0	.2500E+00	.0000E+00	.0000E+00	.0000E+00
122	136	121	122	137	0	1	0	.2500E+00	.0000E+00	.0000E+00	.0000E+00
123	122	123	138	137	0	1	0	.2500E+00	.0000E+00	.0000E+00	.0000E+00
124	124	139	138	123	0	1	0	.2500E+00	.0000E+00	.0000E+00	.0000E+00
125	141	143	116	114	0	1	0	.2500E+00	.0000E+00	.0000E+00	.0000E+00
126	118	133	142	125	0	1	0	.2500E+00	.0000E+00	.0000E+00	.0000E+00
127	154	117	116	143	0	1	0	.2500E+00	.0000E+00	.0000E+00	.0000E+00
128	142	152	128	125	0	1	0	.2500E+00	.0000E+00	.0000E+00	.0000E+00
129	136	147	150	135	0	1	0	.2500E+00	.0000E+00	.0000E+00	.0000E+00
130	147	136	137	144	0	1	0	.2500E+00	.0000E+00	.0000E+00	.0000E+00
131	137	138	145	144	0	1	0	.2500E+00	.0000E+00	.0000E+00	.0000E+00
132	139	146	145	138	0	1	0	.2500E+00	.0000E+00	.0000E+00	.0000E+00
133	133	134	149	148	0	1	0	.2500E+00	.0000E+00	.0000E+00	.0000E+00
134	134	135	150	149	0	1	0	.2500E+00	.0000E+00	.0000E+00	.0000E+00
135	146	139	132	151	0	1	0	.2500E+00	.0000E+00	.0000E+00	.0000E+00





136	132	131	153	151	0	1	0	.2500E+00	.0000E+00	.0000E+00	.0000E+00
137	131	130	155	153	0	1	0	.2500E+00	.0000E+00	.0000E+00	.0000E+00
138	130	129	156	155	0	1	0	.2500E+00	.0000E+00	.0000E+00	.0000E+00
139	152	158	140	128	0	1	0	.2500E+00	.0000E+00	.0000E+00	.0000E+00
140	129	127	162	156	0	1	0	.2500E+00	.0000E+00	.0000E+00	.0000E+00
141	133	148	159	142	0	1	0	.2500E+00	.0000E+00	.0000E+00	.0000E+00
142	126	167	162	127	0	1	0	.2500E+00	.0000E+00	.0000E+00	.0000E+00
143	158	169	141	140	0	1	0	.2500E+00	.0000E+00	.0000E+00	.0000E+00
144	160	161	144	145	0	1	0	.2500E+00	.0000E+00	.0000E+00	.0000E+00
145	157	160	145	146	0	1	0	.2500E+00	.0000E+00	.0000E+00	.0000E+00
146	164	165	149	150	0	1	0	.2500E+00	.0000E+00	.0000E+00	.0000E+00
147	163	164	150	147	0	1	0	.2500E+00	.0000E+00	.0000E+00	.0000E+00
148	161	163	147	144	0	1	0	.2500E+00	.0000E+00	.0000E+00	.0000E+00
149	166	148	149	165	0	1	0	.2500E+00	.0000E+00	.0000E+00	.0000E+00
150	168	157	146	151	0	1	0	.2500E+00	.0000E+00	.0000E+00	.0000E+00
151	159	170	152	142	0	1	0	.2500E+00	.0000E+00	.0000E+00	.0000E+00
152	169	173	143	141	0	1	0	.2500E+00	.0000E+00	.0000E+00	.0000E+00
153	172	168	151	153	0	1	0	.2500E+00	.0000E+00	.0000E+00	.0000E+00
154	148	166	174	159	0	1	0	.2500E+00	.0000E+00	.0000E+00	.0000E+00
155	180	172	153	155	0	1	0	.2500E+00	.0000E+00	.0000E+00	.0000E+00
156	187	154	143	173	0	1	0	.2500E+00	.0000E+00	.0000E+00	.0000E+00
157	157	168	171	0	0	1	0	.2500E+00	.0000E+00	.0000E+00	.0000E+00
158	170	184	158	152	0	1	0	.2500E+00	.0000E+00	.0000E+00	.0000E+00
159	160	157	175	176	0	1	0	.2500E+00	.0000E+00	.0000E+00	.0000E+00
160	161	160	176	177	0	1	0	.2500E+00	.0000E+00	.0000E+00	.0000E+00
161	175	157	171	0	0	1	0	.2500E+00	.0000E+00	.0000E+00	.0000E+00
162	186	180	155	156	0	1	0	.2500E+00	.0000E+00	.0000E+00	.0000E+00
163	163	161	177	179	0	1	0	.2500E+00	.0000E+00	.0000E+00	.0000E+00
164	164	163	179	181	0	1	0	.2500E+00	.0000E+00	.0000E+00	.0000E+00
165	165	164	181	182	0	1	0	.2500E+00	.0000E+00	.0000E+00	.0000E+00
166	183	166	165	182	0	1	0	.2500E+00	.0000E+00	.0000E+00	.0000E+00
167	174	166	178	0	0	1	0	.2500E+00	.0000E+00	.0000E+00	.0000E+00
168	166	183	178	0	0	1	0	.2500E+00	.0000E+00	.0000E+00	.0000E+00
169	168	172	185	171	0	1	0	.2500E+00	.0000E+00	.0000E+00	.0000E+00
170	188	186	156	162	0	1	0	.2500E+00	.0000E+00	.0000E+00	.0000E+00
171	174	189	170	159	0	1	0	.2500E+00	.0000E+00	.0000E+00	.0000E+00
172	184	191	169	158	0	1	0	.2500E+00	.0000E+00	.0000E+00	.0000E+00
173	167	200	188	162	0	1	0	.2500E+00	.0000E+00	.0000E+00	.0000E+00
174	192	175	171	185	0	1	0	.2500E+00	.0000E+00	.0000E+00	.0000E+00
175	172	180	195	185	0	1	0	.2500E+00	.0000E+00	.0000E+00	.0000E+00
176	189	174	178	190	0	1	0	.2500E+00	.0000E+00	.0000E+00	.0000E+00
177	175	192	194	176	0	1	0	.2500E+00	.0000E+00	.0000E+00	.0000E+00
178	191	201	173	169	0	1	0	.2500E+00	.0000E+00	.0000E+00	.0000E+00
179	176	194	193	177	0	1	0	.2500E+00	.0000E+00	.0000E+00	.0000E+00
180	183	198	190	178	0	1	0	.2500E+00	.0000E+00	.0000E+00	.0000E+00
181	181	196	199	182	0	1	0	.2500E+00	.0000E+00	.0000E+00	.0000E+00
182	179	197	196	181	0	1	0	.2500E+00	.0000E+00	.0000E+00	.0000E+00
183	177	193	197	179	0	1	0	.2500E+00	.0000E+00	.0000E+00	.0000E+00
184	198	183	182	199	0	1	0	.2500E+00	.0000E+00	.0000E+00	.0000E+00
185	189	202	184	170	0	1	0	.2500E+00	.0000E+00	.0000E+00	.0000E+00
186	180	186	203	195	0	1	0	.2500E+00	.0000E+00	.0000E+00	.0000E+00
187	205	192	185	195	0	1	0	.2500E+00	.0000E+00	.0000E+00	.0000E+00
188	212	187	173	201	0	1	0	.2500E+00	.0000E+00	.0000E+00	.0000E+00
189	186	188	213	203	0	1	0	.2500E+00	.0000E+00	.0000E+00	.0000E+00
190	202	189	190	204	0	1	0	.2500E+00	.0000E+00	.0000E+00	.0000E+00





191	202	214	191	184	0	1	0	.2500E+00	.0000E+00	.0000E+00	.0000E+00
192	198	211	204	190	0	1	0	.2500E+00	.0000E+00	.0000E+00	.0000E+00
193	194	208	207	193	0	1	0	.2500E+00	.0000E+00	.0000E+00	.0000E+00
194	192	205	208	194	0	1	0	.2500E+00	.0000E+00	.0000E+00	.0000E+00
195	193	207	206	197	0	1	0	.2500E+00	.0000E+00	.0000E+00	.0000E+00
196	211	198	199	209	0	1	0	.2500E+00	.0000E+00	.0000E+00	.0000E+00
197	196	210	209	199	0	1	0	.2500E+00	.0000E+00	.0000E+00	.0000E+00
198	197	206	210	196	0	1	0	.2500E+00	.0000E+00	.0000E+00	.0000E+00
199	200	223	213	188	0	1	0	.2500E+00	.0000E+00	.0000E+00	.0000E+00
200	217	205	195	203	0	1	0	.2500E+00	.0000E+00	.0000E+00	.0000E+00
201	214	224	201	191	0	1	0	.2500E+00	.0000E+00	.0000E+00	.0000E+00
202	214	202	204	215	0	1	0	.2500E+00	.0000E+00	.0000E+00	.0000E+00
203	211	218	215	204	0	1	0	.2500E+00	.0000E+00	.0000E+00	.0000E+00
204	208	216	222	207	0	1	0	.2500E+00	.0000E+00	.0000E+00	.0000E+00
205	205	217	216	208	0	1	0	.2500E+00	.0000E+00	.0000E+00	.0000E+00
206	207	222	221	206	0	1	0	.2500E+00	.0000E+00	.0000E+00	.0000E+00
207	218	211	209	219	0	1	0	.2500E+00	.0000E+00	.0000E+00	.0000E+00
208	210	220	219	209	0	1	0	.2500E+00	.0000E+00	.0000E+00	.0000E+00
209	206	221	220	210	0	1	0	.2500E+00	.0000E+00	.0000E+00	.0000E+00
210	232	217	203	213	0	1	0	.2500E+00	.0000E+00	.0000E+00	.0000E+00
211	233	212	201	224	0	1	0	.2500E+00	.0000E+00	.0000E+00	.0000E+00
212	224	214	215	225	0	1	0	.2500E+00	.0000E+00	.0000E+00	.0000E+00
213	218	226	225	215	0	1	0	.2500E+00	.0000E+00	.0000E+00	.0000E+00
214	217	232	231	216	0	1	0	.2500E+00	.0000E+00	.0000E+00	.0000E+00
215	226	218	219	227	0	1	0	.2500E+00	.0000E+00	.0000E+00	.0000E+00
216	220	228	227	219	0	1	0	.2500E+00	.0000E+00	.0000E+00	.0000E+00
217	221	229	228	220	0	1	0	.2500E+00	.0000E+00	.0000E+00	.0000E+00
218	222	230	229	221	0	1	0	.2500E+00	.0000E+00	.0000E+00	.0000E+00
219	216	231	230	222	0	1	0	.2500E+00	.0000E+00	.0000E+00	.0000E+00
220	223	241	232	213	0	1	0	.2500E+00	.0000E+00	.0000E+00	.0000E+00
221	234	233	224	225	0	1	0	.2500E+00	.0000E+00	.0000E+00	.0000E+00
222	235	234	225	226	0	1	0	.2500E+00	.0000E+00	.0000E+00	.0000E+00
223	236	235	226	227	0	1	0	.2500E+00	.0000E+00	.0000E+00	.0000E+00
224	237	236	227	228	0	1	0	.2500E+00	.0000E+00	.0000E+00	.0000E+00
225	238	237	228	229	0	1	0	.2500E+00	.0000E+00	.0000E+00	.0000E+00
226	239	238	229	230	0	1	0	.2500E+00	.0000E+00	.0000E+00	.0000E+00
227	240	239	230	231	0	1	0	.2500E+00	.0000E+00	.0000E+00	.0000E+00
228	241	240	231	232	0	1	0	.2500E+00	.0000E+00	.0000E+00	.0000E+00

(Beam element material properties and connectivity table.)

2	80	3	0	1	0	0	0	0	0	0
1	.3000E+08	.3000E+00	.0000E+00	.2830E+00	.00E+00	.00E+00	.00E+00	.00E+00	.0000	
1	.3200E+00	.4800E-01	.4800E-01	.4015E-01	.2010E-01	.2010E-01	.2010E-01	.0001E+00	.0000	.0000
.0000										
2	.3200E+00	.4800E-01	.4800E-01	.4015E-01	.2010E-01	.2010E-01	.2010E-01	.0001E+00	.0000	.0000
.0000										
3	.3200E+00	.4800E-01	.4800E-01	.4015E-01	.2010E-01	.2010E-01	.2010E-01	.0001E+00	.0000	.0000
.0000										
.0000E+00	.0000E+00	.0000E+00	.0000E+00	.0000E+00						
.0000E+00	.0000E+00	.0000E+00	.0000E+00	.0000E+00						
.0000E+00	.0000E+00	.0000E+00	.0000E+00	.0000E+00						
1	293	322	246	1	3	0	0	0	0	0
2	291	293	246	1	3	0	0	0	0	0



3	289	291	246	1	3	0	0	0	0	0	0	0	0
4	287	289	246	1	3	0	0	0	0	0	0	0	0
5	284	287	246	1	3	0	0	0	0	0	0	0	0
6	282	284	246	1	3	0	0	0	0	0	0	0	0
7	280	282	246	1	3	0	0	0	0	0	0	0	0
8	278	280	246	1	3	0	0	0	0	0	0	0	0
9	276	278	246	1	3	0	0	0	0	0	0	0	0
10	256	276	246	1	3	0	0	0	0	0	0	0	0
11	166	313	323	1	1	0	0	0	0	0	0	0	0
12	313	314	323	1	1	0	0	0	0	0	0	0	0
13	314	315	323	1	1	0	0	0	0	0	0	0	0
14	315	316	323	1	1	0	0	0	0	0	0	0	0
15	316	317	323	1	1	0	0	0	0	0	0	0	0
16	317	318	323	1	1	0	0	0	0	0	0	0	0
17	318	319	323	1	1	0	0	0	0	0	0	0	0
18	319	320	323	1	1	0	0	0	0	0	0	0	0
19	320	321	323	1	1	0	0	0	0	0	0	0	0
20	321	322	323	1	1	0	0	0	0	0	0	0	0
21	75	247	323	1	1	0	0	0	0	0	0	0	0
22	247	248	323	1	1	0	0	0	0	0	0	0	0
23	248	249	323	1	1	0	0	0	0	0	0	0	0
24	249	250	323	1	1	0	0	0	0	0	0	0	0
25	250	251	323	1	1	0	0	0	0	0	0	0	0
26	251	252	323	1	1	0	0	0	0	0	0	0	0
27	252	253	323	1	1	0	0	0	0	0	0	0	0
28	253	254	323	1	1	0	0	0	0	0	0	0	0
29	254	255	323	1	1	0	0	0	0	0	0	0	0
30	255	256	323	1	1	0	0	0	0	0	0	0	0
31	266	267	323	1	2	0	0	0	0	0	0	0	0
32	267	268	323	1	2	0	0	0	0	0	0	0	0
33	268	269	323	1	2	0	0	0	0	0	0	0	0
34	269	270	323	1	2	0	0	0	0	0	0	0	0
35	270	271	323	1	2	0	0	0	0	0	0	0	0
36	271	272	323	1	2	0	0	0	0	0	0	0	0
37	272	273	323	1	2	0	0	0	0	0	0	0	0
38	273	274	323	1	2	0	0	0	0	0	0	0	0
39	274	275	323	1	2	0	0	0	0	0	0	0	0
40	275	277	246	1	2	0	0	0	0	0	0	0	0
41	277	279	246	1	2	0	0	0	0	0	0	0	0
42	279	281	246	1	2	0	0	0	0	0	0	0	0
43	281	283	246	1	2	0	0	0	0	0	0	0	0
44	283	285	246	1	2	0	0	0	0	0	0	0	0
45	285	286	246	1	2	0	0	0	0	0	0	0	0
46	286	288	246	1	2	0	0	0	0	0	0	0	0
47	288	290	246	1	2	0	0	0	0	0	0	0	0
48	290	292	246	1	2	0	0	0	0	0	0	0	0
49	292	303	246	1	2	0	0	0	0	0	0	0	0
50	302	303	323	1	2	0	0	0	0	0	0	0	0
51	301	302	323	1	2	0	0	0	0	0	0	0	0
52	300	301	323	1	2	0	0	0	0	0	0	0	0
53	299	300	323	1	2	0	0	0	0	0	0	0	0
54	298	299	323	1	2	0	0	0	0	0	0	0	0
55	297	298	323	1	2	0	0	0	0	0	0	0	0
56	296	297	323	1	2	0	0	0	0	0	0	0	0
57	295	296	323	1	2	0	0	0	0	0	0	0	0



58	294	295	323	1	2	0	0	0	0	0	0	0	0
59	157	294	323	1	2	0	0	0	0	0	0	0	0
60	81	266	323	1	2	0	0	0	0	0	0	0	0
61	256	257	323	1	1	0	0	0	0	0	0	0	0
62	257	258	323	1	1	0	0	0	0	0	0	0	0
63	258	259	323	1	1	0	0	0	0	0	0	0	0
64	259	260	323	1	1	0	0	0	0	0	0	0	0
65	260	261	323	1	1	0	0	0	0	0	0	0	0
66	261	262	323	1	1	0	0	0	0	0	0	0	0
67	262	263	323	1	1	0	0	0	0	0	0	0	0
68	263	264	323	1	1	0	0	0	0	0	0	0	0
69	264	265	323	1	1	0	0	0	0	0	0	0	0
70	265	275	323	1	1	0	0	0	0	0	0	0	0
71	312	322	323	1	1	0	0	0	0	0	0	0	0
72	311	312	323	1	1	0	0	0	0	0	0	0	0
73	310	311	323	1	1	0	0	0	0	0	0	0	0
74	309	310	323	1	1	0	0	0	0	0	0	0	0
75	308	309	323	1	1	0	0	0	0	0	0	0	0
76	307	308	323	1	1	0	0	0	0	0	0	0	0
77	306	307	323	1	1	0	0	0	0	0	0	0	0
78	305	306	323	1	1	0	0	0	0	0	0	0	0
79	304	305	323	1	1	0	0	0	0	0	0	0	0
80	303	304	323	1	1	0	0	0	0	0	0	0	0

(Nodal loading data.)

1	0	.3950E-03	.3950E-03	.3950E-03	.0000E+00	.0000E+00	.0000E+00	0
2	0	.3384E-03	.3384E-03	.3384E-03	.0000E+00	.0000E+00	.0000E+00	0
3	0	.3401E-03	.3401E-03	.3401E-03	.0000E+00	.0000E+00	.0000E+00	0
4	0	.3419E-03	.3419E-03	.3419E-03	.0000E+00	.0000E+00	.0000E+00	0
5	0	.3436E-03	.3436E-03	.3436E-03	.0000E+00	.0000E+00	.0000E+00	0
6	0	.3454E-03	.3454E-03	.3454E-03	.0000E+00	.0000E+00	.0000E+00	0
7	0	.3334E-03	.3334E-03	.3334E-03	.0000E+00	.0000E+00	.0000E+00	0
8	0	.3206E-03	.3206E-03	.3206E-03	.0000E+00	.0000E+00	.0000E+00	0
9	0	.7285E-03	.7285E-03	.7285E-03	.0000E+00	.0000E+00	.0000E+00	0
10	0	.3181E-03	.3181E-03	.3181E-03	.0000E+00	.0000E+00	.0000E+00	0
11	0	.6396E-03	.6396E-03	.6396E-03	.0000E+00	.0000E+00	.0000E+00	0
12	0	.6431E-03	.6431E-03	.6431E-03	.0000E+00	.0000E+00	.0000E+00	0
13	0	.6466E-03	.6466E-03	.6466E-03	.0000E+00	.0000E+00	.0000E+00	0
14	0	.6502E-03	.6502E-03	.6502E-03	.0000E+00	.0000E+00	.0000E+00	0
15	0	.6174E-03	.6174E-03	.6174E-03	.0000E+00	.0000E+00	.0000E+00	0
16	0	.6919E-03	.6919E-03	.6919E-03	.0000E+00	.0000E+00	.0000E+00	0
17	0	.5829E-03	.5829E-03	.5829E-03	.0000E+00	.0000E+00	.0000E+00	0
18	0	.6427E-03	.6427E-03	.6427E-03	.0000E+00	.0000E+00	.0000E+00	0
19	0	.6056E-03	.6056E-03	.6056E-03	.0000E+00	.0000E+00	.0000E+00	0
20	0	.2774E-03	.2774E-03	.2774E-03	.0000E+00	.0000E+00	.0000E+00	0
21	0	.5584E-03	.5584E-03	.5584E-03	.0000E+00	.0000E+00	.0000E+00	0
22	0	.5618E-03	.5618E-03	.5618E-03	.0000E+00	.0000E+00	.0000E+00	0
23	0	.5654E-03	.5654E-03	.5654E-03	.0000E+00	.0000E+00	.0000E+00	0
24	0	.5689E-03	.5689E-03	.5689E-03	.0000E+00	.0000E+00	.0000E+00	0
25	0	.5225E-03	.5225E-03	.5225E-03	.0000E+00	.0000E+00	.0000E+00	0
26	0	.9049E-03	.9049E-03	.9049E-03	.0000E+00	.0000E+00	.0000E+00	0
27	0	.4663E-03	.4663E-03	.4663E-03	.0000E+00	.0000E+00	.0000E+00	0
28	0	.5443E-03	.5443E-03	.5443E-03	.0000E+00	.0000E+00	.0000E+00	0





29 0.4113E-03 .4113E-03 .4113E-03 .0000E+00 .0000E+00 .0000E+00 0  
 30 0.4827E-03 .4827E-03 .4827E-03 .0000E+00 .0000E+00 .0000E+00 0  
 31 0.4736E-03 .4736E-03 .4736E-03 .0000E+00 .0000E+00 .0000E+00 0  
 32 0.4771E-03 .4771E-03 .4771E-03 .0000E+00 .0000E+00 .0000E+00 0  
 33 0.4806E-03 .4806E-03 .4806E-03 .0000E+00 .0000E+00 .0000E+00 0  
 34 0.4841E-03 .4841E-03 .4841E-03 .0000E+00 .0000E+00 .0000E+00 0  
 35 0.7426E-03 .7426E-03 .7426E-03 .0000E+00 .0000E+00 .0000E+00 0  
 36 0.4880E-03 .4880E-03 .4880E-03 .0000E+00 .0000E+00 .0000E+00 0  
 37 0.4195E-03 .4195E-03 .4195E-03 .0000E+00 .0000E+00 .0000E+00 0  
 38 0.3497E-03 .3497E-03 .3497E-03 .0000E+00 .0000E+00 .0000E+00 0  
 39 0.6581E-03 .6581E-03 .6581E-03 .0000E+00 .0000E+00 .0000E+00 0  
 40 0.4459E-03 .4459E-03 .4459E-03 .0000E+00 .0000E+00 .0000E+00 0  
 41 0.7025E-03 .7025E-03 .7025E-03 .0000E+00 .0000E+00 .0000E+00 0  
 42 0.3582E-03 .3582E-03 .3582E-03 .0000E+00 .0000E+00 .0000E+00 0  
 43 0.3923E-03 .3923E-03 .3923E-03 .0000E+00 .0000E+00 .0000E+00 0  
 44 0.3958E-03 .3958E-03 .3958E-03 .0000E+00 .0000E+00 .0000E+00 0  
 45 0.3993E-03 .3993E-03 .3993E-03 .0000E+00 .0000E+00 .0000E+00 0  
 46 0.4028E-03 .4028E-03 .4028E-03 .0000E+00 .0000E+00 .0000E+00 0  
 47 0.2032E-03 .2032E-03 .2032E-03 .0000E+00 .0000E+00 .0000E+00 0  
 48 0.3206E-03 .3206E-03 .3206E-03 .0000E+00 .0000E+00 .0000E+00 0  
 49 0.4936E-03 .4936E-03 .4936E-03 .0000E+00 .0000E+00 .0000E+00 0  
 50 0.2332E-03 .2332E-03 .2332E-03 .0000E+00 .0000E+00 .0000E+00 0  
 51 0.6223E-03 .6223E-03 .6223E-03 .0000E+00 .0000E+00 .0000E+00 0  
 52 0.3475E-03 .3475E-03 .3475E-03 .0000E+00 .0000E+00 .0000E+00 0  
 53 0.8141E-03 .8141E-03 .8141E-03 .0000E+00 .0000E+00 .0000E+00 0  
 54 0.3291E-03 .3291E-03 .3291E-03 .0000E+00 .0000E+00 .0000E+00 0  
 55 0.3774E-03 .3774E-03 .3774E-03 .0000E+00 .0000E+00 .0000E+00 0  
 56 0.2329E-03 .2329E-03 .2329E-03 .0000E+00 .0000E+00 .0000E+00 0  
 57 0.5421E-03 .5421E-03 .5421E-03 .0000E+00 .0000E+00 .0000E+00 0  
 58 0.3070E-03 .3070E-03 .3070E-03 .0000E+00 .0000E+00 .0000E+00 0  
 59 0.6363E-03 .6363E-03 .6363E-03 .0000E+00 .0000E+00 .0000E+00 0  
 60 0.3145E-03 .3145E-03 .3145E-03 .0000E+00 .0000E+00 .0000E+00 0  
 61 0.7426E-03 .7426E-03 .7426E-03 .0000E+00 .0000E+00 .0000E+00 0  
 62 0.3181E-03 .3181E-03 .3181E-03 .0000E+00 .0000E+00 .0000E+00 0  
 63 0.3215E-03 .3215E-03 .3215E-03 .0000E+00 .0000E+00 .0000E+00 0  
 64 0.3251E-03 .3251E-03 .3251E-03 .0000E+00 .0000E+00 .0000E+00 0  
 65 0.2217E-03 .2217E-03 .2217E-03 .0000E+00 .0000E+00 .0000E+00 0  
 66 0.1166E-03 .1166E-03 .1166E-03 .0000E+00 .0000E+00 .0000E+00 0  
 67 0.5178E-03 .5178E-03 .5178E-03 .0000E+00 .0000E+00 .0000E+00 0  
 68 0.2491E-03 .2491E-03 .2491E-03 .0000E+00 .0000E+00 .0000E+00 0  
 69 0.1645E-03 .1645E-03 .1645E-03 .0000E+00 .0000E+00 .0000E+00 0  
 70 0.7025E-03 .7025E-03 .7025E-03 .0000E+00 .0000E+00 .0000E+00 0  
 71 0.4027E-03 .4027E-03 .4027E-03 .0000E+00 .0000E+00 .0000E+00 0  
 72 0.4619E-03 .4619E-03 .4619E-03 .0000E+00 .0000E+00 .0000E+00 0  
 73 0.2808E-03 .2808E-03 .2808E-03 .0000E+00 .0000E+00 .0000E+00 0  
 74 0.6223E-03 .6223E-03 .6223E-03 .0000E+00 .0000E+00 .0000E+00 0  
 75 0.1972E-03 .1972E-03 .1972E-03 .0000E+00 .0000E+00 .0000E+00 0  
 76 0.2306E-03 .2306E-03 .2306E-03 .0000E+00 .0000E+00 .0000E+00 0  
 77 0.2312E-03 .2312E-03 .2312E-03 .0000E+00 .0000E+00 .0000E+00 0  
 78 0.1159E-03 .1159E-03 .1159E-03 .0000E+00 .0000E+00 .0000E+00 0  
 79 0.2324E-03 .2324E-03 .2324E-03 .0000E+00 .0000E+00 .0000E+00 0  
 80 0.2330E-03 .2330E-03 .2330E-03 .0000E+00 .0000E+00 .0000E+00 0  
 81 0.1849E-03 .1849E-03 .1849E-03 .0000E+00 .0000E+00 .0000E+00 0  
 82 0.3817E-03 .3817E-03 .3817E-03 .0000E+00 .0000E+00 .0000E+00 0  
 83 0.5421E-03 .5421E-03 .5421E-03 .0000E+00 .0000E+00 .0000E+00 0





```

84 0.7233E-03 .7233E-03 .7233E-03 .0000E+00 .0000E+00 .0000E+00 0
85 0.6870E-03 .6870E-03 .6870E-03 .0000E+00 .0000E+00 .0000E+00 0
86 0.6145E-03 .6145E-03 .6145E-03 .0000E+00 .0000E+00 .0000E+00 0
87 0.5421E-03 .5421E-03 .5421E-03 .0000E+00 .0000E+00 .0000E+00 0
88 0.4696E-03 .4696E-03 .4696E-03 .0000E+00 .0000E+00 .0000E+00 0
89 0.3971E-03 .3971E-03 .3971E-03 .0000E+00 .0000E+00 .0000E+00 0
90 0.4619E-03 .4619E-03 .4619E-03 .0000E+00 .0000E+00 .0000E+00 0
91 0.2764E-03 .2764E-03 .2764E-03 .0000E+00 .0000E+00 .0000E+00 0
92 0.9535E-04 .9535E-04 .9535E-04 .0000E+00 .0000E+00 .0000E+00 0
93 0.1885E-03 .1885E-03 .1885E-03 .0000E+00 .0000E+00 .0000E+00 0
94 0.1862E-03 .1862E-03 .1862E-03 .0000E+00 .0000E+00 .0000E+00 0
95 0.1838E-03 .1838E-03 .1838E-03 .0000E+00 .0000E+00 .0000E+00 0
96 0.1815E-03 .1815E-03 .1815E-03 .0000E+00 .0000E+00 .0000E+00 0
97 0.2610E-03 .2610E-03 .2610E-03 .0000E+00 .0000E+00 .0000E+00 0
98 0.7426E-03 .7426E-03 .7426E-03 .0000E+00 .0000E+00 .0000E+00 0
99 0.3817E-03 .3817E-03 .3817E-03 .0000E+00 .0000E+00 .0000E+00 0
100 0.7025E-03 .7025E-03 .7025E-03 .0000E+00 .0000E+00 .0000E+00 0
101 0.6223E-03 .6223E-03 .6223E-03 .0000E+00 .0000E+00 .0000E+00 0
102 0.2764E-03 .2764E-03 .2764E-03 .0000E+00 .0000E+00 .0000E+00 0
103 0.1908E-03 .1908E-03 .1908E-03 .0000E+00 .0000E+00 .0000E+00 0
104 0.1885E-03 .1885E-03 .1885E-03 .0000E+00 .0000E+00 .0000E+00 0
105 0.1862E-03 .1862E-03 .1862E-03 .0000E+00 .0000E+00 .0000E+00 0
106 0.1838E-03 .1838E-03 .1838E-03 .0000E+00 .0000E+00 .0000E+00 0
107 0.1815E-03 .1815E-03 .1815E-03 .0000E+00 .0000E+00 .0000E+00 0
108 0.2610E-03 .2610E-03 .2610E-03 .0000E+00 .0000E+00 .0000E+00 0
109 0.5421E-03 .5421E-03 .5421E-03 .0000E+00 .0000E+00 .0000E+00 0
110 0.3971E-03 .3971E-03 .3971E-03 .0000E+00 .0000E+00 .0000E+00 0
111 0.2348E-03 .2348E-03 .2348E-03 .0000E+00 .0000E+00 .0000E+00 0
112 0.4619E-03 .4619E-03 .4619E-03 .0000E+00 .0000E+00 .0000E+00 0
113 0.5421E-03 .5421E-03 .5421E-03 .0000E+00 .0000E+00 .0000E+00 0
114 0.6145E-03 .6145E-03 .6145E-03 .0000E+00 .0000E+00 .0000E+00 0
115 0.3817E-03 .3817E-03 .3817E-03 .0000E+00 .0000E+00 .0000E+00 0
116 0.6870E-03 .6870E-03 .6870E-03 .0000E+00 .0000E+00 .0000E+00 0
117 0.7233E-03 .7233E-03 .7233E-03 .0000E+00 .0000E+00 .0000E+00 0
118 0.7277E-03 .7277E-03 .7277E-03 .0000E+00 .0000E+00 .0000E+00 0
119 0.1908E-03 .1908E-03 .1908E-03 .0000E+00 .0000E+00 .0000E+00 0
120 0.9423E-04 .9423E-04 .9423E-04 .0000E+00 .0000E+00 .0000E+00 0
121 0.1862E-03 .1862E-03 .1862E-03 .0000E+00 .0000E+00 .0000E+00 0
122 0.1838E-03 .1838E-03 .1838E-03 .0000E+00 .0000E+00 .0000E+00 0
123 0.1815E-03 .1815E-03 .1815E-03 .0000E+00 .0000E+00 .0000E+00 0
124 0.2610E-03 .2610E-03 .2610E-03 .0000E+00 .0000E+00 .0000E+00 0
125 0.3971E-03 .3971E-03 .3971E-03 .0000E+00 .0000E+00 .0000E+00 0
126 0.7426E-03 .7426E-03 .7426E-03 .0000E+00 .0000E+00 .0000E+00 0
127 0.7025E-03 .7025E-03 .7025E-03 .0000E+00 .0000E+00 .0000E+00 0
128 0.4696E-03 .4696E-03 .4696E-03 .0000E+00 .0000E+00 .0000E+00 0
129 0.6223E-03 .6223E-03 .6223E-03 .0000E+00 .0000E+00 .0000E+00 0
130 0.5421E-03 .5421E-03 .5421E-03 .0000E+00 .0000E+00 .0000E+00 0
131 0.4619E-03 .4619E-03 .4619E-03 .0000E+00 .0000E+00 .0000E+00 0
132 0.3817E-03 .3817E-03 .3817E-03 .0000E+00 .0000E+00 .0000E+00 0
133 0.2764E-03 .2764E-03 .2764E-03 .0000E+00 .0000E+00 .0000E+00 0
134 0.1908E-03 .1908E-03 .1908E-03 .0000E+00 .0000E+00 .0000E+00 0
135 0.1885E-03 .1885E-03 .1885E-03 .0000E+00 .0000E+00 .0000E+00 0
136 0.1862E-03 .1862E-03 .1862E-03 .0000E+00 .0000E+00 .0000E+00 0
137 0.1838E-03 .1838E-03 .1838E-03 .0000E+00 .0000E+00 .0000E+00 0
138 0.1815E-03 .1815E-03 .1815E-03 .0000E+00 .0000E+00 .0000E+00 0

```



```

139 0.2610E-03 .2610E-03 .2610E-03 .0000E+00 .0000E+00 .0000E+00 0
140 0.5421E-03 .5421E-03 .5421E-03 .0000E+00 .0000E+00 .0000E+00 0
141 0.6145E-03 .6145E-03 .6145E-03 .0000E+00 .0000E+00 .0000E+00 0
142 0.3971E-03 .3971E-03 .3971E-03 .0000E+00 .0000E+00 .0000E+00 0
143 0.6870E-03 .6870E-03 .6870E-03 .0000E+00 .0000E+00 .0000E+00 0
144 0.1838E-03 .1838E-03 .1838E-03 .0000E+00 .0000E+00 .0000E+00 0
145 0.1815E-03 .1815E-03 .1815E-03 .0000E+00 .0000E+00 .0000E+00 0
146 0.2610E-03 .2610E-03 .2610E-03 .0000E+00 .0000E+00 .0000E+00 0
147 0.1862E-03 .1862E-03 .1862E-03 .0000E+00 .0000E+00 .0000E+00 0
148 0.1382E-03 .1382E-03 .1382E-03 .0000E+00 .0000E+00 .0000E+00 0
149 0.1908E-03 .1908E-03 .1908E-03 .0000E+00 .0000E+00 .0000E+00 0
150 0.1885E-03 .1885E-03 .1885E-03 .0000E+00 .0000E+00 .0000E+00 0
151 0.3817E-03 .3817E-03 .3817E-03 .0000E+00 .0000E+00 .0000E+00 0
152 0.4696E-03 .4696E-03 .4696E-03 .0000E+00 .0000E+00 .0000E+00 0
153 0.4619E-03 .4619E-03 .4619E-03 .0000E+00 .0000E+00 .0000E+00 0
154 0.7233E-03 .7233E-03 .7233E-03 .0000E+00 .0000E+00 .0000E+00 0
155 0.5421E-03 .5421E-03 .5421E-03 .0000E+00 .0000E+00 .0000E+00 0
156 0.6223E-03 .6223E-03 .6223E-03 .0000E+00 .0000E+00 .0000E+00 0
157 0.1925E-03 .1925E-03 .1925E-03 .0000E+00 .0000E+00 .0000E+00 0
158 0.5421E-03 .5421E-03 .5421E-03 .0000E+00 .0000E+00 .0000E+00 0
159 0.3971E-03 .3971E-03 .3971E-03 .0000E+00 .0000E+00 .0000E+00 0
160 0.2370E-03 .2370E-03 .2370E-03 .0000E+00 .0000E+00 .0000E+00 0
161 0.1181E-03 .1181E-03 .1181E-03 .0000E+00 .0000E+00 .0000E+00 0
162 0.7025E-03 .7025E-03 .7025E-03 .0000E+00 .0000E+00 .0000E+00 0
163 0.2355E-03 .2355E-03 .2355E-03 .0000E+00 .0000E+00 .0000E+00 0
164 0.2347E-03 .2347E-03 .2347E-03 .0000E+00 .0000E+00 .0000E+00 0
165 0.2340E-03 .2340E-03 .2340E-03 .0000E+00 .0000E+00 .0000E+00 0
166 0.1846E-03 .1846E-03 .1846E-03 .0000E+00 .0000E+00 .0000E+00 0
167 0.7426E-03 .7426E-03 .7426E-03 .0000E+00 .0000E+00 .0000E+00 0
168 0.2639E-03 .2639E-03 .2639E-03 .0000E+00 .0000E+00 .0000E+00 0
169 0.6145E-03 .6145E-03 .6145E-03 .0000E+00 .0000E+00 .0000E+00 0
170 0.4696E-03 .4696E-03 .4696E-03 .0000E+00 .0000E+00 .0000E+00 0
171 0.1461E-03 .1461E-03 .1461E-03 .0000E+00 .0000E+00 .0000E+00 0
172 0.3770E-03 .3770E-03 .3770E-03 .0000E+00 .0000E+00 .0000E+00 0
173 0.6870E-03 .6870E-03 .6870E-03 .0000E+00 .0000E+00 .0000E+00 0
174 0.2462E-03 .2462E-03 .2462E-03 .0000E+00 .0000E+00 .0000E+00 0
175 0.2431E-03 .2431E-03 .2431E-03 .0000E+00 .0000E+00 .0000E+00 0
176 0.3383E-03 .3383E-03 .3383E-03 .0000E+00 .0000E+00 .0000E+00 0
177 0.3345E-03 .3345E-03 .3345E-03 .0000E+00 .0000E+00 .0000E+00 0
178 0.9531E-04 .9531E-04 .9531E-04 .0000E+00 .0000E+00 .0000E+00 0
179 0.3307E-03 .3307E-03 .3307E-03 .0000E+00 .0000E+00 .0000E+00 0
180 0.4902E-03 .4902E-03 .4902E-03 .0000E+00 .0000E+00 .0000E+00 0
181 0.1635E-03 .1635E-03 .1635E-03 .0000E+00 .0000E+00 .0000E+00 0
182 0.3302E-03 .3302E-03 .3302E-03 .0000E+00 .0000E+00 .0000E+00 0
183 0.2082E-03 .2082E-03 .2082E-03 .0000E+00 .0000E+00 .0000E+00 0
184 0.5421E-03 .5421E-03 .5421E-03 .0000E+00 .0000E+00 .0000E+00 0
185 0.2922E-03 .2922E-03 .2922E-03 .0000E+00 .0000E+00 .0000E+00 0
186 0.6034E-03 .6034E-03 .6034E-03 .0000E+00 .0000E+00 .0000E+00 0
187 0.7233E-03 .7233E-03 .7233E-03 .0000E+00 .0000E+00 .0000E+00 0
188 0.7165E-03 .7165E-03 .7165E-03 .0000E+00 .0000E+00 .0000E+00 0
189 0.3302E-03 .3302E-03 .3302E-03 .0000E+00 .0000E+00 .0000E+00 0
190 0.1908E-03 .1908E-03 .1908E-03 .0000E+00 .0000E+00 .0000E+00 0
191 0.6145E-03 .6145E-03 .6145E-03 .0000E+00 .0000E+00 .0000E+00 0
192 0.3621E-03 .3621E-03 .3621E-03 .0000E+00 .0000E+00 .0000E+00 0
193 0.4262E-03 .4262E-03 .4262E-03 .0000E+00 .0000E+00 .0000E+00 0

```





194	0.2150E-03	.2150E-03	.2150E-03	.0000E+00	.0000E+00	.0000E+00	0
195	0.4384E-03	.4384E-03	.4384E-03	.0000E+00	.0000E+00	.0000E+00	0
196	0.4186E-03	.4186E-03	.4186E-03	.0000E+00	.0000E+00	.0000E+00	0
197	0.4224E-03	.4224E-03	.4224E-03	.0000E+00	.0000E+00	.0000E+00	0
198	0.3019E-03	.3019E-03	.3019E-03	.0000E+00	.0000E+00	.0000E+00	0
199	0.4148E-03	.4148E-03	.4148E-03	.0000E+00	.0000E+00	.0000E+00	0
200	0.7731E-03	.7731E-03	.7731E-03	.0000E+00	.0000E+00	.0000E+00	0
201	0.6870E-03	.6870E-03	.6870E-03	.0000E+00	.0000E+00	.0000E+00	0
202	0.4142E-03	.4142E-03	.4142E-03	.0000E+00	.0000E+00	.0000E+00	0
203	0.5844E-03	.5844E-03	.5844E-03	.0000E+00	.0000E+00	.0000E+00	0
204	0.2863E-03	.2863E-03	.2863E-03	.0000E+00	.0000E+00	.0000E+00	0
205	0.4810E-03	.4810E-03	.4810E-03	.0000E+00	.0000E+00	.0000E+00	0
206	0.2570E-03	.2570E-03	.2570E-03	.0000E+00	.0000E+00	.0000E+00	0
207	0.5179E-03	.5179E-03	.5179E-03	.0000E+00	.0000E+00	.0000E+00	0
208	0.5217E-03	.5217E-03	.5217E-03	.0000E+00	.0000E+00	.0000E+00	0
209	0.5065E-03	.5065E-03	.5065E-03	.0000E+00	.0000E+00	.0000E+00	0
210	0.5103E-03	.5103E-03	.5103E-03	.0000E+00	.0000E+00	.0000E+00	0
211	0.3954E-03	.3954E-03	.3954E-03	.0000E+00	.0000E+00	.0000E+00	0
212	0.7233E-03	.7233E-03	.7233E-03	.0000E+00	.0000E+00	.0000E+00	0
213	0.7306E-03	.7306E-03	.7306E-03	.0000E+00	.0000E+00	.0000E+00	0
214	0.4981E-03	.4981E-03	.4981E-03	.0000E+00	.0000E+00	.0000E+00	0
215	0.3817E-03	.3817E-03	.3817E-03	.0000E+00	.0000E+00	.0000E+00	0
216	0.6135E-03	.6135E-03	.6135E-03	.0000E+00	.0000E+00	.0000E+00	0
217	0.3000E-03	.3000E-03	.3000E-03	.0000E+00	.0000E+00	.0000E+00	0
218	0.4890E-03	.4890E-03	.4890E-03	.0000E+00	.0000E+00	.0000E+00	0
219	0.5982E-03	.5982E-03	.5982E-03	.0000E+00	.0000E+00	.0000E+00	0
220	0.6020E-03	.6020E-03	.6020E-03	.0000E+00	.0000E+00	.0000E+00	0
221	0.6058E-03	.6058E-03	.6058E-03	.0000E+00	.0000E+00	.0000E+00	0
222	0.6096E-03	.6096E-03	.6096E-03	.0000E+00	.0000E+00	.0000E+00	0
223	0.8036E-03	.8036E-03	.8036E-03	.0000E+00	.0000E+00	.0000E+00	0
224	0.5821E-03	.5821E-03	.5821E-03	.0000E+00	.0000E+00	.0000E+00	0
225	0.4771E-03	.4771E-03	.4771E-03	.0000E+00	.0000E+00	.0000E+00	0
226	0.5825E-03	.5825E-03	.5825E-03	.0000E+00	.0000E+00	.0000E+00	0
227	0.3450E-03	.3450E-03	.3450E-03	.0000E+00	.0000E+00	.0000E+00	0
228	0.3468E-03	.3468E-03	.3468E-03	.0000E+00	.0000E+00	.0000E+00	0
229	0.3488E-03	.3488E-03	.3488E-03	.0000E+00	.0000E+00	.0000E+00	0
230	0.3487E-03	.3487E-03	.3487E-03	.0000E+00	.0000E+00	.0000E+00	0
231	0.3526E-03	.3526E-03	.3526E-03	.0000E+00	.0000E+00	.0000E+00	0
232	0.3594E-03	.3594E-03	.3594E-03	.0000E+00	.0000E+00	.0000E+00	0
233	0.3120E-03	.3120E-03	.3120E-03	.0000E+00	.0000E+00	.0000E+00	0
234	0.2624E-03	.2624E-03	.2624E-03	.0000E+00	.0000E+00	.0000E+00	0
235	0.3147E-03	.3147E-03	.3147E-03	.0000E+00	.0000E+00	.0000E+00	0
236	0.3679E-03	.3679E-03	.3679E-03	.0000E+00	.0000E+00	.0000E+00	0
237	0.3698E-03	.3698E-03	.3698E-03	.0000E+00	.0000E+00	.0000E+00	0
238	0.3717E-03	.3717E-03	.3717E-03	.0000E+00	.0000E+00	.0000E+00	0
239	0.3736E-03	.3736E-03	.3736E-03	.0000E+00	.0000E+00	.0000E+00	0
240	0.3755E-03	.3755E-03	.3755E-03	.0000E+00	.0000E+00	.0000E+00	0
241	0.3891E-03	.3891E-03	.3891E-03	.0000E+00	.0000E+00	.0000E+00	0
303	0.1295E-02	.1295E-02	.1295E-02	.0000E+00	.0000E+00	.0000E+00	0

(Frequency analysis data.)



0 0 .0000E+00 .0000E+00 .0000E+00 .0000E+00 .0000E+00 .0000E+00 0  
.0000E+00 .0000E+00 .0000E+00 .0000E+00  
0 0 0 .0000E+00 .6000E+03 0 6 9700





## APPENDIX C. BOUNDARY ELEMENT PROGRAM INPUT FILE

TITLE=FREQ 450-500 FORCE=1.225 DIR=Z NODE=303

EXTERIOR

BAFFLE,B=0.0,RH=-1.0,0.0

SPEED=58320,DENS=.0361,PREF=2.90E-9

GEOM

NODES

1	.00000	5.50000	.00000
2	.00000	11.08333	.00000
3	.00000	16.66667	.00000
4	.00000	22.25000	.00000
5	.00000	27.83334	.00000
6	.00000	33.41667	.00000
7	.00000	39.00000	.00000
8	1.50000	43.50000	.00000
9	2.83333	7.66667	.00000
10	2.86113	17.58881	.00000
11	2.88887	27.49442	.00000
12	2.91667	37.41667	.00000
13	3.00000	48.00000	.00000
14	5.41667	44.91667	.00000
15	5.66667	9.83333	.00000
16	5.69458	14.18841	.00000
17	5.72229	18.51097	.00000
18	5.75000	22.83333	.00000
19	5.77771	27.15551	.00000
20	5.80541	31.47749	.00000
21	5.83333	35.83333	.00000
22	6.50000	2.75000	.00000
23	6.83333	38.83333	.00000
24	7.83333	41.83333	.00000
25	8.50000	12.00000	.00000
26	8.58352	19.43315	.00000
27	8.66648	26.81660	.00000
28	8.62500	48.00000	.00000



29	8.75000	34.25000	.00000
30	10.00000	8.00000	.00000
31	10.25000	38.75000	.00000
32	11.33333	14.16667	.00000
33	11.38968	17.29377	.00000
34	11.44484	20.35536	.00000
35	11.50000	23.41667	.00000
36	11.55515	26.47771	.00000
37	11.61030	29.53848	.00000
38	11.66667	32.66667	.00000
39	12.16667	34.16667	.00000
40	12.28333	41.83333	.00000
41	12.66667	35.66667	.00000
42	13.00000	.00000	.00000
43	13.50000	13.25000	.00000
44	13.66667	3.08333	.00000
45	14.16667	16.33333	.00000
46	14.33333	6.16667	.00000
47	14.30634	21.27762	.00000
48	14.25000	48.00000	.00000
49	14.44366	26.13883	.00000
50	14.58333	31.08334	.00000
51	15.00000	9.25000	.00000
52	15.08333	32.58334	.00000
53	15.50833	44.91667	.00000
54	15.66667	12.33333	.00000
55	15.94166	35.66667	.00000
56	16.33333	15.41667	.00000
57	16.76666	41.83333	.00000
58	17.00000	18.50000	.00000
59	17.08636	20.40000	.00000
60	17.16818	22.20000	.00000
61	17.25000	24.00000	.00000
62	17.33182	25.80000	.00000
63	17.41364	27.60000	.00000
64	17.50000	29.50000	.00000



65	18.02500	38.75000	.00000
66	18.45833	.00000	.00000
67	18.77222	6.16667	.00000
68	19.08611	12.33333	.00000
69	19.28333	35.66667	.00000
70	19.40000	18.50000	.00000
71	19.46727	22.20000	.00000
72	19.53273	25.80000	.00000
73	19.60000	29.50000	.00000
74	19.87500	48.00000	.00000
75	20.54166	32.58334	.00000
76	21.25000	41.83333	.00000
77	21.70000	18.50000	.00000
78	21.71727	20.40000	.00000
79	21.73364	22.20000	.00000
80	21.75000	24.00000	.00000
81	21.76636	25.80000	.00000
82	21.78273	27.60000	.00000
83	21.80000	29.50000	.00000
84	22.06944	15.41667	.00000
85	22.43889	12.33333	.00000
86	22.62500	35.66667	.00000
87	22.80833	9.25000	.00000
88	23.17778	6.16667	.00000
89	23.54722	3.08333	.00000
90	23.91667	.00000	.00000
91	24.00000	18.50000	.00000
92	24.00000	22.20000	.00000
93	24.00000	25.80000	.00000
94	24.00000	29.50000	.00000
95	25.50000	48.00000	.00000
96	25.61667	44.91667	.00000
97	25.79167	12.33333	.00000
98	25.73333	41.83333	.00000
99	25.85000	38.75000	.00000
100	25.96667	35.66667	.00000



101	26.08333	32.58334	.00000
102	26.30000	18.50000	.00000
103	26.28273	20.40000	.00000
104	26.26636	22.20000	.00000
105	26.25000	24.00000	.00000
106	26.23364	25.80000	.00000
107	26.21727	27.60000	.00000
108	26.20000	29.50000	.00000
109	27.58333	6.16667	.00000
110	27.72222	15.41667	.00000
111	28.46727	25.80000	.00000
112	28.40000	29.50000	.00000
113	28.60000	18.50000	.00000
114	28.53273	22.20000	.00000
115	29.14444	12.33333	.00000
116	29.30833	35.66667	.00000
117	29.37500	.00000	.00000
118	30.21667	41.83333	.00000
119	30.50000	29.50000	.00000
120	30.56667	9.25000	.00000
121	30.58636	27.60000	.00000
122	30.66818	25.80000	.00000
123	30.75000	24.00000	.00000
124	30.83182	22.20000	.00000
125	30.91364	20.40000	.00000
126	31.00000	18.50000	.00000
127	31.12500	48.00000	.00000
128	31.54166	32.58334	.00000
129	31.98889	6.16667	.00000
130	32.49722	12.33333	.00000
131	32.58333	35.66667	.00000
132	33.41111	3.08333	.00000
133	33.45834	15.41667	.00000
134	33.41666	31.91666	.00000
135	33.55632	26.80538	.00000
136	33.62500	38.75000	.00000





137	33.69369	21.77770	.00000
138	33.83334	16.66667	.00000
139	34.45833	35.00000	.00000
140	34.66666	41.83333	.00000
141	34.83334	.00000	.00000
142	35.70833	44.91667	.00000
143	35.91667	12.33333	.00000
144	36.29167	13.58333	.00000
145	36.39445	6.16667	.00000
146	36.33333	34.33333	.00000
147	36.44483	27.81089	.00000
148	36.38966	31.03815	.00000
149	36.55518	21.35546	.00000
150	36.50000	24.58333	.00000
151	36.66667	14.83333	.00000
152	36.61036	18.12727	.00000
153	36.75000	48.00000	.00000
154	38.37500	9.25000	.00000
155	38.41667	40.50000	.00000
156	39.25000	36.75000	.00000
157	39.33351	28.81646	.00000
158	39.41649	20.93325	.00000
159	39.50000	13.00000	.00000
160	40.29167	.00000	.00000
161	40.83333	6.16667	.00000
162	41.58334	8.66667	.00000
163	42.19458	34.47726	.00000
164	42.16666	39.16666	.00000
165	42.33334	11.16667	.00000
166	42.30543	15.85520	.00000
167	42.27771	20.51105	.00000
168	42.25000	25.16667	.00000
169	42.22229	29.82207	.00000
170	42.37500	46.00000	.00000
171	43.29167	3.08333	.00000
172	45.16667	9.33333	.00000



173 45.13887 20.08885 .00000  
 174 45.11113 30.82770 .00000  
 175 45.08333 41.58333 .00000  
 176 45.75000 .00000 .00000  
 177 46.87500 3.75000 .00000  
 178 48.00000 7.50000 .00000  
 179 48.00000 13.58333 .00000  
 180 48.00000 19.66667 .00000  
 181 48.00000 25.75000 .00000  
 182 48.00000 31.83333 .00000  
 183 48.00000 37.91667 .00000  
 184 48.00000 44.00000 .00000

END

# ELEMENTS

1 1 3 17 15 9 2 10 16  
 2 3 5 19 17 10 4 11 18  
 3 5 7 21 19 11 6 12 20  
 4 7 13 24 21 12 8 14 23  
 5 1 15 46 42 22 9 30 44  
 6 15 17 34 32 25 16 26 33  
 7 17 19 36 34 26 18 27 35  
 8 19 21 38 36 27 20 29 37  
 9 21 24 41 38 29 23 31 39  
 10 13 48 57 24 14 28 53 40  
 11 15 32 54 46 30 25 43 51  
 12 24 57 69 41 31 40 65 55  
 13 32 34 60 58 45 33 47 59  
 14 34 36 62 60 47 35 49 61  
 15 36 38 64 62 49 37 50 63  
 16 38 41 41 64 50 39 41 52  
 17 32 58 58 54 43 45 58 56  
 18 41 69 83 64 52 55 75 73  
 19 42 46 88 90 66 44 67 89  
 20 46 54 85 88 67 51 68 87  
 21 54 58 77 85 68 56 70 84  
 22 58 60 79 77 70 59 71 78



23 60 62 81 79 71 61 72 80  
24 62 64 83 81 72 63 73 82  
25 48 95 98 57 53 74 96 76  
26 57 98 100 69 65 76 99 86  
27 69 100 108 83 75 86 101 94  
28 81 83 108 106 93 82 94 107  
29 79 81 106 104 92 80 93 105  
30 77 79 104 102 91 78 92 103  
31 77 102 115 85 84 91 110 97  
32 85 115 129 88 87 97 120 109  
33 88 129 141 90 89 109 132 117  
34 95 153 140 98 96 127 142 118  
35 98 140 131 100 99 118 136 116  
36 100 131 119 108 101 116 128 112  
37 102 104 124 126 113 103 114 125  
38 102 126 143 115 110 113 133 130  
39 104 106 122 124 114 105 111 123  
40 106 108 119 122 111 107 112 121  
41 115 143 161 129 120 130 154 145  
42 119 131 131 146 134 128 131 139  
43 119 146 147 122 121 134 148 135  
44 122 147 149 124 123 135 150 137  
45 124 149 151 126 125 137 152 138  
46 126 151 151 143 133 138 151 144  
47 129 161 176 141 132 145 171 160  
48 131 140 164 146 139 136 155 156  
49 140 153 184 164 155 142 170 175  
50 143 151 165 161 154 144 159 162  
51 146 164 169 147 148 156 163 157  
52 147 169 167 149 150 157 168 158  
53 149 167 165 151 152 158 166 159  
54 161 165 178 176 171 162 172 177  
55 164 184 182 169 163 175 183 174  
56 165 167 180 178 172 166 173 179  
57 167 169 182 180 173 168 174 181

END



CHIEF=24.0,24.0,10.0

FIELD

1	12.0	12.0	10.0
2	36.0	36.0	10.0
3	24.0	-106.0	-75.0
4	24.0	-51.0	-130.0
5	24.0	24.0	-150.0
6	24.0	99.0	-130.0
7	24.0	154.0	-75.0
8	154.0	24.0	-75.0
9	99.0	24.0	-130.0
10	-51.0	24.0	-130.0
11	-106.0	24.0	-75.0

END

MODAL

BC,FREQ=450.,FILE=A450.DAT

END

BC,FREQ=451.,FILE=A451.DAT

END

BC,FREQ=452.,FILE=A452.DAT

END

BC,FREQ=453.,FILE=A453.DAT

END

BC,FREQ=454.,FILE=A454.DAT

END

BC,FREQ=455.,FILE=A455.DAT

END

BC,FREQ=456.,FILE=A456.DAT

END

BC,FREQ=457.,FILE=A457.DAT

END

BC,FREQ=458.,FILE=A458.DAT

END

BC,FREQ=459.,FILE=A459.DAT

END

BC,FREQ=460.,FILE=A460.DAT





END  
BC,FREQ=461.,FILE=A461.DAT  
END  
BC,FREQ=462.,FILE=A462.DAT  
END  
BC,FREQ=463.,FILE=A463.DAT  
END  
BC,FREQ=464.,FILE=A464.DAT  
END  
BC,FREQ=465.,FILE=A465.DAT  
END  
BC,FREQ=466.,FILE=A466.DAT  
END  
BC,FREQ=467.,FILE=A467.DAT  
END  
BC,FREQ=468.,FILE=A468.DAT  
END  
BC,FREQ=469.,FILE=A469.DAT  
END  
BC,FREQ=470.,FILE=A470.DAT  
END  
BC,FREQ=471.,FILE=A471.DAT  
END  
BC,FREQ=472.,FILE=A472.DAT  
END  
BC,FREQ=473.,FILE=A473.DAT  
END  
BC,FREQ=474.,FILE=A474.DAT  
END  
BC,FREQ=475.,FILE=A475.DAT  
END  
BC,FREQ=476.,FILE=A476.DAT  
END  
BC,FREQ=477.,FILE=A477.DAT  
END  
BC,FREQ=478.,FILE=A478.DAT



END  
BC,FREQ=479.,FILE=A479.DAT  
END  
BC,FREQ=480.,FILE=A480.DAT  
END  
BC,FREQ=481.,FILE=A481.DAT  
END  
BC,FREQ=482.,FILE=A482.DAT  
END  
BC,FREQ=483.,FILE=A483.DAT  
END  
BC,FREQ=484.,FILE=A484.DAT  
END  
BC,FREQ=485.,FILE=A485.DAT  
END  
BC,FREQ=486.,FILE=A486.DAT  
END  
BC,FREQ=487.,FILE=A487.DAT  
END  
BC,FREQ=488.,FILE=A488.DAT  
END  
BC,FREQ=489.,FILE=A489.DAT  
END  
BC,FREQ=490.,FILE=A490.DAT  
END  
BC,FREQ=491.,FILE=A491.DAT  
END  
BC,FREQ=492.,FILE=A492.DAT  
END  
BC,FREQ=493.,FILE=A493.DAT  
END  
BC,FREQ=494.,FILE=A494.DAT  
END  
BC,FREQ=495.,FILE=A495.DAT  
END  
BC,FREQ=496.,FILE=A496.DAT



END  
BC,FREQ=497.,FILE=A497.DAT  
END  
BC,FREQ=498.,FILE=A498.DAT  
END  
BC,FREQ=499.,FILE=A499.DAT  
END  
BC,FREQ=500.,FILE=A500.DAT  
END



## APPENDIX D. FORTRAN PROGRAMS

```
C          MODAL
C
C      THIS PROGRAM MAKES A BEMAP INPUT FILE USING INPUTS
C      FROM AN ALGOR DECODER OUTPUT FILE FOR NODE POINTS AND
C      MULTIPLE EDITED FREQUENCY RESPONSE OUTPUT FILES WITH
C      AUXILLIARY FILES CONTAINING INFORMATION ABOUT BEMAP
C      ELEMENT CONECTIVITY ('ELEMENTS'), FIELD POINTS ('FIELD'),
C      AND A FILE OF UNUSED ALGOR NODES ('BAD').
C      08 APRIL 1991
C
C*****
C
10  CHARACTER*12 A,E
20  CHARACTER*60 C,D
30  DIMENSION M(57,8),E(50),FREQ(50),II(323,8),JJ(25)
40  DIMENSION X(323),Y(323),Z(323),F(323)
50  WRITE(*,*)'INPUT ALGOR INPUT FILE NAME'
60  READ(*,70)A
70  FORMAT(A12)
80  OPEN(UNIT=10,FILE=A)
90  WRITE(*,*)'INPUT NUMBER OF FREQUENCY RESPONSE FILES'
110 READ(*,*)IRESP
120 ICOUNT=1
130 IF (IRESP-ICOUNT)190,140,140
140 WRITE(*,150)ICOUNT
150 FORMAT(1X,'INPUT FREQUENCY RESPONSE FILE AND FREQUENCY NUMBER',I2)
160 READ(*,200)E(ICOUNT),FREQ(ICOUNT)
170 ICOUNT=ICOUNT+1
180 GO TO 130
190 CONTINUE
200 FORMAT(A8,1X,F4.0)
210 OPEN(UNIT=11,FILE='INPUT')
220 OPEN(UNIT=12,FILE='ELEMENTS')
```





```

230  OPEN(UNIT=13,FILE='BAD')
240  OPEN(UNIT=14,FILE='FIELD')
250  WRITE(*,*)'INPUT TITLE FOR BEMAP INPUT FILE'
260  READ(*,270)C
270  FORMAT(A60)
280  WRITE(*,*)'INPUT NUMBER OF BOUNDARY ELEMENTS'
290  READ(*,*)NUMBER
300  IZ1=0
310  IZ2=0
320  IZ3=0
330  IZ4=0
340  IO1=1
C*****
C
C READ HEADER DATA
C
C*****
350  READ(10,360)D,NODES,(JJ(L),L=1,16),GRAV
360  FORMAT(A60,/,4I5,I3,I2,4I5,3I1,4I5,F10.0)
C*****
C
C READ IN NODAL LOCATIONS
C
C*****
370  READ(10,380)(II(1,L),L=1,7),X(1),Y(1),Z(1),II(1,8),F(1),J1,J2
380  FORMAT(I6,6I2,3E14.7,I5,E12.5,2I2)
390  DO 420 I=2,NODES
400  READ(10,410)(II(I,L1),L1=1,7),X(I),Y(I),Z(I),II(I,8),F(I)
410  FORMAT(I6,6I2,3E14.7,I5,E12.5)
420  CONTINUE
C*****
C
C RENUMBER NODES TO DELETE THOSE NOT USED BY BEMAP
C
C*****
430  DO 490 I=1,NUMBER

```



```

440  READ(13,*)K
450  DO 490 J=K,241
460  X(J)=X(J+1)
470  Y(J)=Y(J+1)
480  Z(J)=Z(J+1)
490  CONTINUE
C*****
C
C START CREATING BEMAP INPUT FILE
C
C*****
500  WRITE(11,510)C
510  FORMAT('TITLE=',A60)
520  WRITE(11,530)
530  FORMAT('EXTERIOR')
540  WRITE(11,550)
550  FORMAT('BAFFLE,B=0.0,RH=-1.0,0.0')
560  WRITE(11,570)
570  FORMAT('SPEED=58320,DENS=.0361,PREF=2.00E-9')
580  WRITE(11,590)
590  FORMAT('GEOM')
600  WRITE(11,610)
610  FORMAT('NODES')
620  DO 650 I=1,(241-NUMBER)
630  WRITE(11,640)II(I,1),Z(I),Y(I),X(I)
640  FORMAT(I5,3F9.5)
650  CONTINUE
660  WRITE(11,670)
670  FORMAT('END')
680  WRITE(11,690)
690  FORMAT('ELEMENTS')
C*****
C
C INPUT BEMAP ELEMENT CONECTIVITY DATA FROM THE FILE "ELEMENTS"
C
C*****

```



```

700  READ(12,*)I, (M(I,J), J=1,8)
710  WRITE(11,720)I, (M(I,J),J=1,8)
720  FORMAT(9I5)
730  IF (I-NUMBER) 700,740,740
740  WRITE(11,670)
C*****
C
C INPUT CHIEF POINTS AND FIELD POINTS
C
C*****
750  WRITE(11,760)
760  FORMAT('CHIEF=24.0,24.0,10.0')
770  WRITE(11,780)
780  FORMAT('FIELD')
790  DO 830 I=1,11
800  READ(14,*)X1,X2,X3
810  WRITE(11,820)I,X1,X2,X3
820  FORMAT(I2,2X,F7.4,2X,F7.4,2X,F7.4)
830  CONTINUE
840  WRITE(11,670)
C*****
C
C WRITE BEMAP BOUNDARY CONDITION FILES
C
C*****
850  WRITE(11,860)
860  FORMAT('MODAL')
870  DO 910 I=1,IRESP
880  WRITE(11,890)FREQ(I),E(I)
890  FORMAT('BC,FREQ=',F4.0,',FILE=',A8)
900  WRITE(11,670)
910  CONTINUE
920  END

```



```

C          BCFILE
C
C  THIS PROGRAM MAKES A BEMAP INPUT FILE USING INPUTS
C  FROM AN ALGOR EDITED FREQUENCY RESPONSE OUTPUT FILE
C  08 APRIL 1991
C
C*****
10  CHARACTER*24 A,E
20  DIMENSION M(57,8)
30  DIMENSION XDISP(323),XPHAS(323)
40  WRITE(*,*)'INPUT BC FILE NAME TO BE CREATED'
50  READ(*,60)A
60  FORMAT(A24)
70  OPEN(UNIT=11,FILE=A)
80  WRITE(*,*)'INPUT FREQUENCY RESPONSE FILE NAME'
90  READ(*,60)E
100 OPEN(UNIT=9,FILE=E)
110 OPEN(UNIT=13,FILE='BAD')
120 OPEN(UNIT=12,FILE='ELEMENTS')
130 WRITE(*,*)'INPUT FREQUENCY'
140 READ(*,*)FREQ
C*****
C
C INPUT PLATE NODE DISPLACEMENTS FROM THE FREQUENCY RESPONSE OUTPUT FILE
C THE OUTPUT FILE MUST HAVE BEEN EDITED SO THAT ONLY THE NODAL
C DISPLACEMENT DATA REMAINS IN THE FILE
C
C*****
150 DO 180 I=1,317
160 READ(9,170)I1,XDISP(I),F1,F2,F3,F4,F5
170 FORMAT(I6,6E12.4)
180 CONTINUE
190 DO 220 I=1,317
200 READ(9,210)I1,XPHAS(I),F1,F2,F3,F4,F5
210 FORMAT(I6,6E12.4)
220 CONTINUE

```





```

C*****
C
C CONVERT DISPLACEMENTS TO VELOCITIES
C
C*****
230   DO 270 I=1,241
240   XPHAS(I)=XPHAS(I)*.0174532
250   XDISP(I)=XDISP(I)*6.2831853*FREQ
260   XPHAS(I)=XPHAS(I)+1.5707963
270   CONTINUE
C*****
C
C RENUMBER NODES TO DELETE THOSE NOT USED BY BEMAP
C
C*****
280   DO 330 I=1,57
290   READ(13,*)K
300   DO 330 J=K,241
310   XDISP(J)=XDISP(J+1)
320   XPHAS(J)=XPHAS(J+1)
330   CONTINUE
C*****
C
C INPUT BEMAP ELEMENT CONECTIVITY DATA FROM THE FILE "ELEMENTS"
C
C*****
340   READ(12,*)I, (M(I,J), J=1,8)
350   IF (I-57) 340,360,360
360   CONTINUE
C*****
C
C START CREATING BEMAP INPUT FILE
C
C*****
370   IZ1=0
380   IO1=1

```



```

C*****
C
C INPUT BEMAP BOUNDARY CONDITIONS
C
C*****
390   DO 430 I=1,57
400   DO 430 J=1,8
410   WRITE(11,420)J,I,IZ1,IZ1,IO1,IZ1,XDISP(M(I,J)),XPHAS(M(I,J))
420   FORMAT(6I5,2E11.4)
430   CONTINUE
440   WRITE(11,*)'END'
450   END

```



```

C          TEST
C
C THIS PROGRAM TAKES THE ALGOR INPUT FILE WITH MASS LOADING
C APPLIED AND CHANGES THE MASS LOADING BASED ON A NEW INPUT
C FREQUENCY
C APRIL 08 1991
C
C*****
10  CHARACTER*8 A,A1
20  CHARACTER*60 B
30  DIMENSION X(330),Y(330),Z(330),F(330),F1(56),F3(16)
40  DIMENSION AREA(241),XL(241)
50  DIMENSION F2(230,4),F4(4,4),F5(5,4),F7(3,6),F8(3,5)
60  DIMENSION I(330,8),K(230,8),M(80,14)
70  DIMENSION J(26),JJ(25)
80  WRITE(*,*)'INPUT ALGOR FILE NAME'
90  READ(*,120)A
100 WRITE(*,*)'INPUT NEW ALGOR FILE NAME'
110 READ(*,120)A1
120 FORMAT(A8)
130 WRITE(*,*)'INPUT FREQUENCY (HZ)'
140 READ(*,*)FREQ
150 OPEN(UNIT=11,FILE=A)
160 OPEN(UNIT=12,FILE='AREA')
170 OPEN(UNIT=13,FILE=A1)
C*****
C
C READ IN HEADER DATA
C
C*****
180 READ(11,190)B,NODES,(JJ(L),L=1,16),FX
190 FORMAT(A60,/,4I5,I3,I2,4I5,I3,2I1,4I5,F10.1)
C*****
C
C READ IN THE NODAL LOCATIONS
C

```



```

C*****
200  READ(11,210) (I(1,L),L=1,7),X(1),Y(1),Z(1),I(1,8),F(1),J1,J2
210  FORMAT(I6,6I2,3E14.7,I5,E12.5,2I2)
220  DO 250 L=2,NODES
230  READ(11,240)(I(L,L1),L1=1,7),X(L),Y(L),Z(L),I(L,8),F(L)
240  FORMAT(I6,6I2,3E14.7,I5,E12.5)
250  CONTINUE
C*****
C
C READ IN THE PLATE DATA
C
C*****
260  READ(11,270)(J(L),L=1,11)
270  FORMAT(11I5)
280  READ(11,290)JJ(17),(F1(L),L=1,5)
290  FORMAT(I10,10X,5E10.4)
300  READ(11,310)(F1(L),L=6,11)
310  FORMAT(6E10.4)
320  DO 350 L=1,5
330  READ(11,340) (F5(L,L1),L1=1,4)
340  FORMAT(4E10.4)
350  CONTINUE
C*****
C
C READ IN THE PLATE CONECTIVITY DATA
C
C*****
360  DO 390 L=1,J(2)
370  READ(11,380)(K(L,L1),L1=1,8),(F2(L,L2),L2=1,4)
380  FORMAT(8I5,4E10.4)
390  CONTINUE
C*****
C
C READ IN THE BEAM DATA
C
C*****

```





```

400  READ(11,410)(J(L),L=12,22)
410  FORMAT(11I5)
420  READ(11,430)J(23),(F1(L),L=32,38),F3(1)
430  FORMAT(I5,4E10.4,3E8.2,F8.3)
440  DO 480 L=1,3
450  READ(11,460)J(23+L),(F7(L,L1),L1=1,6),(F8(L,L2),L2=1,5)
470  FORMAT(I5,6E10.4,2F5.3,3F10.4)
480  CONTINUE
490  DO 520 L=1,3
500  READ(11,510)(F4(L,L1),L1=1,4)
510  FORMAT(4E10.4)
520  CONTINUE
C*****
C
C READ IN THE BEAM CONECTIVITY DATA
C
C*****
530  DO 560 L=1,J(13)
540  READ(11,550)(M(L,L1),L1=1,14)
550  FORMAT(10I5,2I7,I4,I2)
560  CONTINUE
C*****
C
C MAKE NEW NODAL LOADS
C
C*****
570  RHOS=.07075
580  RHOFW=.0361
590  D=42926.0
600  W=6.2831853*FREQ
610  ACK=W/58320
620  PLK=2.0
630  PLK1=((RHOS*W**2/D)+(RHOFW*W**2)/(D*SQRT(PLK**2-ACK**2)))*.25
640  CHECK=PLK-PLK1
650  IF (CHECK-.0000001)680,660,660
660  PLK=PLK1

```



```

670   GO TO 630
680   READ(12,690) (AREA(L),L=1,241)
690   FORMAT(F6.3)
700   DO 720 L=1,241
710   XL(L)=AREA(L)*RHOFW/(PLK1*386.1)
720   CONTINUE
C*****
C
C READ BUT DO NOT SAVE OLD NODAL LOADS
C
C*****
730   DO 760 L=1,242
740   READ(11,750)N1,N2,D1,D2,D3,D4,D5,D6,N3
750   FORMAT(2I5,6E10.4,I2)
760   CONTINUE
C*****
C
C READ ZERO LINE
C
C*****
770   READ(11,750)N4,N5,D7,D8,D9,D10,D11,D12,N6
C*****
C
C READ IN END DATA
C
C*****
780   IZ=0
790   FZ=0.0
800   READ(11,810)(F4(4,L),L=1,4)
810   FORMAT(4E10.4)
820   READ(11,830)I17,I18,I19,FA,FB,I20,I21
830   FORMAT(3I5,2E10.4,2I5)
C*****
C
C WRITE HEADER DATA TO NEW FILE
C

```



```

C*****
840  WRITE(13,190)B,NODES,(JJ(L),L=1,16),FX
C*****
C
C WRITE NODAL LOCATIONS
C
C*****
850  WRITE(13,210) (I(1,L),L=1,7),X(1),Y(1),Z(1),I(1,8),F(1),J1,J2
860  DO 880 L=2,NODES
870  WRITE(13,240) (I(L,L1),L1=1,7),X(L),Y(L),Z(L),I(L,8),F(L)
880  CONTINUE
C*****
C
C WRITE PLATE DATA
C
C*****
890  WRITE(13,270)(J(L),L=1,11)
900  WRITE(13,290)JJ(17),(F1(L),L=1,5)
910  WRITE(13,310)(F1(L),L=6,11)
920  DO 940 L=1,5
930  WRITE(13,340) (F5(L,L1),L1=1,4)
940  CONTINUE
C*****
C
C WRITE PLATE CONECTIVITY DATA
C
C*****
950  DO 970 L=1,J(2)
960  WRITE(13,380)(K(L,L1),L1=1,8),(F2(L,L2),L2=1,4)
970  CONTINUE
C*****
C
C WRITE BEAM DATA
C
C*****
980  WRITE(13,410)(J(L),L=12,22)

```



```

990  WRITE(13,430)J(23),(F1(L),L=32,38),F3(1)
1000 DO 1020 L=1,3
1010  WRITE(13,460)J(23+L),(F7(L,L1),L1=1,6),(F8(L,L2),L2=1,5)
1020  CONTINUE
1030 DO 1050 L=1,3
1040  WRITE(13,500)(F4(L,L1),L1=1,4)
1050  CONTINUE
C*****
C
C WRITE BEAM CONECTIVITY DATA
C
C*****
1060 DO 1080 L=1,J(13)
1070  WRITE(13,540)(M(L,L1),L1=1,14)
1080  CONTINUE
C*****
C
C WRITE NEW NODAL LOADS
C
C*****
1090  IN=0
1100 DO 1120 L=1,241
1110  WRITE(13,740)L,IZ,XL(L),XL(L),XL(L),FZ,FZ,FZ,IN
1120  CONTINUE
1130  WRITE(13,740)N1,N2,D1,D2,D3,D4,D5,D6,N3
1140  WRITE(13,740)IZ,IZ,FZ,FZ,FZ,FZ,FZ,FZ,IZ
C*****
C
C WRITE END DATA
C
C*****
1150  WRITE(13,800)(F4(4,L),L=1,4)
1160  I21=6
1170  WRITE(13,1180)I17,I18,I19,FA,FB,I20,I21
1180  FORMAT(3I5,2E10.4,2I5)
1190  END

```





Additional files that are opened in the fortran programs are: AREA - contains a list of the area of each finite element plate element in order from 1 to 241, BAD - contains a list of the finite element plate nodes that are not used in the boundary element plate model, ELEMENTS - contains the connectivity table for plate mode for the boundary element program, FIELD - contains a list of the field points used in the boundary element program.

(AREA, listed in columns to save space.)

8.752	10.814	8.923	4.074	13.618	7.497	8.762
7.498	9.297	10.235	4.023	8.800	7.412	16.027
7.537	7.750	6.223	5.783	15.224	2.112	16.189
7.576	14.583	13.789	12.012	4.074	7.328	11.038
7.615	9.881	4.370	8.800	4.023	10.863	8.458
7.653	15.567	5.109	5.203	5.783	3.622	13.594
7.388	7.937	5.123	10.235	4.125	7.316	6.647
7.104	8.693	2.568	12.012	3.062	4.614	10.836
16.143	8.771	5.149	13.618	4.227	12.012	13.256
7.048	8.848	5.163	8.458	4.176	6.476	13.340
14.174	8.926	4.098	15.224	8.458	13.370	13.425
14.251	4.502	8.458	16.027	10.406	16.027	13.509
14.329	7.105	12.012	16.125	10.235	15.878	17.808
14.407	10.938	16.027	4.227	16.027	7.318	12.898
13.681	5.167	15.224	2.088	12.012	4.229	10.573
15.332	13.789	13.618	4.125	13.789	13.618	12.909
12.917	7.701	12.012	4.074	4.266	8.023	7.644
14.242	18.040	10.406	4.023	12.012	9.445	7.686
13.420	7.292	8.800	5.783	8.800	4.765	7.729
6.148	8.363	10.235	8.800	5.252	9.714	7.726
12.373	5.160	6.125	16.455	2.618	9.275	7.813
12.450	12.012	2.113	15.567	15.567	9.360	7.964
12.528	6.802	4.176	10.406	5.218	6.689	6.914
12.606	14.101	4.125	13.789	5.201	9.191	5.815
11.579	6.970	4.074	12.012	5.185	17.132	6.973
20.052	16.455	4.023	10.235	4.091	15.224	8.152
10.333	7.048	5.783	8.458	16.455	9.178	8.194
12.061	7.125	16.455	6.125	5.848	12.951	8.237
9.115	7.203	8.458	4.227	13.618	6.344	8.279
10.697	4.912	15.567	4.176	10.406	10.659	8.321
10.494	2.583	13.789	4.125	3.238	5.696	8.623
10.572	11.475	6.125	4.074	8.355	11.477	
10.649	5.521	4.227	4.023	15.224	11.561	
10.727	3.646	4.176	5.783	5.456	11.223	
16.455	15.567	4.125	12.012	5.388	11.308	



(BAD, listed in columns to save space.)

231	151	69
229	149	66
227	147	64
225	145	62
213	143	58
209	140	57
208	125	49
206	123	41
204	121	38
201	119	36
195	115	33
184	109	31
182	100	29
179	96	17
178	94	14
176	92	12
171	89	10
162	87	
159	85	
155	82	

(FIELD)

12.0 12.0 10.0  
36.0 36.0 10.0  
24.0 -106.0 -75.0  
24.0 -51.0 -130.0  
24.0 24.0 -150.0  
24.0 99.0 -130.0  
24.0 154.0 -75.0  
154.0 24.0 -75.0  
99.0 24.0 -130.0  
-51.0 24.0 -130.0  
-106.0 24.0 -75.0



(ELEMENTS)

1	1	3	17	15	9	2	10	16
2	3	5	19	17	10	4	11	18
3	5	7	21	19	11	6	12	20
4	7	13	24	21	12	8	14	23
5	1	15	46	42	22	9	30	44
6	15	17	34	32	25	16	26	33
7	17	19	36	34	26	18	27	35
8	19	21	38	36	27	20	29	37
9	21	24	41	38	29	23	31	39
10	13	48	57	24	14	28	53	40
11	15	32	54	46	30	25	43	51
12	24	57	69	41	31	40	65	55
13	32	34	60	58	45	33	47	59
14	34	36	62	60	47	35	49	61
15	36	38	64	62	49	37	50	63
16	38	41	41	64	50	39	41	52
17	32	58	58	54	43	45	58	56
18	41	69	83	64	52	55	75	73
19	42	46	88	90	66	44	67	89
20	46	54	85	88	67	51	68	87
21	54	58	77	85	68	56	70	84
22	58	60	79	77	70	59	71	78
23	60	62	81	79	71	61	72	80
24	62	64	83	81	72	63	73	82
25	48	95	98	57	53	74	96	76
26	57	98	100	69	65	76	99	86
27	69	100	108	83	75	86	101	94
28	81	83	108	106	93	82	94	107
29	79	81	106	104	92	80	93	105
30	77	79	104	102	91	78	92	103
31	77	102	115	85	84	91	110	97
32	85	115	129	88	87	97	120	109
33	88	129	141	90	89	109	132	117
34	95	153	140	98	96	127	142	118
35	98	140	131	100	99	118	136	116
36	100	131	119	108	101	116	128	112
37	102	104	124	126	113	103	114	125
38	102	126	143	115	110	113	133	130
39	104	106	122	124	114	105	111	123
40	106	108	119	122	111	107	112	121
41	115	143	161	129	120	130	154	145
42	119	131	131	146	134	128	131	139
43	119	146	147	122	121	134	148	135
44	122	147	149	124	123	135	150	137
45	124	149	151	126	125	137	152	138
46	126	151	151	143	133	138	151	144
47	129	161	176	141	132	145	171	160
48	131	140	164	146	139	136	155	156
49	140	153	184	164	155	142	170	175
50	143	151	165	161	154	144	159	162
51	146	164	169	147	148	156	163	157
52	147	169	167	149	150	157	168	158



53 149 167 165 151 152 158 166 159  
54 161 165 178 176 171 162 172 177  
55 164 184 182 169 163 175 183 174  
56 165 167 180 178 172 166 173 179  
57 167 169 182 180 173 168 174 181





## APPENDIX E. MODAL FREQUENCY DATA

Run # 0, Unmodified Model Modal Frequencies

1\*\*\*\* Algor (c) Dynamic Modal Analysis - SSAP1H 3/3/89, Ver 8.002D/387

1\*\*\*\* PRINT OF NATURAL FREQUENCIES

Mode Number	Circular Frequency (rad/sec)	Frequency (Hz)	Period (sec)
1	1.0000E-10	1.5915E-11	6.2832E+10
2	1.0000E-10	1.5915E-11	6.2832E+10
3	2.0917E-04	3.3290E-05	3.0039E+04
4	5.7103E-04	9.0883E-05	1.1003E+04
5	6.3749E-04	1.0146E-04	9.8561E+03
6	3.0002E+00	4.7750E-01	2.0943E+00
7	1.0393E+02	1.6541E+01	6.0454E-02
8	1.3081E+02	2.0820E+01	4.8031E-02
9	1.6431E+02	2.6151E+01	3.8240E-02
10	2.1119E+02	3.3612E+01	2.9751E-02
11	2.2595E+02	3.5961E+01	2.7808E-02
12	3.3242E+02	5.2907E+01	1.8901E-02
13	3.3930E+02	5.4002E+01	1.8518E-02
14	3.9201E+02	6.2390E+01	1.6028E-02
15	4.0862E+02	6.5034E+01	1.5377E-02
16	5.4355E+02	8.6508E+01	1.1560E-02
17	5.7257E+02	9.1128E+01	1.0974E-02
18	5.9760E+02	9.5112E+01	1.0514E-02
19	6.9862E+02	1.1119E+02	8.9937E-03
20	7.2078E+02	1.1472E+02	8.7173E-03
21	7.4868E+02	1.1916E+02	8.3923E-03
22	7.7378E+02	1.2315E+02	8.1201E-03
23	7.8497E+02	1.2493E+02	8.0043E-03
24	8.1494E+02	1.2970E+02	7.7100E-03
25	8.7881E+02	1.3987E+02	7.1497E-03
26	9.3917E+02	1.4947E+02	6.6901E-03
27	9.7474E+02	1.5513E+02	6.4460E-03



Mode Number	Circular Frequency (rad/sec)	Frequency (Hz)	Period (sec)
28	1.0600E+03	1.6871E+02	5.9275E-03
29	1.1087E+03	1.7646E+02	5.6671E-03
30	1.1427E+03	1.8186E+02	5.4987E-03
31	1.2145E+03	1.9330E+02	5.1733E-03
32	1.2795E+03	2.0363E+02	4.9108E-03
33	1.2917E+03	2.0559E+02	4.8641E-03
34	1.3243E+03	2.1077E+02	4.7446E-03
35	1.4072E+03	2.2396E+02	4.4650E-03
36	1.4861E+03	2.3652E+02	4.2279E-03
37	1.5784E+03	2.5121E+02	3.9807E-03
38	1.6101E+03	2.5626E+02	3.9023E-03
39	1.6764E+03	2.6680E+02	3.7481E-03
40	1.7050E+03	2.7135E+02	3.6852E-03
41	1.7328E+03	2.7578E+02	3.6261E-03
42	1.7495E+03	2.7845E+02	3.5914E-03
43	1.8203E+03	2.8971E+02	3.4517E-03
44	1.9158E+03	3.0490E+02	3.2797E-03
45	1.9278E+03	3.0682E+02	3.2592E-03
46	2.0788E+03	3.3086E+02	3.0224E-03
47	2.0905E+03	3.3272E+02	3.0056E-03
48	2.1000E+03	3.3423E+02	2.9920E-03
49	2.1894E+03	3.4846E+02	2.8698E-03
50	2.2766E+03	3.6233E+02	2.7599E-03
51	2.2978E+03	3.6571E+02	2.7344E-03
52	2.3729E+03	3.7765E+02	2.6479E-03
53	2.4219E+03	3.8546E+02	2.5943E-03
54	2.5173E+03	4.0065E+02	2.4960E-03
55	2.5688E+03	4.0884E+02	2.4459E-03
56	2.5986E+03	4.1358E+02	2.4179E-03
57	2.6319E+03	4.1888E+02	2.3873E-03
58	2.6961E+03	4.2910E+02	2.3305E-03
59	2.7443E+03	4.3677E+02	2.2896E-03
60	2.8007E+03	4.4575E+02	2.2434E-03
61	2.8400E+03	4.5200E+02	2.2124E-03
62	2.8850E+03	4.5916E+02	2.1779E-03



Mode Number	Circular Frequency (rad/sec)	Frequency (Hz)	Period (sec)
63	2.9391E+03	4.6778E+02	2.1378E-03
64	2.9997E+03	4.7741E+02	2.0946E-03
65	3.0487E+03	4.8522E+02	2.0609E-03
66	3.0764E+03	4.8962E+02	2.0424E-03
67	3.1230E+03	4.9704E+02	2.0119E-03
68	3.2043E+03	5.0998E+02	1.9609E-03
69	3.2359E+03	5.1502E+02	1.9417E-03
70	3.2708E+03	5.2057E+02	1.9210E-03
71	3.3428E+03	5.3202E+02	1.8796E-03
72	3.4087E+03	5.4251E+02	1.8433E-03
73	3.4310E+03	5.4606E+02	1.8313E-03
74	3.4532E+03	5.4960E+02	1.8195E-03
75	3.6043E+03	5.7364E+02	1.7433E-03
76	3.6283E+03	5.7747E+02	1.7317E-03
77	3.6955E+03	5.8816E+02	1.7002E-03
78	3.7361E+03	5.9461E+02	1.6818E-03
79	3.7917E+03	6.0347E+02	1.6571E-03

The Sturm sequence check didn't find any missing frequency.

1\*\*\*\* End of file



Run # 1, Modal Frequencies for Model With .375 lb Weight Added

1\*\*\*\* Algor (c) Dynamic Modal Analysis - SSAP1H 3/3/89, Ver 8.002D/387

1\*\*\*\* PRINT OF NATURAL FREQUENCIES

Mode Number	Circular Frequency (rad/sec)	Frequency (Hertz)	Period (sec)
1	1.0000E-10	1.5915E-11	6.2832E+10
2	1.0000E-10	1.5915E-11	6.2832E+10
3	5.3779E-05	8.5592E-06	1.1683E+05
4	5.5804E-04	8.8815E-05	1.1259E+04
5	6.7341E-04	1.0718E-04	9.3304E+03
6	3.0000E+00	4.7746E-01	2.0944E+00
7	1.0393E+02	1.6541E+01	6.0454E-02
8	1.3081E+02	2.0820E+01	4.8032E-02
9	1.6429E+02	2.6147E+01	3.8245E-02
10	2.1112E+02	3.3600E+01	2.9762E-02
11	2.2586E+02	3.5947E+01	2.7818E-02
12	3.3200E+02	5.2840E+01	1.8925E-02
13	3.3773E+02	5.3751E+01	1.8604E-02
14	3.9198E+02	6.2386E+01	1.6029E-02
15	4.0862E+02	6.5033E+01	1.5377E-02
16	5.4299E+02	8.6420E+01	1.1571E-02
17	5.6709E+02	9.0256E+01	1.1080E-02
18	5.9638E+02	9.4916E+01	1.0536E-02
19	6.8468E+02	1.0897E+02	9.1769E-03
20	7.2015E+02	1.1462E+02	8.7248E-03
21	7.4776E+02	1.1901E+02	8.4027E-03
22	7.7370E+02	1.2314E+02	8.1210E-03
23	7.8461E+02	1.2487E+02	8.0080E-03
24	8.1465E+02	1.2966E+02	7.7127E-03
25	8.7862E+02	1.3984E+02	7.1512E-03
26	9.3870E+02	1.4940E+02	6.6935E-03
27	9.7473E+02	1.5513E+02	6.4461E-03
28	1.0600E+03	1.6871E+02	5.9275E-03
29	1.1087E+03	1.7645E+02	5.6674E-03
30	1.1424E+03	1.8182E+02	5.5000E-03





Mode Number	Circular Frequency (rad/sec)	Frequency (Hertz)	Period (sec)
31	1.2143E+03	1.9326E+02	5.1743E-03
32	1.2792E+03	2.0360E+02	4.9116E-03
33	1.2915E+03	2.0555E+02	4.8650E-03
34	1.3238E+03	2.1069E+02	4.7463E-03
35	1.4071E+03	2.2395E+02	4.4653E-03
36	1.4860E+03	2.3651E+02	4.2282E-03
37	1.5778E+03	2.5111E+02	3.9823E-03
38	1.5964E+03	2.5408E+02	3.9357E-03
39	1.6723E+03	2.6616E+02	3.7572E-03
40	1.7046E+03	2.7130E+02	3.6859E-03
41	1.7327E+03	2.7577E+02	3.6262E-03
42	1.7492E+03	2.7840E+02	3.5919E-03
43	1.8203E+03	2.8970E+02	3.4518E-03
44	1.9156E+03	3.0488E+02	3.2800E-03
45	1.9278E+03	3.0682E+02	3.2593E-03
46	2.0788E+03	3.3086E+02	3.0224E-03
47	2.0899E+03	3.3262E+02	3.0064E-03
48	2.1000E+03	3.3422E+02	2.9920E-03
49	2.1891E+03	3.4841E+02	2.8702E-03
50	2.2764E+03	3.6230E+02	2.7601E-03
51	2.2973E+03	3.6563E+02	2.7350E-03
52	2.3723E+03	3.7757E+02	2.6485E-03
53	2.4218E+03	3.8545E+02	2.5944E-03
54	2.5173E+03	4.0063E+02	2.4961E-03
55	2.5687E+03	4.0882E+02	2.4461E-03
56	2.5983E+03	4.1354E+02	2.4182E-03
57	2.6313E+03	4.1878E+02	2.3879E-03
58	2.6955E+03	4.2901E+02	2.3309E-03
59	2.7436E+03	4.3667E+02	2.2901E-03
60	2.7991E+03	4.4549E+02	2.2447E-03
61	2.8394E+03	4.5191E+02	2.2129E-03
62	2.8835E+03	4.5892E+02	2.1790E-03
63	2.9389E+03	4.6775E+02	2.1379E-03
64	2.9971E+03	4.7700E+02	2.0964E-03
65	3.0435E+03	4.8438E+02	2.0645E-03



Mode Number	Circular Frequency (rad/sec)	Frequency (Hertz)	Period (sec)
66	3.0547E+03	4.8617E+02	2.0569E-03
67	3.1225E+03	4.9697E+02	2.0122E-03
68	3.2032E+03	5.0981E+02	1.9615E-03
69	3.2358E+03	5.1499E+02	1.9418E-03
70	3.2685E+03	5.2019E+02	1.9224E-03
71	3.3413E+03	5.3179E+02	1.8804E-03
72	3.3965E+03	5.4058E+02	1.8499E-03
73	3.4266E+03	5.4537E+02	1.8336E-03
74	3.4480E+03	5.4876E+02	1.8223E-03
75	3.6037E+03	5.7354E+02	1.7435E-03
76	3.6276E+03	5.7734E+02	1.7321E-03
77	3.6950E+03	5.8807E+02	1.7005E-03
78	3.7337E+03	5.9423E+02	1.6828E-03
79	3.7828E+03	6.0205E+02	1.6610E-03

The Stum sequence check didn't find any missing frequency.

1\*\*\*\* End of file



Run # 2, Modal Frequencies for Model With .75 lb Weight Added

1\*\*\*\* Algor (c) Dynamic Modal Analysis - SSAP1H 3/3/89, Ver 8.002D/387

1\*\*\*\* PRINT OF NATURAL FREQUENCIES

Mode Number	Circular Frequency (rad/sec)	Frequency (Hz)	Period (sec)
1	1.0000E-10	1.5915E-11	6.2832E+10
2	1.0000E-10	1.5915E-11	6.2832E+10
3	1.3724E-04	2.1843E-05	4.5781E+04
4	5.1110E-04	8.1344E-05	1.2293E+04
5	7.6412E-04	1.2161E-04	8.2227E+03
6	3.0002E+00	4.7749E-01	2.0943E+00
7	1.0393E+02	1.6541E+01	6.0456E-02
8	1.3080E+02	2.0818E+01	4.8035E-02
9	1.6389E+02	2.6084E+01	3.8338E-02
10	2.1114E+02	3.3604E+01	2.9758E-02
11	2.2593E+02	3.5958E+01	2.7810E-02
12	3.3150E+02	5.2760E+01	1.8954E-02
13	3.3887E+02	5.3933E+01	1.8541E-02
14	3.9169E+02	6.2340E+01	1.6041E-02
15	4.0853E+02	6.5019E+01	1.5380E-02
16	5.4345E+02	8.6492E+01	1.1562E-02
17	5.7130E+02	9.0924E+01	1.0998E-02
18	5.9675E+02	9.4976E+01	1.0529E-02
19	6.9561E+02	1.1071E+02	9.0327E-03
20	7.2053E+02	1.1468E+02	8.7203E-03
21	7.4687E+02	1.1887E+02	8.4127E-03
22	7.7340E+02	1.2309E+02	8.1241E-03
23	7.8468E+02	1.2489E+02	8.0073E-03
24	8.1423E+02	1.2959E+02	7.7168E-03
25	8.7873E+02	1.3985E+02	7.1503E-03
26	9.3900E+02	1.4945E+02	6.6914E-03
27	9.7461E+02	1.5511E+02	6.4469E-03
28	1.0600E+03	1.6871E+02	5.9275E-03
29	1.1073E+03	1.7623E+02	5.6745E-03
30	1.1378E+03	1.8109E+02	5.5222E-03



Mode Number	Circular Frequency (rad/sec)	Frequency (Hertz)	Period (sec)
31	1.2141E+03	1.9323E+02	5.1751E-03
32	1.2778E+03	2.0338E+02	4.9170E-03
33	1.2915E+03	2.0554E+02	4.8651E-03
34	1.3235E+03	2.1064E+02	4.7474E-03
35	1.4068E+03	2.2390E+02	4.4663E-03
36	1.4852E+03	2.3638E+02	4.2305E-03
37	1.5762E+03	2.5086E+02	3.9862E-03
38	1.6071E+03	2.5577E+02	3.9097E-03
39	1.6744E+03	2.6649E+02	3.7525E-03
40	1.6977E+03	2.7020E+02	3.7009E-03
41	1.7327E+03	2.7576E+02	3.6263E-03
42	1.7433E+03	2.7746E+02	3.6041E-03
43	1.8185E+03	2.8942E+02	3.4552E-03
44	1.9114E+03	3.0421E+02	3.2873E-03
45	1.9268E+03	3.0667E+02	3.2609E-03
46	2.0696E+03	3.2939E+02	3.0359E-03
47	2.0788E+03	3.3086E+02	3.0224E-03
48	2.0999E+03	3.3421E+02	2.9922E-03
49	2.1783E+03	3.4669E+02	2.8844E-03
50	2.2665E+03	3.6072E+02	2.7722E-03
51	2.2857E+03	3.6378E+02	2.7489E-03
52	2.3581E+03	3.7530E+02	2.6645E-03
53	2.4199E+03	3.8514E+02	2.5964E-03
54	2.5081E+03	3.9917E+02	2.5052E-03
55	2.5468E+03	4.0533E+02	2.4671E-03
56	2.5747E+03	4.0978E+02	2.4404E-03
57	2.5992E+03	4.1367E+02	2.4174E-03
58	2.6559E+03	4.2270E+02	2.3657E-03
59	2.7126E+03	4.3173E+02	2.3163E-03
60	2.7592E+03	4.3914E+02	2.2772E-03
61	2.8270E+03	4.4993E+02	2.2226E-03
62	2.8610E+03	4.5533E+02	2.1962E-03
63	2.9370E+03	4.6744E+02	2.1393E-03
64	2.9443E+03	4.6860E+02	2.1340E-03
65	3.0095E+03	4.7898E+02	2.0878E-03





Mode Number	Circular Frequency (rad/sec)	Frequency (Hertz)	Period (sec)
66	3.0448E+03	4.8460E+02	2.0636E-03
67	3.0846E+03	4.9093E+02	2.0370E-03
68	3.1316E+03	4.9841E+02	2.0064E-03
69	3.2153E+03	5.1173E+02	1.9542E-03
70	3.2364E+03	5.1509E+02	1.9414E-03
71	3.2885E+03	5.2338E+02	1.9107E-03
72	3.3482E+03	5.3288E+02	1.8766E-03
73	3.4198E+03	5.4428E+02	1.8373E-03
74	3.4424E+03	5.4788E+02	1.8252E-03
75	3.6003E+03	5.7300E+02	1.7452E-03
76	3.6259E+03	5.7708E+02	1.7329E-03
77	3.6805E+03	5.8577E+02	1.7072E-03
78	3.7099E+03	5.9045E+02	1.6936E-03
79	3.7489E+03	5.9666E+02	1.6760E-03
80	3.8140E+03	6.0702E+02	1.6474E-03

The Sturm sequence check didn't find any missing frequency.

1\*\*\*\* End of file



Run # 3, Modal Frequencies for Model With 1.50 lb Weight Added

1\*\*\*\* Algor (c) Dynamic Modal Analysis - SSAP1H 3/3/89, Ver 8.002D/387

1\*\*\*\* PRINT OF NATURAL FREQUENCIES

Mode Number	Circular Frequency (rad/sec)	Frequency (Hz)	Period (sec)
1	1.0000E-10	1.5915E-11	6.2832E+10
2	1.0000E-10	1.5915E-11	6.2832E+10
3	5.1019E-05	8.1200E-06	1.2315E+05
4	5.0116E-04	7.9762E-05	1.2537E+04
5	6.5347E-04	1.0400E-04	9.6151E+03
6	3.0001E+00	4.7748E-01	2.0943E+00
7	1.0393E+02	1.6541E+01	6.0455E-02
8	1.3081E+02	2.0819E+01	4.8032E-02
9	1.6422E+02	2.6137E+01	3.8260E-02
10	2.1113E+02	3.3603E+01	2.9759E-02
11	2.2591E+02	3.5955E+01	2.7813E-02
12	3.3152E+02	5.2763E+01	1.8953E-02
13	3.3854E+02	5.3880E+01	1.8560E-02
14	3.9194E+02	6.2379E+01	1.6031E-02
15	4.0860E+02	6.5031E+01	1.5377E-02
16	5.4335E+02	8.6477E+01	1.1564E-02
17	5.7009E+02	9.0733E+01	1.1021E-02
18	5.9608E+02	9.4869E+01	1.0541E-02
19	6.9274E+02	1.1025E+02	9.0701E-03
20	7.2042E+02	1.1466E+02	8.7215E-03
21	7.4553E+02	1.1865E+02	8.4279E-03
22	7.7367E+02	1.2313E+02	8.1213E-03
23	7.8448E+02	1.2485E+02	8.0094E-03
24	8.1389E+02	1.2953E+02	7.7200E-03
25	8.7871E+02	1.3985E+02	7.1504E-03
26	9.3896E+02	1.4944E+02	6.6917E-03
27	9.7471E+02	1.5513E+02	6.4462E-03
28	1.0600E+03	1.6871E+02	5.9275E-03
29	1.1085E+03	1.7642E+02	5.6684E-03
30	1.1417E+03	1.8171E+02	5.5034E-03



Mode Number	Circular Frequency (rad/sec)	Frequency (Hz)	Period (sec)
31	1.2144E+03	1.9327E+02	5.1740E-03
32	1.2791E+03	2.0358E+02	4.9121E-03
33	1.2916E+03	2.0557E+02	4.8646E-03
34	1.3240E+03	2.1072E+02	4.7457E-03
35	1.4071E+03	2.2395E+02	4.4653E-03
36	1.4859E+03	2.3650E+02	4.2284E-03
37	1.5779E+03	2.5113E+02	3.9819E-03
38	1.6043E+03	2.5534E+02	3.9164E-03
39	1.6743E+03	2.6648E+02	3.7527E-03
40	1.7039E+03	2.7119E+02	3.6875E-03
41	1.7327E+03	2.7577E+02	3.6262E-03
42	1.7485E+03	2.7828E+02	3.5935E-03
43	1.8200E+03	2.8967E+02	3.4522E-03
44	1.9152E+03	3.0481E+02	3.2807E-03
45	1.9277E+03	3.0680E+02	3.2595E-03
46	2.0788E+03	3.3086E+02	3.0225E-03
47	2.0880E+03	3.3232E+02	3.0092E-03
48	2.1000E+03	3.3422E+02	2.9920E-03
49	2.1881E+03	3.4824E+02	2.8716E-03
50	2.2760E+03	3.6223E+02	2.7607E-03
51	2.2959E+03	3.6541E+02	2.7367E-03
52	2.3707E+03	3.7731E+02	2.6504E-03
53	2.4216E+03	3.8541E+02	2.5947E-03
54	2.5170E+03	4.0059E+02	2.4963E-03
55	2.5685E+03	4.0880E+02	2.4462E-03
56	2.5984E+03	4.1355E+02	2.4181E-03
57	2.6290E+03	4.1841E+02	2.3900E-03
58	2.6933E+03	4.2865E+02	2.3329E-03
59	2.7411E+03	4.3626E+02	2.2922E-03
60	2.7928E+03	4.4448E+02	2.2498E-03
61	2.8373E+03	4.5157E+02	2.2145E-03
62	2.8792E+03	4.5824E+02	2.1823E-03
63	2.9388E+03	4.6773E+02	2.1380E-03
64	2.9594E+03	4.7101E+02	2.1231E-03
65	2.9948E+03	4.7664E+02	2.0980E-03



Mode Number	Circular Frequency (rad/sec)	Frequency (Hz)	Period (sec)
66	3.0496E+03	4.8535E+02	2.0604E-03
67	3.1212E+03	4.9675E+02	2.0131E-03
68	3.1970E+03	5.0881E+02	1.9654E-03
69	3.2354E+03	5.1493E+02	1.9420E-03
70	3.2557E+03	5.1816E+02	1.9299E-03
71	3.3267E+03	5.2946E+02	1.8887E-03
72	3.3590E+03	5.3459E+02	1.8706E-03
73	3.4217E+03	5.4458E+02	1.8363E-03
74	3.4441E+03	5.4815E+02	1.8243E-03
75	3.6024E+03	5.7334E+02	1.7442E-03
76	3.6262E+03	5.7712E+02	1.7327E-03
77	3.6930E+03	5.8777E+02	1.7014E-03
78	3.7286E+03	5.9343E+02	1.6851E-03
79	3.7647E+03	5.9917E+02	1.6690E-03
80	3.8107E+03	6.0650E+02	1.6488E-03

The Sturm sequence check didn't find any missing frequency.

1\*\*\*\* End of file





Run # 4, Modal Frequencies for Model With 0.75 lb Weight Added at Node # 277

1\*\*\*\* Algor (c) Dynamic Modal Analysis - SSAP1H 3/3/89, Ver 8.002D/387

1\*\*\*\* PRINT OF NATURAL FREQUENCIES

Mode Number	Circular Frequency (rad/sec)	Frequency (Hz)	Period (sec)
1	1.0000E-10	1.5915E-11	6.2832E+10
2	1.0000E-10	1.5915E-11	6.2832E+10
3	8.0877E-05	1.2872E-05	7.7688E+04
4	5.9605E-04	9.4865E-05	1.0541E+04
5	6.8167E-04	1.0849E-04	9.2173E+03
6	3.0001E+00	4.7748E-01	2.0943E+00
7	1.0393E+02	1.6541E+01	6.0454E-02
8	1.3081E+02	2.0820E+01	4.8032E-02
9	1.6427E+02	2.6144E+01	3.8250E-02
10	2.1115E+02	3.3606E+01	2.9756E-02
11	2.2593E+02	3.5957E+01	2.7811E-02
12	3.3196E+02	5.2833E+01	1.8927E-02
13	3.3891E+02	5.3939E+01	1.8539E-02
14	3.9198E+02	6.2386E+01	1.6029E-02
15	4.0861E+02	6.5033E+01	1.5377E-02
16	5.4330E+02	8.6469E+01	1.1565E-02
17	5.7140E+02	9.0942E+01	1.0996E-02
18	5.9689E+02	9.4998E+01	1.0527E-02
19	6.9502E+02	1.1062E+02	9.0403E-03
20	7.2058E+02	1.1468E+02	8.7196E-03
21	7.4794E+02	1.1904E+02	8.4007E-03
22	7.7363E+02	1.2313E+02	8.1217E-03
23	7.8317E+02	1.2465E+02	8.0227E-03
24	8.1346E+02	1.2947E+02	7.7240E-03
25	8.7856E+02	1.3983E+02	7.1517E-03
26	9.3898E+02	1.4944E+02	6.6915E-03
27	9.7473E+02	1.5513E+02	6.4461E-03
28	1.0600E+03	1.6871E+02	5.9275E-03
29	1.1087E+03	1.7645E+02	5.6673E-03
30	1.1419E+03	1.8175E+02	5.5022E-03



Mode Number	Circular Frequency (rad/sec)	Frequency (Hz)	Period (sec)
31	1.2145E+03	1.9329E+02	5.1735E-03
32	1.2794E+03	2.0362E+02	4.9112E-03
33	1.2915E+03	2.0555E+02	4.8651E-03
34	1.3236E+03	2.1065E+02	4.7471E-03
35	1.4068E+03	2.2391E+02	4.4661E-03
36	1.4861E+03	2.3652E+02	4.2280E-03
37	1.5781E+03	2.5116E+02	3.9815E-03
38	1.6033E+03	2.5518E+02	3.9188E-03
39	1.6743E+03	2.6648E+02	3.7527E-03
40	1.7045E+03	2.7128E+02	3.6862E-03
41	1.7326E+03	2.7576E+02	3.6264E-03
42	1.7493E+03	2.7842E+02	3.5917E-03
43	1.8198E+03	2.8964E+02	3.4526E-03
44	1.9157E+03	3.0489E+02	3.2799E-03
45	1.9278E+03	3.0682E+02	3.2592E-03
46	2.0788E+03	3.3086E+02	3.0225E-03
47	2.0900E+03	3.3264E+02	3.0063E-03
48	2.0999E+03	3.3421E+02	2.9921E-03
49	2.1889E+03	3.4837E+02	2.8705E-03
50	2.2766E+03	3.6233E+02	2.7599E-03
51	2.2970E+03	3.6559E+02	2.7353E-03
52	2.3722E+03	3.7755E+02	2.6487E-03
53	2.4219E+03	3.8546E+02	2.5943E-03
54	2.5165E+03	4.0052E+02	2.4968E-03
55	2.5688E+03	4.0884E+02	2.4460E-03
56	2.5985E+03	4.1357E+02	2.4180E-03
57	2.6317E+03	4.1884E+02	2.3875E-03
58	2.6958E+03	4.2905E+02	2.3307E-03
59	2.7437E+03	4.3668E+02	2.2900E-03
60	2.8001E+03	4.4565E+02	2.2439E-03
61	2.8392E+03	4.5187E+02	2.2130E-03
62	2.8843E+03	4.5905E+02	2.1784E-03
63	2.9390E+03	4.6776E+02	2.1378E-03
64	2.9978E+03	4.7712E+02	2.0959E-03
65	3.0483E+03	4.8515E+02	2.0612E-03



Mode Number	Circular Frequency (rad/sec)	Frequency (Hz)	Period (sec)
66	3.0704E+03	4.8867E+02	2.0464E-03
67	3.1230E+03	4.9704E+02	2.0119E-03
68	3.2041E+03	5.0995E+02	1.9610E-03
69	3.2359E+03	5.1501E+02	1.9417E-03
70	3.2705E+03	5.2051E+02	1.9212E-03
71	3.3409E+03	5.3173E+02	1.8807E-03
72	3.4082E+03	5.4244E+02	1.8435E-03
73	3.4304E+03	5.4597E+02	1.8316E-03
74	3.4520E+03	5.4941E+02	1.8201E-03
75	3.6043E+03	5.7364E+02	1.7433E-03
76	3.6279E+03	5.7741E+02	1.7319E-03
77	3.6953E+03	5.8812E+02	1.7003E-03
78	3.7358E+03	5.9458E+02	1.6819E-03
79	3.7906E+03	6.0329E+02	1.6576E-03

The Sturm sequence check didn't find any missing frequency.

1\*\*\*\* End of file



Run # 5, Modal Frequencies for Model With 0.75 lb Weight Added to Opposite Beams

1\*\*\*\* Algor (c) Dynamic Modal Analysis - SSAP1H 3/3/89, Ver 8.002D/387

1\*\*\*\* PRINT OF NATURAL FREQUENCIES

Mode Number	Circular Frequency (rad/sec)	Frequency (Hz)	Period (sec)
1	1.0000E-10	1.5915E-11	6.2832E+10
2	1.0000E-10	1.5915E-11	6.2832E+10
3	1.0000E-10	1.5915E-11	6.2832E+10
4	4.8223E-04	7.6749E-05	1.3030E+04
5	6.3061E-04	1.0036E-04	9.9636E+03
6	3.0001E+00	4.7748E-01	2.0943E+00
7	1.0393E+02	1.6541E+01	6.0455E-02
8	1.3081E+02	2.0819E+01	4.8032E-02
9	1.6423E+02	2.6138E+01	3.8259E-02
10	2.1114E+02	3.3604E+01	2.9758E-02
11	2.2591E+02	3.5955E+01	2.7812E-02
12	3.3163E+02	5.2780E+01	1.8947E-02
13	3.3868E+02	5.3903E+01	1.8552E-02
14	3.9195E+02	6.2381E+01	1.6031E-02
15	4.0860E+02	6.5031E+01	1.5377E-02
16	5.4344E+02	8.6492E+01	1.1562E-02
17	5.7082E+02	9.0848E+01	1.1007E-02
18	5.9623E+02	9.4894E+01	1.0538E-02
19	6.9563E+02	1.1071E+02	9.0324E-03
20	7.2055E+02	1.1468E+02	8.7199E-03
21	7.4479E+02	1.1854E+02	8.4361E-03
22	7.7326E+02	1.2307E+02	8.1256E-03
23	7.8238E+02	1.2452E+02	8.0309E-03
24	8.1296E+02	1.2939E+02	7.7288E-03
25	8.7812E+02	1.3976E+02	7.1553E-03
26	9.3862E+02	1.4939E+02	6.6941E-03
27	9.7467E+02	1.5512E+02	6.4465E-03
28	1.0600E+03	1.6871E+02	5.9275E-03
29	1.1084E+03	1.7641E+02	5.6686E-03
30	1.1416E+03	1.8169E+02	5.5037E-03





Mode Number	Circular Frequency (rad/sec)	Frequency (Hz)	Period (sec)
31	1.2143E+03	1.9326E+02	5.1743E-03
32	1.2791E+03	2.0357E+02	4.9123E-03
33	1.2916E+03	2.0557E+02	4.8646E-03
34	1.3238E+03	2.1068E+02	4.7465E-03
35	1.4071E+03	2.2395E+02	4.4653E-03
36	1.4859E+03	2.3649E+02	4.2284E-03
37	1.5777E+03	2.5111E+02	3.9824E-03
38	1.6013E+03	2.5486E+02	3.9237E-03
39	1.6735E+03	2.6634E+02	3.7546E-03
40	1.7034E+03	2.7111E+02	3.6885E-03
41	1.7326E+03	2.7575E+02	3.6264E-03
42	1.7489E+03	2.7834E+02	3.5927E-03
43	1.8197E+03	2.8961E+02	3.4529E-03
44	1.9150E+03	3.0478E+02	3.2811E-03
45	1.9273E+03	3.0674E+02	3.2601E-03
46	2.0787E+03	3.3083E+02	3.0227E-03
47	2.0887E+03	3.3243E+02	3.0082E-03
48	2.1000E+03	3.3422E+02	2.9920E-03
49	2.1880E+03	3.4823E+02	2.8716E-03
50	2.2748E+03	3.6204E+02	2.7621E-03
51	2.2963E+03	3.6546E+02	2.7362E-03
52	2.3713E+03	3.7740E+02	2.6497E-03
53	2.4216E+03	3.8541E+02	2.5946E-03
54	2.5171E+03	4.0061E+02	2.4962E-03
55	2.5685E+03	4.0878E+02	2.4463E-03
56	2.5984E+03	4.1354E+02	2.4181E-03
57	2.6291E+03	4.1843E+02	2.3899E-03
58	2.6942E+03	4.2880E+02	2.3321E-03
59	2.7428E+03	4.3654E+02	2.2908E-03
60	2.7923E+03	4.4440E+02	2.2502E-03
61	2.8309E+03	4.5055E+02	2.2195E-03
62	2.8815E+03	4.5860E+02	2.1806E-03
63	2.9379E+03	4.6758E+02	2.1387E-03
64	2.9426E+03	4.6833E+02	2.1353E-03
65	2.9974E+03	4.7705E+02	2.0962E-03



Mode Number	Circular Frequency (rad/sec)	Frequency (Hz)	Period (sec)
66	3.0478E+03	4.8507E+02	2.0616E-03
67	3.1199E+03	4.9655E+02	2.0139E-03
68	3.2003E+03	5.0935E+02	1.9633E-03
69	3.2344E+03	5.1477E+02	1.9426E-03
70	3.2654E+03	5.1970E+02	1.9242E-03
71	3.3303E+03	5.3003E+02	1.8867E-03
72	3.3441E+03	5.3223E+02	1.8789E-03
73	3.4216E+03	5.4456E+02	1.8363E-03
74	3.4455E+03	5.4837E+02	1.8236E-03
75	3.5985E+03	5.7272E+02	1.7461E-03
76	3.6257E+03	5.7704E+02	1.7330E-03
77	3.6942E+03	5.8795E+02	1.7008E-03
78	3.7058E+03	5.8979E+02	1.6955E-03
79	3.7455E+03	5.9611E+02	1.6775E-03
80	3.8104E+03	6.0645E+02	1.6489E-03

The Sturm sequence check didn't find an missing frequency.

1\*\*\*\* End of file



## APPENDIX F. RADIATED POWER DATA

The boundary element program output contains the pressure, velocity, and intensity at each node on the plate. It also calculates the power radiated from each element and integrates it over the entire plate to get the total radiated power. These tables summarize the total radiated power from the boundary element model into a semi-infinite acoustic medium in the frequency band 450 - 500 Hz. Each of the data tables is for a different loading of the model foundation.

Forcing applied at node # 303, amplitude = .75 lb rms.

Run # 0, foundation unloaded.

Freq (Hz)	k (in <sup>-1</sup> )	Power (in-lb/sec)	Power (Watts)	Radiation Efficiency
450	4.85E-02	6.41E-03	2.90E-05	1.40E-10
451	4.86E-02	3.05E-03	1.38E-05	6.60E-11
452	4.87E-02	3.61E-04	1.63E-06	7.64E-12
453	4.88E-02	4.47E-03	2.02E-05	9.22E-11
454	4.89E-02	5.67E-03	2.56E-05	1.14E-10
455	4.90E-02	7.56E-03	3.42E-05	1.49E-10
456	4.91E-02	6.50E-03	2.94E-05	1.24E-10
457	4.92E-02	2.61E-03	1.18E-05	5.21E-11
458	4.93E-02	3.38E-03	1.53E-05	6.57E-11
459	4.95E-02	4.70E-03	2.12E-05	8.82E-11
460	4.96E-02	5.38E-03	2.43E-05	9.82E-11
461	4.97E-02	5.68E-03	2.57E-05	1.07E-10
462	4.98E-02	5.01E-03	2.27E-05	9.19E-11
463	4.99E-02	4.02E-03	1.82E-05	7.58E-11
464	5.00E-02	5.24E-03	2.37E-05	1.06E-10



Freq (Hz)	k (in <sup>-1</sup> )	Power (in-lb/sec)	Power (Watts)	Radiation Efficiency
465	5.01E-02	3.27E-03	1.48E-05	6.33E-11
466	5.02E-02	6.39E-03	2.89E-05	1.20E-10
467	5.03E-02	4.25E-03	1.92E-05	7.77E-11
468	5.04E-02	8.04E-03	3.63E-05	1.42E-10
469	5.05E-02	8.05E-03	3.64E-05	1.41E-10
470	5.06E-02	5.09E-03	2.30E-05	9.28E-11
471	5.07E-02	1.04E-02	4.70E-05	1.94E-10
472	5.09E-02	9.66E-03	4.37E-05	1.80E-10
473	5.10E-02	1.37E-02	6.17E-05	2.45E-10
474	5.11E-02	1.31E-02	5.94E-05	2.37E-10
475	5.12E-02	8.41E-03	3.80E-05	1.51E-10
476	5.13E-02	7.08E-03	3.20E-05	1.29E-10
477	5.14E-02	4.70E-03	2.12E-05	8.32E-11
478	5.15E-02	1.38E-02	6.25E-05	2.38E-10
479	5.16E-02	1.10E-02	4.99E-05	1.96E-10
480	5.17E-02	1.29E-02	5.82E-05	2.18E-10
481	5.18E-02	7.49E-03	3.38E-05	1.34E-10
482	5.19E-02	1.14E-02	5.17E-05	1.95E-10
483	5.20E-02	1.24E-02	5.61E-05	2.06E-10
484	5.21E-02	8.47E-03	3.83E-05	1.43E-10
485	5.22E-02	7.95E-03	3.59E-05	1.34E-10
486	5.24E-02	4.61E-03	2.08E-05	7.58E-11
487	5.25E-02	5.40E-03	2.44E-05	8.66E-11
488	5.26E-02	3.91E-03	1.77E-05	6.24E-11
489	5.27E-02	8.76E-03	3.96E-05	1.36E-10
490	5.28E-02	8.19E-03	3.70E-05	1.27E-10
491	5.29E-02	6.60E-03	2.98E-05	1.00E-10
492	5.30E-02	1.11E-02	5.02E-05	1.62E-10
493	5.31E-02	1.46E-02	6.62E-05	2.11E-10
494	5.32E-02	8.59E-03	3.88E-05	1.25E-10
495	5.33E-02	1.04E-02	4.70E-05	1.50E-10
496	5.34E-02	1.42E-02	6.43E-05	2.10E-10
497	5.35E-02	1.28E-02	5.77E-05	1.94E-10
498	5.37E-02	9.03E-03	4.08E-05	1.41E-10
499	5.38E-02	9.67E-03	4.37E-05	1.53E-10
500	5.39E-02	1.37E-02	6.20E-05	2.17E-10





Forcing applied at node # 303, amplitude = .75 lb rms.

Run # 1, foundation modified with .375 lb weight added to node # 285

Freq (Hz)	k (in <sup>-1</sup> )	Power (in-lb/sec)	Power (Watts)	Radiation Efficiency
450	4.85E-02	7.34E-03	3.32E-05	1.53E-10
451	4.86E-02	3.35E-03	1.52E-05	7.15E-11
452	4.87E-02	3.26E-04	1.47E-06	6.85E-12
453	4.88E-02	4.48E-03	2.03E-05	9.16E-11
454	4.89E-02	5.65E-03	2.56E-05	1.12E-10
455	4.90E-02	7.68E-03	3.47E-05	1.50E-10
456	4.91E-02	6.05E-03	2.73E-05	7.50E-12
457	4.92E-02	2.62E-03	1.18E-05	5.20E-11
458	4.93E-02	3.39E-03	1.53E-05	6.57E-11
459	4.95E-02	4.71E-03	2.13E-05	8.79E-11
460	4.96E-02	4.50E-03	2.03E-05	8.54E-11
461	4.97E-02	5.34E-03	2.41E-05	9.96E-11
462	4.98E-02	4.78E-03	2.16E-05	8.89E-11
463	4.99E-02	4.70E-03	2.13E-05	8.92E-11
464	5.00E-02	5.27E-03	2.38E-05	1.07E-10
465	5.01E-02	2.00E-03	9.05E-06	4.05E-11
466	5.02E-02	6.42E-03	2.90E-05	1.20E-10
467	5.03E-02	4.28E-03	1.93E-05	7.78E-11
468	5.04E-02	8.11E-03	3.66E-05	1.43E-10
469	5.05E-02	7.85E-03	3.55E-05	1.38E-10
470	5.06E-02	6.58E-03	2.98E-05	1.17E-10
471	5.07E-02	1.04E-02	4.69E-05	2.01E-10
472	5.09E-02	9.87E-03	4.46E-05	1.81E-10
473	5.10E-02	1.37E-02	6.20E-05	2.45E-10
474	5.11E-02	1.32E-02	5.97E-05	2.37E-10
475	5.12E-02	8.46E-03	3.82E-05	1.51E-10
476	5.13E-02	7.11E-03	3.22E-05	1.29E-10
477	5.14E-02	4.70E-03	2.13E-05	8.30E-11
478	5.15E-02	1.39E-02	6.27E-05	2.38E-10
479	5.16E-02	1.11E-02	5.01E-05	1.96E-10
480	5.17E-02	1.34E-02	6.04E-05	2.22E-10



Freq (Hz)	k (in <sup>-1</sup> )	Power (in-lb/sec)	Power (Watts)	Radiation Efficiency
481	5.18E-02	7.52E-03	3.40E-05	1.34E-10
482	5.19E-02	1.15E-02	5.18E-05	1.94E-10
483	5.20E-02	1.17E-02	5.31E-05	2.02E-10
484	5.21E-02	8.49E-03	3.84E-05	1.42E-10
485	5.22E-02	7.97E-03	3.60E-05	1.34E-10
486	5.24E-02	4.59E-03	2.07E-05	7.51E-11
487	5.25E-02	5.40E-03	2.44E-05	8.62E-11
488	5.26E-02	3.90E-03	1.76E-05	6.20E-11
489	5.27E-02	8.82E-03	3.99E-05	1.39E-10
490	5.28E-02	8.22E-03	3.72E-05	1.26E-10
491	5.29E-02	6.52E-03	2.95E-05	9.88E-11
492	5.30E-02	1.02E-02	4.63E-05	1.52E-10
493	5.31E-02	1.46E-02	6.60E-05	2.10E-10
494	5.32E-02	8.55E-03	3.86E-05	1.24E-10
495	5.33E-02	1.04E-02	4.68E-05	1.49E-10
496	5.34E-02	1.42E-02	6.42E-05	2.10E-10
497	5.35E-02	1.27E-02	5.76E-05	1.93E-10
498	5.37E-02	9.05E-03	4.09E-05	1.41E-10
499	5.38E-02	9.66E-03	4.37E-05	1.53E-10
500	5.39E-02	1.37E-02	6.19E-05	2.17E-10



Forcing applied at node # 303, amplitude = .75 lb rms.

Run # 2, foundation modified with .75 lb weight added to node # 285

Freq (Hz)	k (in <sup>-1</sup> )	Power (in-lb/sec)	Power (Watts)	Radiation Efficiency
450	4.85E-02	6.46E-03	2.92E-05	1.30E-10
451	4.86E-02	2.23E-03	1.01E-05	4.56E-11
452	4.87E-02	-1.72E-03	-7.80E-06	-3.44E-11
453	4.88E-02	4.70E-03	2.12E-05	9.27E-11
454	4.89E-02	5.06E-03	2.29E-05	9.94E-11
455	4.90E-02	7.66E-03	3.46E-05	1.48E-10
456	4.91E-02	6.45E-03	2.91E-05	1.20E-10
457	4.92E-02	3.54E-03	1.60E-05	7.05E-11
458	4.93E-02	3.61E-03	1.63E-05	7.34E-11
459	4.95E-02	5.54E-03	2.51E-05	1.13E-10
460	4.96E-02	5.48E-03	2.48E-05	1.06E-10
461	4.97E-02	7.24E-03	3.27E-05	1.37E-10
462	4.98E-02	8.18E-03	3.70E-05	1.64E-10
463	4.99E-02	5.89E-03	2.66E-05	1.16E-10
464	5.00E-02	5.71E-03	2.58E-05	1.10E-10
465	5.01E-02	2.74E-03	1.24E-05	5.46E-11
466	5.02E-02	6.83E-03	3.09E-05	1.34E-10
467	5.03E-02	5.45E-03	2.46E-05	1.04E-10
468	5.04E-02	8.52E-03	3.85E-05	1.59E-10
469	5.05E-02	8.56E-03	3.87E-05	1.54E-10
470	5.06E-02	7.35E-03	3.32E-05	1.30E-10
471	5.07E-02	1.08E-02	4.89E-05	1.79E-10
472	5.09E-02	1.06E-02	4.81E-05	1.71E-10
473	5.10E-02	1.31E-02	5.92E-05	2.06E-10
474	5.11E-02	1.29E-02	5.83E-05	2.09E-10
475	5.12E-02	7.32E-03	3.31E-05	1.16E-10
476	5.13E-02	6.22E-03	2.81E-05	1.03E-10
477	5.14E-02	5.92E-03	2.67E-05	9.84E-11
478	5.15E-02	1.46E-02	6.61E-05	2.47E-10
479	5.16E-02	1.09E-02	4.92E-05	1.78E-10
480	5.17E-02	1.05E-02	4.75E-05	1.86E-10



Freq (Hz)	k (in <sup>-1</sup> )	Power (in-lb/sec)	Power (Watts)	Radiation Efficiency
481	5.18E-02	7.37E-03	3.33E-05	1.27E-10
482	5.19E-02	1.08E-02	4.90E-05	1.91E-10
483	5.20E-02	1.19E-02	5.40E-05	2.07E-10
484	5.21E-02	7.78E-03	3.52E-05	1.36E-10
485	5.22E-02	7.56E-03	3.42E-05	1.28E-10
486	5.24E-02	3.40E-03	1.54E-05	5.71E-11
487	5.25E-02	4.71E-03	2.13E-05	7.71E-12
488	5.26E-02	3.42E-03	1.54E-05	5.48E-12
489	5.27E-02	8.70E-03	3.93E-05	1.32E-10
490	5.28E-02	8.18E-03	3.70E-05	1.24E-10
491	5.29E-02	6.27E-03	2.83E-05	9.35E-11
492	5.30E-02	9.85E-03	4.45E-05	1.45E-10
493	5.31E-02	1.44E-02	6.53E-05	2.06E-10
494	5.32E-02	8.58E-03	3.88E-05	1.24E-10
495	5.33E-02	1.01E-02	4.55E-05	1.44E-10
496	5.34E-02	1.39E-02	6.30E-05	2.06E-10
497	5.35E-02	1.17E-02	5.28E-05	1.83E-10
498	5.37E-02	8.87E-03	4.01E-05	1.44E-10
499	5.38E-02	9.51E-03	4.30E-05	1.50E-10
500	5.39E-02	1.36E-02	6.14E-05	2.15E-10





Forcing applied at node # 303, amplitude = .75 lb rms.

Run # 3, foundation modified with 1.5 lb weight added to node # 285

Freq (Hz)	k (in <sup>-1</sup> )	Power (in-lb/sec)	Power (Watts)	Radiation Efficiency
450	4.85E-02	7.36E-03	3.33E-05	1.52E-10
451	4.86E-02	3.70E-03	1.67E-05	7.52E-11
452	4.87E-02	1.08E-03	4.90E-06	2.17E-11
453	4.88E-02	4.78E-03	2.16E-05	9.54E-11
454	4.89E-02	6.48E-03	2.93E-05	1.24E-10
455	4.90E-02	7.41E-03	3.35E-05	1.43E-10
456	4.91E-02	6.13E-03	2.77E-05	1.15E-10
457	4.92E-02	2.24E-03	1.01E-05	4.30E-11
458	4.93E-02	3.49E-03	1.58E-05	6.59E-11
459	4.95E-02	4.94E-03	2.23E-05	9.09E-11
460	4.96E-02	3.70E-03	1.67E-05	6.78E-11
461	4.97E-02	5.06E-03	2.29E-05	9.53E-11
462	4.98E-02	5.02E-03	2.27E-05	9.58E-11
463	4.99E-02	5.27E-03	2.38E-05	1.07E-10
464	5.00E-02	5.24E-03	2.37E-05	1.02E-10
465	5.01E-02	3.27E-03	1.48E-05	6.34E-11
466	5.02E-02	6.37E-03	2.88E-05	1.20E-10
467	5.03E-02	4.30E-03	1.94E-05	7.84E-11
468	5.04E-02	7.83E-03	3.54E-05	1.40E-10
469	5.05E-02	7.84E-03	3.54E-05	1.37E-10
470	5.06E-02	6.36E-03	2.87E-05	1.24E-10
471	5.07E-02	1.08E-02	4.87E-05	2.07E-10
472	5.09E-02	9.86E-03	4.46E-05	1.81E-10
473	5.10E-02	1.35E-02	6.12E-05	2.50E-10
474	5.11E-02	1.32E-02	5.95E-05	2.37E-10
475	5.12E-02	8.37E-03	3.78E-05	1.49E-10
476	5.13E-02	6.83E-03	3.09E-05	1.19E-10
477	5.14E-02	5.66E-03	2.56E-05	9.58E-11
478	5.15E-02	1.46E-02	6.58E-05	2.37E-10
479	5.16E-02	1.15E-02	5.22E-05	1.97E-10
480	5.17E-02	1.24E-02	5.60E-05	2.09E-10



Freq (Hz)	k (in <sup>-1</sup> )	Power (in-lb/sec)	Power (Watts)	Radiation Efficiency
481	5.18E-02	7.54E-03	3.41E-05	1.34E-10
482	5.19E-02	1.14E-02	5.16E-05	1.93E-10
483	5.20E-02	1.16E-02	5.26E-05	2.00E-10
484	5.21E-02	8.11E-03	3.66E-05	1.40E-10
485	5.22E-02	7.91E-03	3.58E-05	1.33E-10
486	5.24E-02	4.48E-03	2.02E-05	7.31E-11
487	5.25E-02	5.28E-03	2.39E-05	8.38E-11
488	5.26E-02	3.77E-03	1.71E-05	5.94E-11
489	5.27E-02	8.57E-03	3.87E-05	1.31E-10
490	5.28E-02	8.22E-03	3.72E-05	1.25E-10
491	5.29E-02	6.01E-03	2.72E-05	9.08E-11
492	5.30E-02	1.08E-02	4.86E-05	1.56E-10
493	5.31E-02	1.45E-02	6.56E-05	2.06E-10
494	5.32E-02	8.64E-03	3.90E-05	1.25E-10
495	5.33E-02	9.78E-03	4.42E-05	1.43E-10
496	5.34E-02	1.44E-02	6.53E-05	2.09E-10
497	5.35E-02	1.23E-02	5.57E-05	1.84E-10
498	5.37E-02	8.99E-03	4.06E-05	1.38E-10
499	5.38E-02	9.61E-03	4.34E-05	1.53E-10
500	5.39E-02	1.37E-02	6.19E-05	2.18E-10



Forcing applied at node # 303, amplitude = .75 lb rms.

Run # 4, foundation modified with .75 lb weight added to node # 277

Freq (Hz)	k (in <sup>-1</sup> )	Power (in-lb/sec)	Power (Watts)	Radiation Efficiency
450	4.85E-02	7.33E-03	3.31E-05	1.53E-10
451	4.86E-02	3.04E-03	1.38E-05	6.56E-11
452	4.87E-02	3.44E-04	1.56E-06	7.26E-12
453	4.88E-02	4.47E-03	2.02E-05	9.18E-11
454	4.89E-02	5.64E-03	2.55E-05	1.13E-10
455	4.90E-02	7.81E-03	3.53E-05	1.53E-10
456	4.91E-02	6.06E-03	2.74E-05	1.18E-10
457	4.92E-02	2.61E-03	1.18E-05	5.20E-11
458	4.93E-02	3.38E-03	1.53E-05	6.57E-11
459	4.95E-02	4.70E-03	2.12E-05	8.81E-11
460	4.96E-02	5.39E-03	2.44E-05	9.82E-11
461	4.97E-02	5.69E-03	2.57E-05	1.07E-10
462	4.98E-02	5.02E-03	2.27E-05	9.18E-11
463	4.99E-02	4.04E-03	1.82E-05	7.60E-11
464	5.00E-02	5.25E-03	2.37E-05	1.07E-10
465	5.01E-02	3.28E-03	1.48E-05	6.34E-11
466	5.02E-02	6.40E-03	2.89E-05	1.20E-10
467	5.03E-02	4.26E-03	1.92E-05	7.77E-11
468	5.04E-02	8.06E-03	3.64E-05	1.43E-10
469	5.05E-02	8.32E-03	3.76E-05	1.43E-10
470	5.06E-02	5.11E-03	2.31E-05	9.29E-11
471	5.07E-02	1.04E-02	4.71E-05	1.94E-10
472	5.09E-02	9.67E-03	4.37E-05	1.79E-10
473	5.10E-02	1.37E-02	6.19E-05	2.45E-10
474	5.11E-02	1.32E-02	5.95E-05	2.37E-10
475	5.12E-02	8.46E-03	3.82E-05	1.51E-10
476	5.13E-02	6.95E-03	3.14E-05	1.20E-10
477	5.14E-02	4.74E-03	2.14E-05	8.39E-11
478	5.15E-02	1.38E-02	6.26E-05	2.38E-10
479	5.16E-02	1.10E-02	4.99E-05	1.96E-10
480	5.17E-02	1.29E-02	5.82E-05	2.18E-10



Freq (Hz)	k (in <sup>-1</sup> )	Power (in-lb/sec)	Power (Watts)	Radiation Efficiency
481	5.18E-02	7.49E-03	3.38E-05	1.34E-10
482	5.19E-02	1.14E-02	5.16E-05	1.94E-10
483	5.20E-02	1.17E-02	5.29E-05	2.02E-10
484	5.21E-02	8.44E-03	3.82E-05	1.44E-10
485	5.22E-02	7.94E-03	3.59E-05	1.34E-10
486	5.24E-02	4.54E-03	2.05E-05	7.45E-11
487	5.25E-02	5.13E-03	2.32E-05	8.36E-11
488	5.26E-02	3.88E-03	1.75E-05	6.16E-11
489	5.27E-02	8.80E-03	3.98E-05	1.38E-10
490	5.28E-02	8.23E-03	3.72E-05	1.26E-10
491	5.29E-02	6.51E-03	2.94E-05	9.86E-11
492	5.30E-02	1.03E-02	4.64E-05	1.52E-10
493	5.31E-02	1.46E-02	6.61E-05	2.10E-10
494	5.32E-02	8.59E-03	3.88E-05	1.24E-10
495	5.33E-02	1.04E-02	4.72E-05	1.48E-10
496	5.34E-02	1.41E-02	6.36E-05	2.08E-10
497	5.35E-02	1.26E-02	5.70E-05	1.92E-10
498	5.37E-02	8.83E-03	3.99E-05	1.44E-10
499	5.38E-02	9.62E-03	4.35E-05	1.52E-10
500	5.39E-02	1.37E-02	6.17E-05	2.16E-10





Forcing applied at node # 303, amplitude = .75 lb rms.

Run # 5, foundation modified with two .75 lb weights added to node # 285 and # 284.

Freq (Hz)	k (in <sup>-1</sup> )	Power (in-lb/sec)	Power (Watts)	Radiation Efficiency
450	4.85E-02	7.41E-03	3.35E-05	1.55E-10
451	4.86E-02	2.98E-03	1.35E-05	6.40E-11
452	4.87E-02	2.63E-04	1.19E-06	5.52E-12
453	4.88E-02	4.83E-03	2.18E-05	9.82E-11
454	4.89E-02	5.68E-03	2.57E-05	1.13E-10
455	4.90E-02	7.04E-03	3.18E-05	1.43E-10
456	4.91E-02	6.10E-03	2.76E-05	1.19E-10
457	4.92E-02	2.76E-03	1.25E-05	5.42E-11
458	4.93E-02	3.41E-03	1.54E-05	6.61E-11
459	4.95E-02	4.58E-03	2.07E-05	8.63E-11
460	4.96E-02	5.43E-03	2.45E-05	9.88E-11
461	4.97E-02	5.50E-03	2.49E-05	1.02E-10
462	4.98E-02	4.54E-03	2.05E-05	8.58E-11
463	4.99E-02	4.68E-03	2.12E-05	8.93E-11
464	5.00E-02	5.24E-03	2.37E-05	1.06E-10
465	5.01E-02	3.29E-03	1.49E-05	6.37E-11
466	5.02E-02	6.38E-03	2.88E-05	1.20E-10
467	5.03E-02	4.27E-03	1.93E-05	7.81E-11
468	5.04E-02	8.07E-03	3.65E-05	1.43E-10
469	5.05E-02	7.78E-03	3.52E-05	1.37E-10
470	5.06E-02	6.08E-03	2.75E-05	1.20E-10
471	5.07E-02	1.08E-02	4.88E-05	1.99E-10
472	5.09E-02	9.81E-03	4.43E-05	1.81E-10
473	5.10E-02	1.37E-02	6.18E-05	2.45E-10
474	5.11E-02	1.31E-02	5.92E-05	2.37E-10
475	5.12E-02	8.36E-03	3.78E-05	1.50E-10
476	5.13E-02	6.81E-03	3.08E-05	1.18E-10
477	5.14E-02	5.73E-03	2.59E-05	9.63E-11
478	5.15E-02	1.38E-02	6.23E-05	2.34E-10
479	5.16E-02	1.12E-02	5.07E-05	1.96E-10
480	5.17E-02	1.28E-02	5.80E-05	2.16E-10



Freq (Hz)	k (in <sup>-1</sup> )	Power (in-lb/sec)	Power (Watts)	Radiation Efficiency
481	5.18E-02	7.49E-03	3.38E-05	1.33E-10
482	5.19E-02	1.14E-02	5.15E-05	1.93E-10
483	5.20E-02	1.16E-02	5.26E-05	2.00E-10
484	5.21E-02	8.39E-03	3.79E-05	1.43E-10
485	5.22E-02	7.86E-03	3.55E-05	1.32E-10
486	5.24E-02	4.44E-03	2.01E-05	7.25E-11
487	5.25E-02	5.20E-03	2.35E-05	8.27E-11
488	5.26E-02	3.67E-03	1.66E-05	5.78E-11
489	5.27E-02	8.60E-03	3.89E-05	1.32E-10
490	5.28E-02	8.12E-03	3.67E-05	1.24E-10
491	5.29E-02	6.91E-03	3.12E-05	1.03E-10
492	5.30E-02	1.06E-02	4.78E-05	1.55E-10
493	5.31E-02	1.59E-02	7.19E-05	2.33E-10
494	5.32E-02	7.95E-03	3.59E-05	1.17E-10
495	5.33E-02	1.01E-02	4.57E-05	1.45E-10
496	5.34E-02	1.43E-02	6.48E-05	2.07E-10
497	5.35E-02	1.27E-02	5.75E-05	1.88E-10
498	5.37E-02	1.03E-02	4.65E-05	1.51E-10
499	5.38E-02	1.04E-02	4.71E-05	1.54E-10
500	5.39E-02	1.34E-02	6.06E-05	2.06E-10







Thesis

B21714 Barber

c.1      Experimental and computational determination of global resonances in ship structures.

Thesis

B21714 Barber

c.1      Experimental and computational determination of global resonances in ship structures.



DUDLEY KNOX LIBRARY



3 2768 00016163 2